Winter College on Optics and Photonics
7 - 25 February 2000

1218-19

"Radiation and Coherence Transport"

A. FRIBERG
Royal Institute of Technology
Department of Physics - Optics
Stockholm, Sweden

RADIATION AND COHERENCE TRANSPORT

Ari T. Friberg

Royal Institute of Technology

Stockholm, Sweden

Mathematics — queen of science

Radiometry — waiting maid, servant

"It is not especially elegant; it is not very popular, it has not been trendy; but it is essential in almost every part of optical engineering"
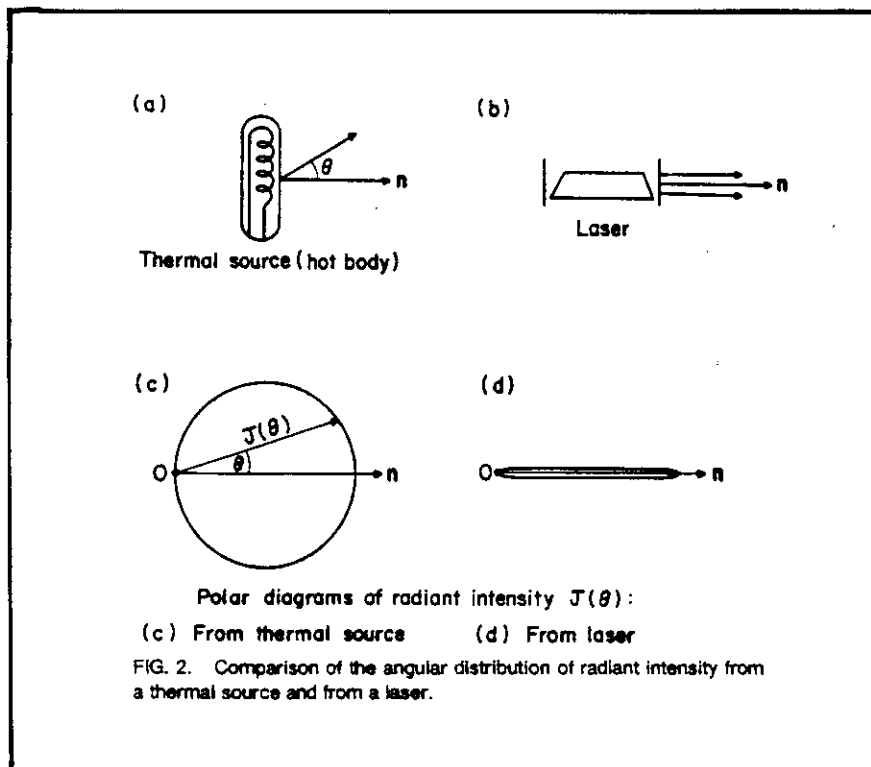
W. L. Wolfe (1998)

[OUTLINE]

I. Conventional radiation transport

II. Optical coherence theory

III. Generalized radiometry

IV. Coherence transport in random fields

Historical Milestones

— 1729 P. Bouguer ⎫
— 1760 J. Lambert ⎬ empirical laws
                    ⎭

— 1900 M. Planck   blackbody spectrum

— ~ 1900   conventional radiometry

— ~ 1960 ⎧ blackbody radiation
          ⎨ quantum theory of coherence
          ⎩ laser

Polar diagrams of radiant intensity $J(\theta)$:

(c) From thermal source   (d) From laser

FIG. 2.   Comparison of the angular distribution of radiant intensity from a thermal source and from a laser.

RADIANCE

(brightness, specific intensity)

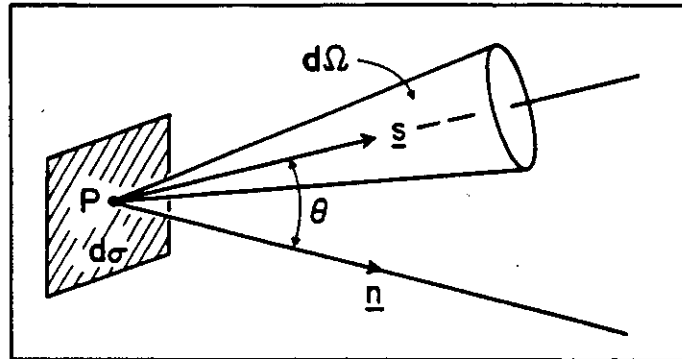Fig. 2. Illustration of the notation relating to the traditional definition of radiance.

$$L \equiv \frac{d^2 \Phi}{d A \cos \Theta \, d\Omega}$$

Equation of radiative transfer:

$$\underline{s} \cdot \nabla L(\underline{r}, \underline{s}) = -\alpha(\underline{r}, \underline{s}) L(\underline{r}, \underline{s})$$

extinction
(absorption,
scattering)

$$+ \int \beta(\underline{r}, \underline{s}, \underline{s}') L(\underline{r}, \underline{s}') d\Omega'$$

$$+ D(\underline{r}, \underline{s})$$

radiation

differential
scattering

CONVENTIONAL RADIOMETRY

- radiance $L(\underline{r}, \underline{s})$

- radiant exitance (emittance)

$$M \equiv \frac{d\bar{\Phi}}{dA} \qquad M(\underline{r}) = \int L(\underline{r}, \underline{s}) \cos\theta \, d\Omega$$

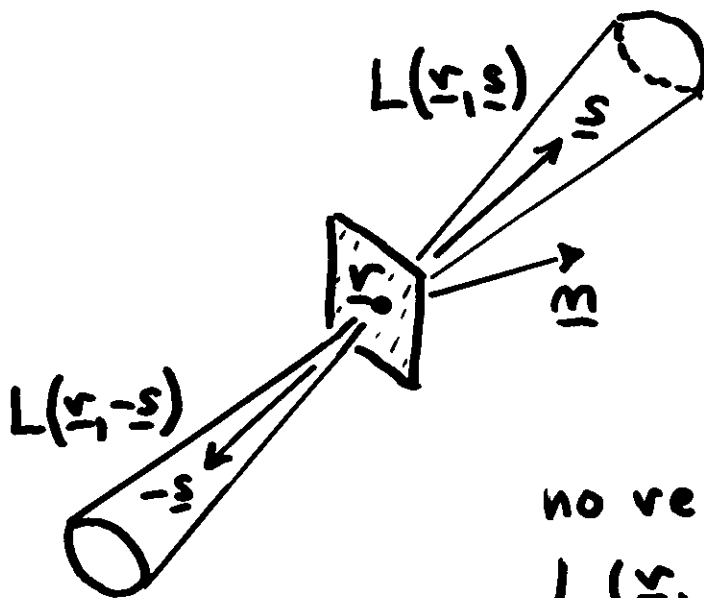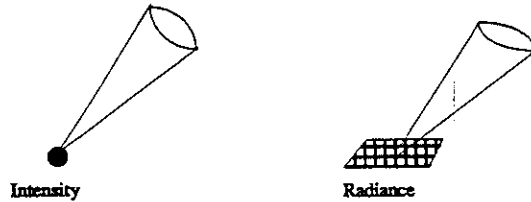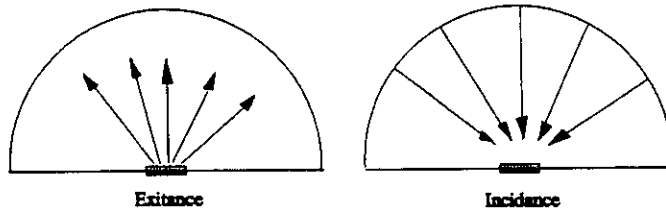radiant incidance (irradiance)

$$E \equiv \frac{d\bar{\Phi}}{dA} \qquad E(\underline{r}) = \int L(\underline{r}, \underline{s}) \cos\theta \, d\Omega$$

- radiant intensity

$$I \equiv \frac{d\bar{\Phi}}{d\Omega} \qquad I(\underline{s}) = \cos\theta \int L(\underline{r}, \underline{s}) \, dA$$

$\Rightarrow$
$$\boxed{\begin{array}{l} \text{On physical grounds} \\ \text{all quantities } (L, M \& E, I) \\ \text{are } \underline{\text{real}} \text{ and } \underline{\text{positive}} \end{array}}$$

(4)

Table 2-1. Basic radiometric quantities.			
Name	Symbol	Equation	Units
Energy	Q		joule, J
Flux	$\Phi\ [P]$	$\partial Q/\partial t$	watt, W
Flux Density		$\partial\Phi/\partial A$	
Exitance	$M\ [W]$	$\partial\Phi/\partial A$	W m^{-2}
Incidance	$E\ [H]$	$\partial\Phi/\partial A$	W m^{-2}
Intensity	$I\ [J]$	$\partial\Phi/\partial\Omega$	W sr^{-1}
Radiance	$L\ [N]$	$\partial\Phi/\partial A\cos\theta\partial\Omega$	W m^{-2} sr^{-1}

Exitance

Incidance

Intensity

Radiance

$$L(\underline{r},\underline{s})$$

$$\underline{s}$$

$$\underline{r}$$

$$\underline{m}$$

$$L(\underline{r},-\underline{s})$$

$$-\underline{s}$$

no relation between
$L(\underline{r},\underline{s})$ and $L(\underline{r},-\underline{s})$

■ Spectral radiometric quantities

$$dL(\underline{r}, \underline{s}) = L(\underline{r}, \underline{s}, \nu)\, d\nu$$

$$= L(\underline{r}, \underline{s}, \lambda)\, d\lambda$$

$$\Rightarrow \quad M(\underline{r}, \nu) \quad E(\underline{r}, \nu) \quad I(\underline{r}, \nu)$$
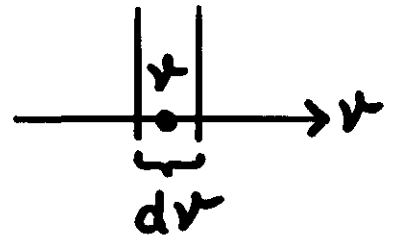
■ Photonic radiometric quantities

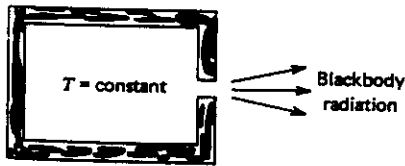$$d\overline{\Phi}_\nu = N_\nu\,(h\nu)\, dt \qquad \text{photon flux}$$

■ Photometric (luminous) quantities

$$\Phi_v = \int V(\lambda)\, \overline{\Phi}(\lambda)\, d\lambda$$

$V(\lambda)$ = absolute spectral response
of the (average) human eye

Lumen

BLACKBODY

— homogeneous
— isotropic
— thermal equilibrium

$$L(\nu) = \frac{2h\nu^3}{(c/n)^2} \frac{1}{e^{h\nu/kT} - 1}$$
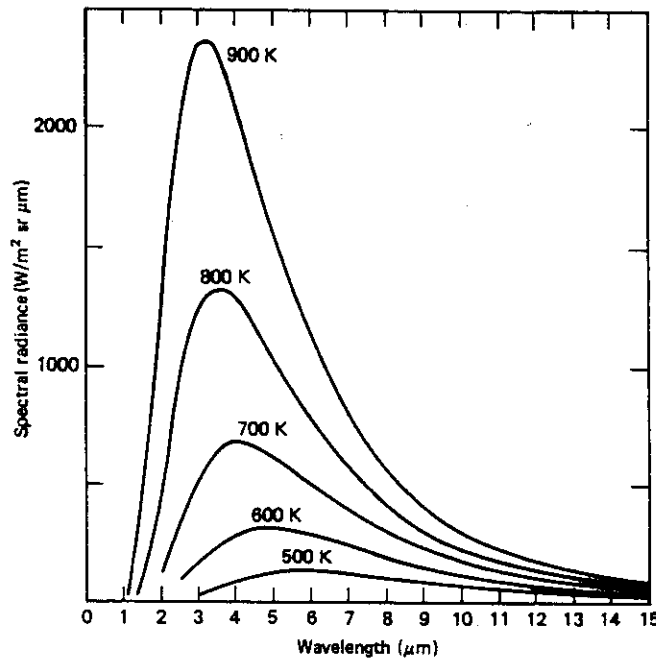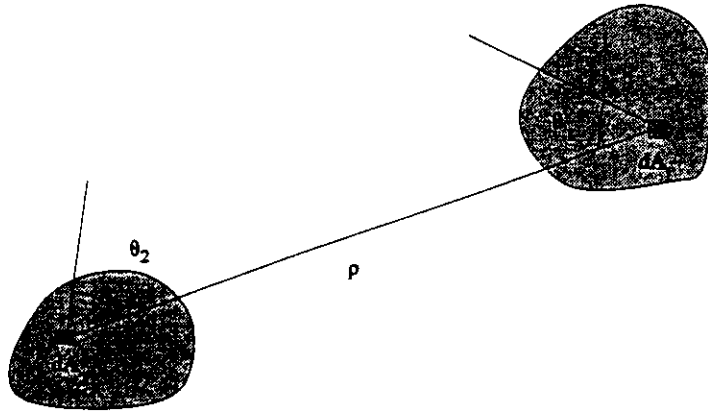
(Planck's radiation law)

Figure 4.4. Planck radiation law for several blackbody temperatures. (Used with permission from R. D. Hudson, *Infrared System Engineering*, Wiley, New York, 1969.)

$$I(s,\nu) = I_o(\nu) \cos\theta$$

Lambertian emitter

(7)

RADIATIVE TRANSFER

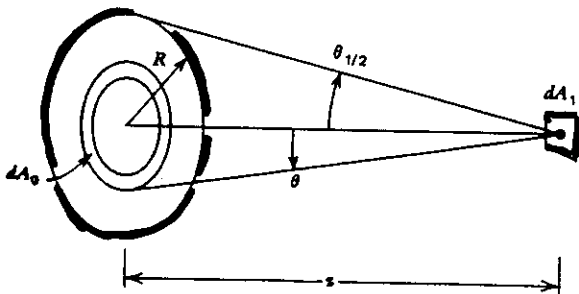Free space $(\underline{s}\cdot\nabla) L(\underline{r},\underline{s}) = \dfrac{dL(\underline{r},\underline{s})}{ds} = 0$

$$d\underline{\Phi} = L \; \frac{dA_1 \cos\theta_1 \; dA_2 \cos\theta_2}{\varrho^2} = L \, d\overline{z}$$
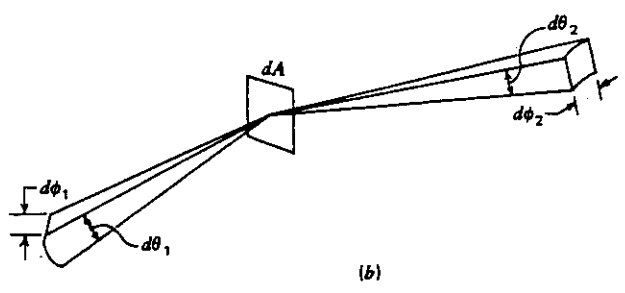
differential throughput
"etendue"

Lambertian disk:

$$M = \pi L \sin^2\theta_{1/2}$$

Figure 2.10. Disk Lambertian source irradiates the area element dA_1.

RADIANCE THEOREM

(a)

(b)
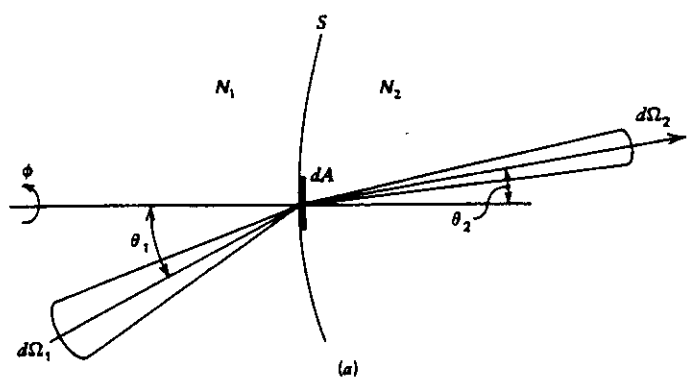
$$d^2\Phi = L_1 \, dA \cos\theta_1 \, d\Omega_1 \qquad d^2\Phi = L_2 \, dA \cos\theta_2 \, d\Omega_2$$

Snell's law:

$$d\phi_1 = d\phi_2$$

$$N_1 \sin\theta_1 = N_2 \sin\theta_2$$

$$N_1 \cos\theta_1 \, d\theta_1 = N_2 \cos\theta_2 \, d\theta_2$$

$$L_2 = L_1 \frac{dA \cos\theta_1 \sin\theta_1 \, d\theta_1 \, d\phi_1}{dA \cos\theta_2 \sin\theta_2 \, d\theta_2 \, d\phi_2} = L_1 \frac{N_2^2}{N_1^2}$$

$$\boxed{\frac{L_1}{N_1^2} = \frac{L_2}{N_2^2}} \quad \text{(Basic radiance)}$$

⑨

SPACE-TIME COHERENCE

✧ scalar theory
✧ stationary & ergodic field

$V(\mathbf{r},t)$
COMPLEX ANALYTIC SIGNAL
(only positive frequencies)

$\Gamma(\mathbf{r}_1,\mathbf{r}_2;\tau) = \langle V^*(\mathbf{r}_1,t)V(\mathbf{r}_2,t+\tau)\rangle$
MUTUAL COHERENCE FUNCTION

$I(\mathbf{r}) = \Gamma(\mathbf{r},\mathbf{r};0) = \langle |V^*(\mathbf{r},t)|^2\rangle$
(AVERAGED) OPTICAL INTENSITY

$\gamma(\mathbf{r}_1,\mathbf{r}_2;\tau) = \dfrac{\Gamma(\mathbf{r}_1,\mathbf{r}_2;\tau)}{\sqrt{I(\mathbf{r}_1)I(\mathbf{r}_2)}}$
COMPLEX DEGREE OF COHERENCE

$$0 \le |\gamma(\mathbf{r}_1,\mathbf{r}_2;\tau)| \le 1$$
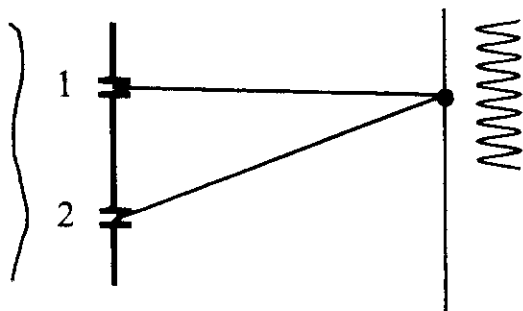
INCOHERENT   COHERENT ➡

DOMAIN $\mathcal{D}$

$\Gamma(\mathbf{r}_1,\mathbf{r}_2;\tau) = U^*(\mathbf{r}_1)U(\mathbf{r}_2)e^{-i\omega\tau}$

STRICTLY MONOCHROMATIC

$(\nabla^2 + k^2)U(\mathbf{r}) = 0$

YOUNG'S INTERFEROMETER

Delay τ

Visibility $\mathcal{V} \propto |\gamma_{12}(\tau)|$

Fringe location $\propto$ phase of γ

SPACE-FREQUENCY COHERENCE

$$\begin{cases} \Gamma(\mathbf{r}_1,\mathbf{r}_2;\tau) = \int\limits_0^\infty W(\mathbf{r}_1,\mathbf{r}_2;\omega)e^{-i\omega\tau}d\omega \\ \left\langle \tilde{V}^*(\mathbf{r}_1,\omega)\tilde{V}(\mathbf{r}_2,\omega')\right\rangle = W(\mathbf{r}_1,\mathbf{r}_2;\omega)\delta(\omega-\omega') \end{cases}$$

WIENER-KHINTCHINE
THEOREM

CROSS-SPECTRAL DENSITY

$$S(\mathbf{r},\omega) = W(\mathbf{r},\mathbf{r};\omega)$$ SPECTRUM (SPECTRAL INTENSITY)

$$\mu(\mathbf{r}_1,\mathbf{r}_2;\omega) = \frac{W(\mathbf{r}_1,\mathbf{r}_2;\omega)}{\sqrt{S(\mathbf{r}_2,\omega)S(\mathbf{r}_1,\omega)}}$$

COMPLEX DEGREE OF
SPECTRAL (SPATIAL)
COHERENCE

$$0 \le \left| \mu(\mathbf{r}_1,\mathbf{r}_2;\omega) \right| \le 1$$

INCOHERENT   COHERENT ➡

DOMAIN $\mathcal{D}$

$$W(\mathbf{r}_1,\mathbf{r}_2;\omega) = U^*(\mathbf{r}_1,\omega)U(\mathbf{r}_2,\omega)$$

FACTORIZATION

$\Rightarrow$ **stationary field may be partially coherent at single frequencies !**

YOUNG + SPECTRAL FILTERS

$T(\omega_0,\Delta\omega)$

1

2
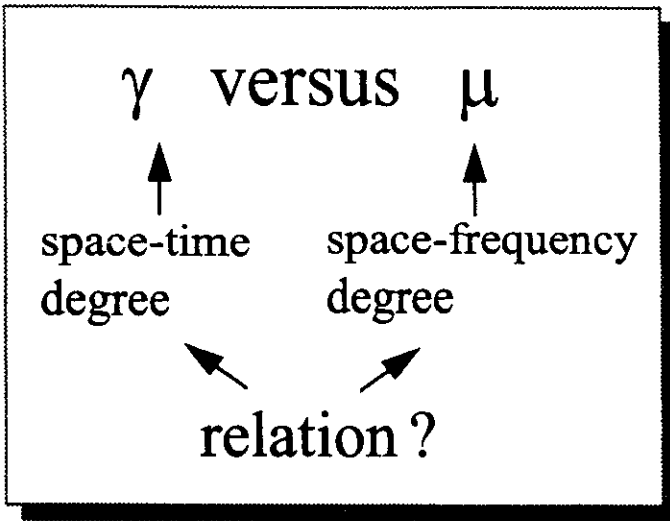
As $\Delta\omega \to 0$

$\gamma(\mathbf{r}_1,r_2;\tau) = \mu(\mathbf{r}_1,r_2;\omega_0)\theta(\tau)$

$\theta(\tau) \sim T(\omega)$

$\theta(0) = 1$

γ versus μ

$\uparrow$ space-time degree

$\uparrow$ space-frequency degree

relation ?
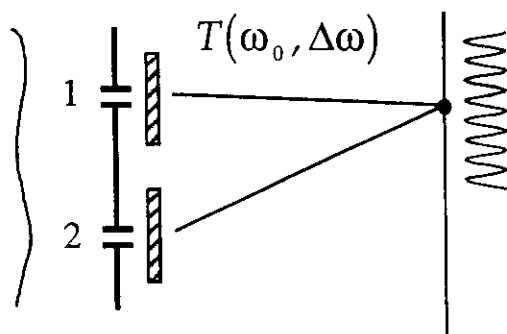
INTENSITY

$$I(\mathbf{r}) = \int_0^\infty S(\mathbf{r},\omega)\,d\omega$$

NORMALIZED SPECTRUM

$$\delta(\mathbf{r},\omega) = \frac{S(\mathbf{r},\omega)}{\int_0^\infty S(\mathbf{r},\omega)\,d\omega}$$

$$\gamma(\mathbf{r}_1,\mathbf{r}_2;\tau) = \int_0^\infty \sqrt{\delta(\mathbf{r}_1,\omega)\delta(\mathbf{r}_2,\omega)}\,\mu(\mathbf{r}_1,\mathbf{r}_2;\omega)\,e^{-i\omega\tau}\,d\omega$$

FT-pair

EXAMPLE: Black-body
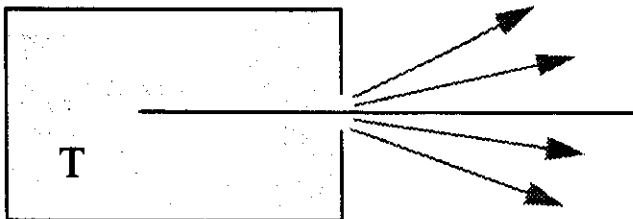
Lambertian

$$\mu(\mathbf{r}_1,\mathbf{r}_2;\omega) = \frac{\sin k|\mathbf{r}_1-\mathbf{r}_2|}{k|\mathbf{r}_1-\mathbf{r}_2|}$$

$\delta(\omega) \sim$ Planck's law

homogeneous, isotropic
E, H vectors
$W = \mathrm{Tr}\{W_{ij}^{(E)}\}$

$$\alpha = \frac{\hbar}{KT}$$

$$\Delta\tau \approx \frac{2\pi}{\omega_{max}} = \frac{2\pi}{2.82}\left(\frac{\hbar}{KT}\right) = 2.23\alpha$$

temporal $|\gamma(0,\tau/\alpha)|$

spatial $\gamma(r/\alpha c,0)$

(12)

PROPAGATION

⬧ Wave equations for $\Gamma(\mathbf{r}_1,\mathbf{r}_2;\tau)$
⬧ Sudarshan's equations
⬧ Helmholtz equations for $W(\mathbf{r}_1,\mathbf{r}_2;\omega)$

$$\left(\nabla_j^2 + k^2\right)W(\mathbf{r}_1,\mathbf{r}_2;\omega) = 0 \qquad (k = \omega/c)$$

⬧ Solutions:
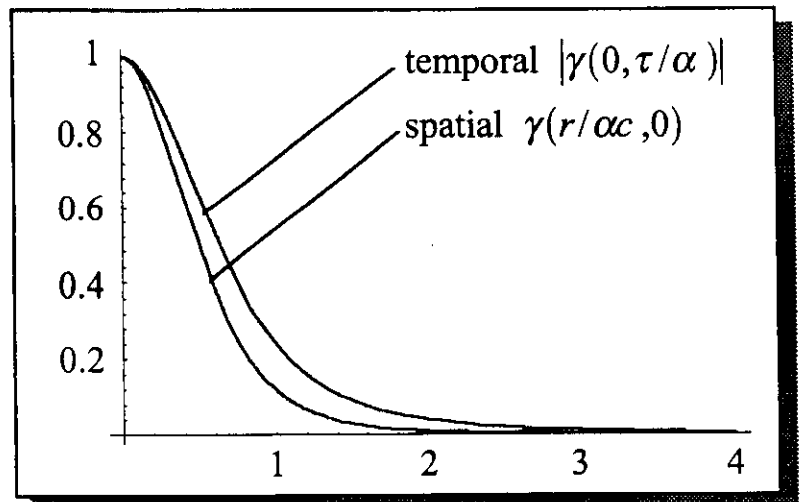
  ◆ Angular spectrum representation (exact)
  ◆ 1st and 2nd Rayleigh Integrals (exact)
  ◆ Extended Fresnel diffraction (beams)

$$\begin{pmatrix} \rho \\ \rho' \end{pmatrix}_{out} = \begin{pmatrix} A & B \\ C & D \end{pmatrix}\begin{pmatrix} \rho \\ \rho' \end{pmatrix}_{in} = M\begin{pmatrix} \rho \\ \rho' \end{pmatrix}_{in}$$

  ◆ symmetric lens systems (2 x 2 ABCD matrices)
  ◆ non-symmetric systems (4 x 4 matrices)
  ◆ tilt & decenter (5 x 5 matrices)

$$U(\rho,z_{out}) = \frac{-ik}{2\pi}e^{ikL}(\det B)^{-1}\iint U(\rho_0,z_{in})$$
$$\times \ \exp\left[ik\left(\rho^T DB^{-1}\rho - 2\rho_0^T B^{-1}\rho + \rho_0^T B^{-1}A\rho_0\right)/2\right]d^2\rho_0$$

EXTENSIONS

⬧ Non-stationary fields (pulses)
⬧ Electromagnetic coherence tensors
  ◆ correlation functions
  ◆ Maxwell's equations
⬧ Partial polarization
  ◆ Blackbody radiation unpolarized
⬧ Higher-order correlations

COHERENT-MODE REPRESENTATION

$W(\mathbf{r}_1, \mathbf{r}_2; \omega)$ continuous in ω

a) $\iint \left| W(\mathbf{r}_1, \mathbf{r}_2; \omega) \right|^2 d^3 r_1 d^3 r_2 < \infty$ (Finite energy, Hilbert-Schmidt)

b) $W(\mathbf{r}_2, \mathbf{r}_1; \omega) = W^*(\mathbf{r}_1, \mathbf{r}_2; \omega)$ (Hermitian)

c) $\iint W(\mathbf{r}_1, \mathbf{r}_2; \omega) f^*(\mathbf{r}_1) f(\mathbf{r}_2)\, d^3 r_1 d^3 r_2 \geq 0$ (Non-negative definite)

$\left[\text{any function } f, \text{ eg. } f(\mathbf{r}) \propto e^{i k s \cdot \mathbf{r}} \text{ far - field} \right]$

$\Rightarrow$ (Mercer's theorem)

$$W(\mathbf{r}_1, \mathbf{r}_2; \omega) = \sum_n \lambda_n(\omega) \psi_n^*(\mathbf{r}_1, \omega) \psi_n(\mathbf{r}_2, \omega) \qquad (\lambda_n \geq 0)$$

$$\int W(\mathbf{r}_1, \mathbf{r}_2; \omega) \psi_n(\mathbf{r}_1, \omega) d^3 r_1 = \lambda_n(\omega) \psi_n(\mathbf{r}_2, \omega) \qquad \left(\int \psi_n^* \psi_m = \delta_{nm} \right)$$

(Fredholm integral equation)

☞   ✧ Factorization $\rightarrow$ each term spatially coherent
                Helmholtz eq. $\rightarrow$ **coherent (natural) modes**

☞   ✧ Let $U(\mathbf{r}) = \sum a_n(\omega) \psi_n(\mathbf{r}, \omega)$

                      $\left\langle a_n^*(\omega) a_m(\omega) \right\rangle = \lambda_n(\omega) \delta_{nm}$

          $\Rightarrow$ $W(\mathbf{r}_1, \mathbf{r}_2; \omega) = \left\langle U^*(\mathbf{r}_1, \omega) U(\mathbf{r}_2, \omega) \right\rangle$

(correlation of ordinary functions !)

Space-time domain	**Space-frequency domain**

$\{Q(\mathbf{r},t)\} \dashrightarrow \{\hat{Q}(\mathbf{r},\omega)\}$

(forbidden)

$\{Q(\mathbf{r},t)\} \dashleftarrow \{U_Q(\mathbf{r},\omega)\}$

(forbidden)

$\Gamma_Q(\mathbf{r}_1,\mathbf{r}_2,\tau) \xrightarrow{\text{FT}} W_Q(\mathbf{r}_1,\mathbf{r}_2,\omega)$

$\Gamma_Q(\mathbf{r}_1,\mathbf{r}_2,\tau) \xleftarrow{\text{FT}} W_Q(\mathbf{r}_1,\mathbf{r}_2,\omega)$

$$\Gamma_Q(\mathbf{r}_1,\mathbf{r}_2,\tau) = \left\langle Q^*(\mathbf{r}_1,t)\,Q(\mathbf{r}_2,t+\tau)\right\rangle_t$$

$$W_Q(\mathbf{r}_1,\mathbf{r}_2,\omega) = \left\langle U_Q^*(\mathbf{r}_1,\omega)\,U_Q(\mathbf{r}_2,\omega)\right\rangle_\omega$$

Source
$\{Q(\mathbf{r},t)\}$
(ϕ_n,λ_n)

D
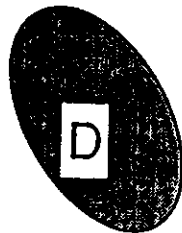
Field
$\{V(\mathbf{r},t)\}$
(ψ_n,λ_n)

$$W_V(\mathbf{r}_1,\mathbf{r}_2,\omega) = \sum_n \lambda_n(\omega)\,\psi_n^*(\mathbf{r}_1,\omega)\,\psi_n(\mathbf{r}_2,\omega)$$

Mode representation of a radiated field.

⑮

EXAMPLE: GAUSSIAN SCHELL-MODEL SOURCES

SCHELL-MODEL: $\quad \mu(\mathbf{r}_1, \mathbf{r}_2; \omega) = g(\mathbf{r}_2 - \mathbf{r}_1; \omega)$
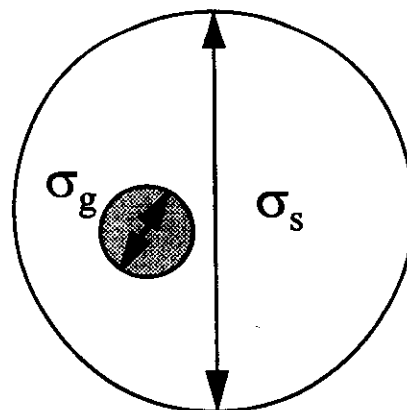
$$\begin{cases} W(\mathbf{r}_1, \mathbf{r}_2; \omega) = \sqrt{S(\mathbf{r}_1, \omega) S(\mathbf{r}_2, \omega)}\, g(\mathbf{r}_2 - \mathbf{r}_1; \omega) \\[2mm] S(\mathbf{r}, \omega) = S(\omega)\, e^{-r^2/2\sigma_S^2} \\[2mm] g(\mathbf{r}'; \omega) = e^{-r'^2/2\sigma_g^2} \end{cases}$$

- ❖ $\sigma_S \gg \sigma_g$ → globally incoherent (quasihomogeneous)
- $\sigma_g \gg \lambda$ → locally coherent
- $\sigma_g \sim \lambda$ → locally incoherent

Coherent modes   (Hermite-Gaussian functions)

$$\psi_n(x, \omega) = \left(\frac{2}{\pi w_S^2 \beta}\right)^{1/4} \frac{1}{\sqrt{2^n n!}} H_n\left(\frac{\sqrt{2}x}{w_S \sqrt{\beta}}\right) e^{-x^2/w_S^2 \beta}$$

$$\lambda_n(\omega) = S(\omega)\sqrt{2\pi}\; w_S \frac{\beta}{1+\beta}\left(\frac{1-\beta}{1+\beta}\right)^n$$

$$w_S = 2\sigma_S$$

$$\alpha = \frac{\sigma_g}{w_S} \quad \begin{array}{l}\text{global degree}\\\text{of coherence}\end{array}$$
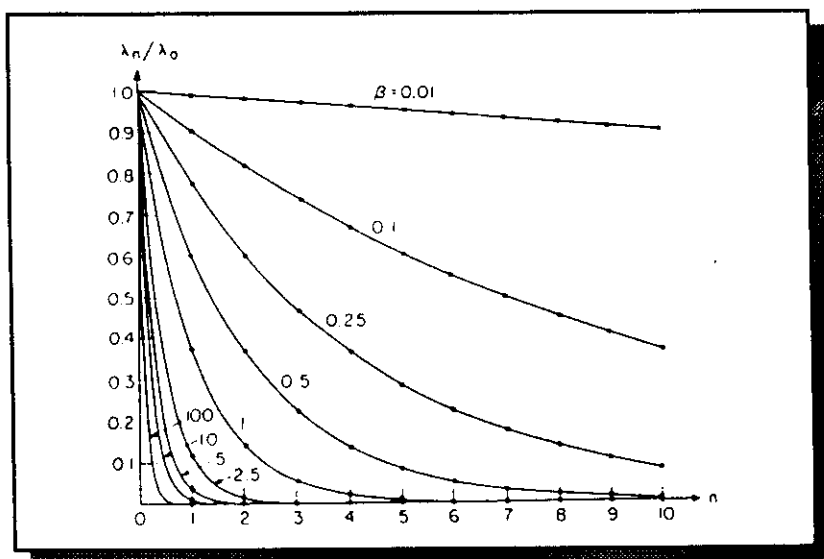
$$\beta = \frac{1}{\sqrt{1 + \alpha^{-2}}} \quad (0 \le \beta \le 1)$$

- ❖ Bessel J_0-correlated sources
- ❖ Short-correlation limit

GENERALIZED RADIANCE
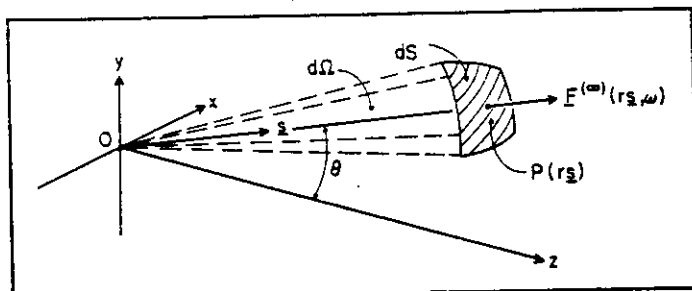
Fig. 3. Energy flow in the far zone of the source.

Power flow
as $r \to \infty$
$$\underline{F}^{(\infty)}(r\underline{s}) \sim S^{(\infty)}(r\underline{s})\,\underline{s}$$

$$J(\underline{s}) = \frac{d\Phi}{d\Omega} = r^2 S^{(\infty)}(r\underline{s})$$

$$= r^2 \langle |U^{(\infty)}(r\underline{s})|^2 \rangle$$

$$= (2\pi k)^2 \cos^2\theta \, \widetilde{W}(k\underline{s}_\perp, -k\underline{s}_\perp)$$

$$= \left(\frac{k}{2\pi}\right)^2 \cos^2\theta \iint\limits_{-\infty}^{\infty} W^{(0)}(\underline{r}_1, \underline{r}_2)$$

$$\cdot e^{-ik\underline{s}_\perp \cdot (\underline{r}_1 - \underline{r}_2)} \, d^2r_1 \, d^2r_2$$

$$J(\underline{s}) = \cos\theta \int_\delta B(\underline{r}, \underline{s}) \, d\delta$$

$$\Rightarrow \quad \text{infinity of possible } B(\underline{r}, \underline{s})$$

17

Requirements:

(i) $\quad B(\underline{r}, \underline{s}) = \mathcal{L}\{W(\underline{r}_1, \underline{r}_2)\}$

(ii) $\quad B(\underline{r}, \underline{s}) \geq 0$

(iii) $\quad B(\underline{r}, \underline{s}) = 0 \quad$ when $\underline{r} \notin \delta$

(iv) $\quad \int_\delta B(\underline{r}, \underline{s}) d\delta = (2\pi k)^2 \cos\theta \, \widetilde{W}(k\underline{s}_\perp, -k\underline{s}_\perp)$

$\Longrightarrow \quad$ No $B(\underline{r}, \underline{s})$ exists that satisfies
all conditions (i) – (iv).

Examples:

$$B^{(1)}(\underline{r}, \underline{s}) = \left(\frac{k}{2\pi}\right)^2 \cos\theta \int W(\underline{r} + \tfrac{1}{2}\underline{r}', \underline{r} - \tfrac{1}{2}\underline{r}') e^{-ik\underline{s}_\perp \cdot \underline{r}'} d^2\underline{r}'$$

(symmetric ordering,
Wigner distribution function)

$$B^{(2)}(\underline{r}, \underline{s}) = \left(\frac{k}{2\pi}\right)^2 \cos\theta \int W(\underline{r}, \underline{r}') e^{-ik\underline{s}_\perp \cdot (\underline{r} - \underline{r}')} d^2\underline{r}'$$

(antinormal ordering)

Commonly asked questions:

1) If $B(\underline{r}, \underline{s})$ is negative, does it mean that energy flows in $-\underline{s}$ direction?

Answer: NO
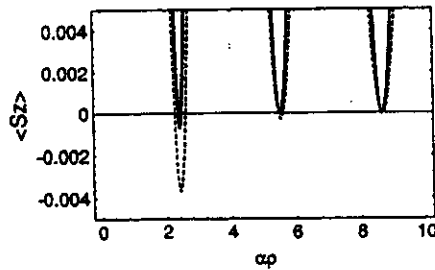
Figure 3. Vertically expanded view of figure 2(b) illustrating the fact that the averaged z-component of the Poynting vector assumes negative values in the regions of its minima.

2) Should $B(\underline{r}, \underline{s})$ vanish when $\langle |U(\underline{r})|^2 \rangle = 0$?

Answer: Hmm...

point sources

π phase shift
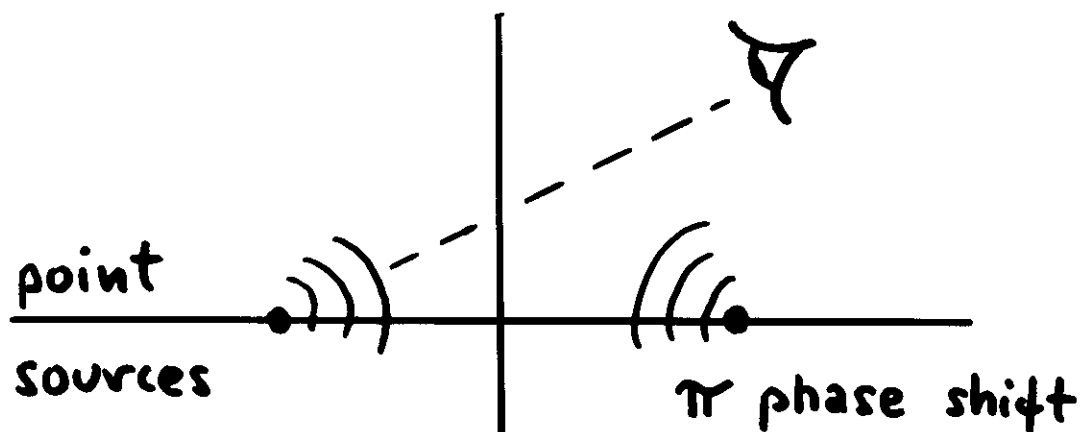
Sommerfeld radiation condition

19

PHASE SPACE

$B(\underline{r}, \underline{s}) \longleftrightarrow \underline{r}$ & $\underline{s}$ conjugate variables

$$(\underline{p} = \hbar \underline{k} = \hbar k \underline{s})$$

RADIANCE	$\underline{r}$	$\underline{s}$
Conventional	Yes	Yes
Wave theory	Yes	No
Quantum mech.	No	No

Marginal distributions:

$$\cos\theta \int\limits_{(z=0)} B(\underline{r}, \underline{s}) \, d^2r = J(\underline{s}) \qquad \text{radiant intensity (physical)}$$

$$\int\limits_{(2\pi)} B(\underline{r}, \underline{s}) \cos\theta \, d\Omega = E(\underline{r}) \qquad \text{generalized radiant emittance}$$

QUASI-HOMOGENEITY

$$\mu(\underline{r}_1, \underline{r}_2, \omega) = g(\underline{r}_1 - \underline{r}_2, \omega)$$

Fast function   Slow function
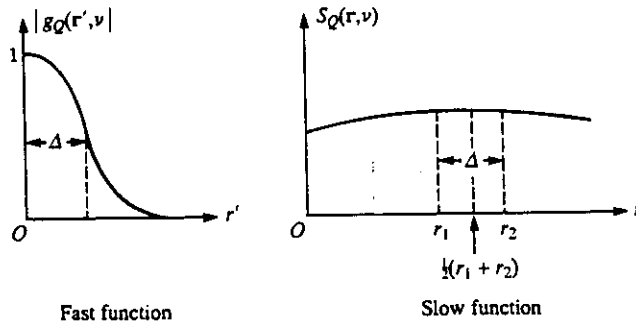
Fig. 5.2 Illustrating the concept of a quasi-homogeneous source. The modulus $|g_Q(\mathbf{r'}, \nu)|$ of the spectral degree of coherence of the source distribution changes much more rapidly with $\mathbf{r'}$ than its spectral density $S_Q(\mathbf{r}, \nu)$ changes with $\mathbf{r}$. For the purpose of illustration, the source is taken to be one-dimensional.

area of coherence
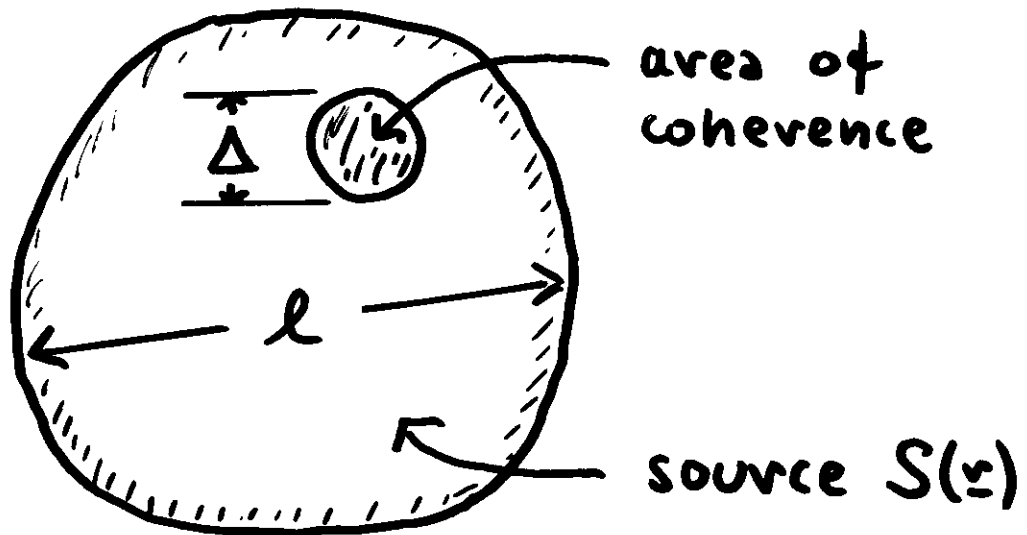
source $S(\underline{r})$

- globally incoherent $\quad \Delta \ll \ell$

- $\begin{cases} \text{locally coherent,} & \text{if} \quad \Delta \gg \lambda \\ \text{locally incoherent,} & \text{if} \quad \Delta \approx \lambda \end{cases}$

GENERALIZED RADIOMETRY

(with quasi-homogeneous sources)

$$B(\underline{r}, \underline{s}) = k^2 \cos\theta\, S^{(0)}(\underline{r})\, \tilde{g}^{(0)}(k\underline{s}_\perp)$$

$$E(\underline{r}) = S^{(0)}(\underline{r}) \underbrace{\int_{-\infty}^{\infty} g^{(0)}(\underline{r}')\, K(\underline{r}')\, d^2 r'}$$

$$C = \text{radiation efficiency}$$

$$K(\underline{r}') = \frac{k^2}{2\sqrt{2\pi}}\, \frac{J_{3/2}(kr')}{(kr')^{3/2}}$$

$$J(\underline{s}) = (2\pi k)^2 \cos^2\theta\, \tilde{S}^{(0)}(0)\, \tilde{g}^{(0)}(k\underline{s}_\perp)$$

$$\Rightarrow$$

coherent*	$J(\underline{s}) \longrightarrow$	$\delta(\theta)$
incoherent	$J(\underline{s}) \sim$	$\cos^2\theta$
Lambertian	$J(\underline{s}) \sim$	$\cos\theta$

---

* uniform

Gaussian correlation $g(\underline{r}') = e^{-r'^2/2\delta_\mu^2}$

$$\frac{B(\underline{r}, \theta)}{B(\underline{r}, o)}$$

Fig. 9. Angular distribution of the normalized radiance from a Gaussian correlated quasihomogeneous planar source.
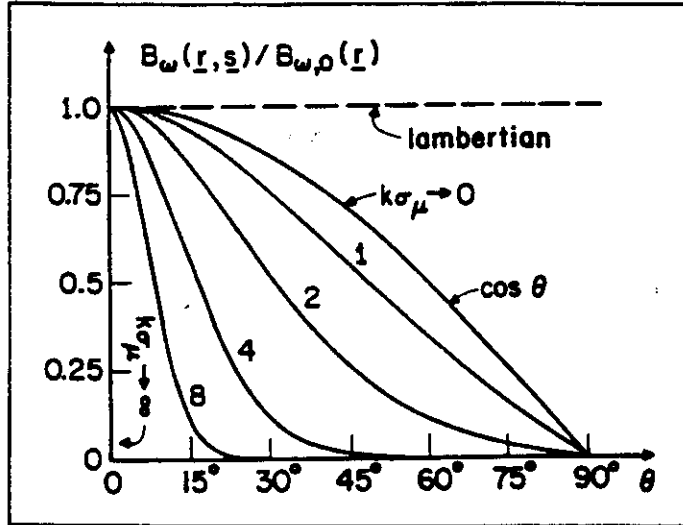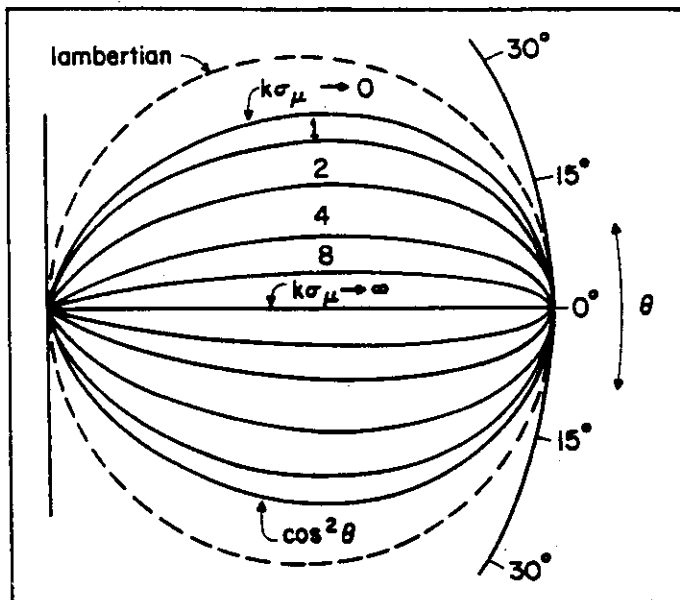
$$\frac{J(\theta)}{J(o)}$$

Fig. 10. Polar diagram of the normalized radiant intensity from a Gaussian correlated quasihomogeneous planar source [after Carter and Wolf[6]].

RADIATION FROM PARTIALLY COHERENT SOURCES

TABLE 1. Radiation from Partially Coherent Model Sources.

	SCHELL	QUASIHOMOGENEOUS		
MODEL	SCHELL	QUASIHOMOGENEOUS		
INTENSITY	GAUSSIAN	NOT RELEVANT		
COHERENCE	GAUSSIAN	GAUSSIAN	EXPONENTIAL	BESSEL
COEFFICIENT OF DIRECTIONALITY	$e^{-r'^2/2\Delta^2}$ $\qquad \dfrac{1}{\Delta^2} = \dfrac{1}{\sigma_\mu^2} + \dfrac{1}{(2\sigma_I)^2}$	$e^{-r'^2/2\sigma_\mu^2}$	$e^{-|r'|/D}$	$\dfrac{2}{\sqrt{\pi}}\,\Gamma\!\left(\nu+\dfrac{3}{2}\right)\dfrac{j_\nu(k|r'|)}{\left(\tfrac{1}{2}k|r'|\right)^\nu}$
RADIANT INTENSITY	$J_{\omega,o}\cos^2\theta\, e^{-\frac{1}{2}(k\Delta)^2\sin^2\theta}$ $\qquad J_{\omega,o} = (k\Delta\sigma_I)^2 I_o$	$J_{\omega,o}\cos^2\theta\, e^{-\frac{1}{2}(k\sigma_\mu)^2\sin^2\theta}$ $\qquad J_{\omega,o} = \dfrac{(k\sigma_\mu)^2}{2\pi}\displaystyle\int I^{(0)}(\underline{r},\omega)\,d^2r$	$J_{\omega,o}\cos^2\theta\,[1+(kD)^2\sin^2\theta]^{-\frac{3}{2}}$ $\qquad J_{\omega,o} = \dfrac{(kD)^2}{2\pi}\displaystyle\int I^{(0)}(\underline{r},\omega)\,d^2r$	$J_{\omega,o}\cos^{2\nu+1}\theta$ $\qquad J_{\omega,o} = \dfrac{1}{\pi}\left(\nu+\dfrac{1}{2}\right)\displaystyle\int I^{(0)}(\underline{r},\omega)\,d^2r$
RADIATION EFFICIENCY	$1 - \dfrac{F(k\Delta/\sqrt{2})}{k\Delta/\sqrt{2}}$ $\qquad F(a) = e^{-a^2}\displaystyle\int_0^a e^{u^2}\,du$	$1 - \dfrac{F(k\sigma_\mu/\sqrt{2})}{k\sigma_\mu/\sqrt{2}}$ $\qquad F(a) = e^{-a^2}\displaystyle\int_0^a e^{u^2}\,du$	$1 - \dfrac{1}{(kD)}\sin^{-1}\!\left(\dfrac{kD}{\sqrt{1+(kD)^2}}\right)$	$\dfrac{2\nu+1}{2\nu+2}$

Fig. 5.12 The spectral degree of coherence $g^{(0)}(\rho', \nu)$ and the distribution of spectral density $S^{(0)}(\rho, \nu)$ across four planar, secondary, Gaussian, Schell-model sources which generate identical distributions of the radiant intensity. The curves in (a) pertain to a completely (spatially) coherent source (e.g. a single-mode laser) and the curves in (d) to a rather incoherent source. The parameters characterizing the four sources are: (a) $\sigma_g = \infty$, $\sigma_S = 1$ mm, $A = 1$ (arbitrary units); (b) $\sigma_g = 5$ mm, $\sigma_S = 1.09$ mm, $A = 0.84$; (c) $\sigma_g = 2.5$ mm, $\sigma_S = 1.67$ mm, $A = 0.36$; (d) $\sigma_g = 2.1$ mm, $\sigma_S = 3.28$ mm, $A = 0.09$. The normalized radiant intensity generated by all these sources is given by the expression (5.4-16), namely $J(\theta)/J(0) = \cos^2\theta \exp[-\frac{1}{2}(k\delta)^2 \sin^2\theta]$, with $\delta = 2$ mm. (After Wolf and Collett, 1978.)

$$\sigma_S \gg \sigma_g,$$
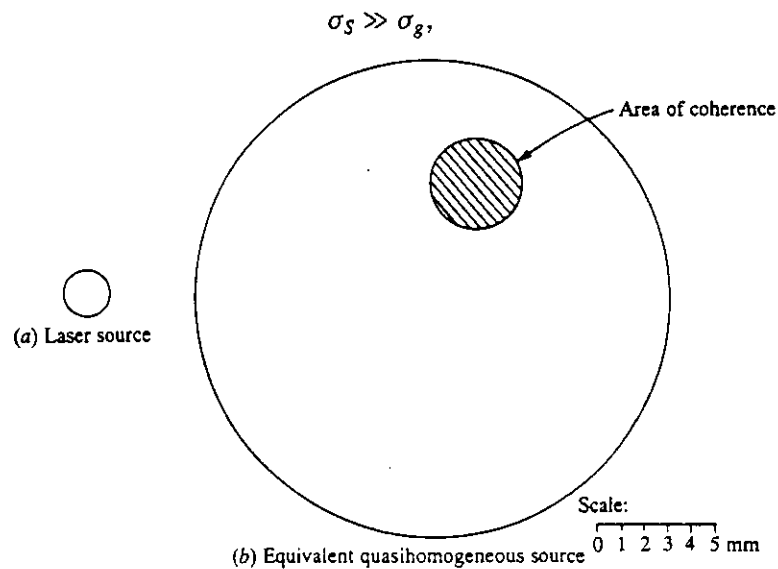
Fig. 5.11 Illustrating the effective sizes of (a) a laser source and of (b) an 'equivalent' quasi-homogeneous source. The coherence area of the quasi-homogeneous source is shown shaded in Fig. (b). (After Wolf, 1978.)

CROSS-SPECTRAL DENSITY OPERATOR

- $(\nabla^2 + k^2) U(\underline{r}) = 0$

$$U(\underline{r}) = \int a(\underline{s}_\perp) e^{ik(\underline{s}_\perp \cdot \underline{\rho} + s_z z)} d^2 s_\perp$$

where

$$s_z = \sqrt{1 - s_\perp^2} \quad , \quad \text{if } |\underline{s}_\perp| \leq 1$$
$$= i\sqrt{s_\perp^2 - 1} \quad , \quad \text{if } |\underline{s}_\perp| > 1$$

In plane $z = 0$

$$-i\lambda \nabla_\perp U(\underline{\rho}) = \int \underline{s}_\perp a(\underline{s}_\perp) e^{ik\underline{s}_\perp \cdot \underline{\rho}} d^2 s_\perp$$

$$\left(\lambda = \frac{\lambda}{2\pi} = \frac{1}{k} \right)$$

- $\Rightarrow$

$$\hat{\underline{s}}_\perp = -i\lambda \nabla_\perp$$
$$\hat{\underline{\rho}} = (\hat{x}, \hat{y})$$

$$[\hat{x}, \hat{s}_x] = i\lambda \qquad [\hat{y}, \hat{s}_y] = i\lambda$$

Commutation relations for classical fields !

(26)

Define
$$\hat{G} = G(\hat{\underline{\rho}}, \hat{\underline{s}}_\perp)$$

$$\langle \underline{\rho}_1 | G(\hat{\underline{\rho}}, \hat{\underline{s}}_\perp) | \underline{\rho}_2 \rangle = W(\underline{\rho}_1, \underline{\rho}_2)$$

Generalized radiance

$$B^{(\Omega)}(\underline{\rho}, \underline{s}) = \left(\frac{k}{2\pi}\right)^2 \cos\theta \, F^{(\Omega)}(\underline{\rho}, \underline{s}_\perp)$$

$$F^{(\Omega)}(\underline{\rho}, \underline{s}_\perp) = (2\pi\lambda)^2 \int \langle \underline{\rho}_1 | G(\hat{\underline{\rho}}, \hat{\underline{s}}_\perp)$$

$$\cdot \Delta^{(\Omega)}(\underline{\rho} - \hat{\underline{\rho}}, \underline{s}_\perp - \hat{\underline{s}}_\perp) | \underline{\rho}_1 \rangle \, d^2\underline{\rho}_1$$

filter functions $\Omega(u,v)$

$$\Rightarrow$$

- As $\lambda \to 0$, operators $\hat{\underline{\rho}}$ and $\hat{\underline{s}}_\perp$ commute;
  all $B^{(\Omega)}(\underline{\rho}, \underline{s})$ will become identical

- For quasi-homogeneous sources
$$B(\underline{\rho}, \underline{s}) = k^2 \cos\theta \, S^{(o)}(\underline{r}) \, \tilde{g}^{(o)}(k\underline{s}_\perp)$$

has all the properties of traditional radiance

ASYMPTOTIC RADIOMETRY

- $B(\underline{\rho}, \underline{s}) = k^2 s_z\, S^{(0)}(\underline{\rho})\, \tilde{q}^{(0)}(k\underline{s}_\perp)$

- $B(\underline{r}, \underline{s})$ constant along straight lines as $k \to \infty$
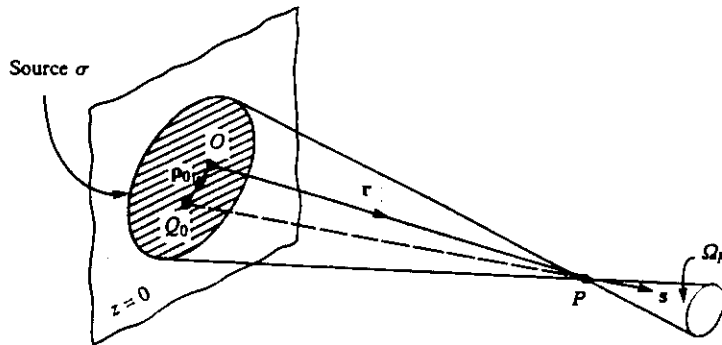
Fig. 5.29 Illustrating the notation relating to the formulas (5.7–108). The point Q_0 in the source plane, whose position vector ρ_0 is given by Eq. (5.7–104), is the point of intersection with the source plane $z = 0$ of the line through the point P in the direction of the real unit vector s.

$$B(\underline{r}, \underline{s}) = k^2 s_z\, S^{(0)}\!\left(\underline{r} - \frac{z}{s_z}\,\underline{s}_\perp\right) \tilde{q}^{(0)}(k\underline{s}_\perp)$$

Geometric result that accounts for the coherence properties of the field !

COHERENCE TRANSPORT

$$W(\underline{r}_1, \underline{r}_2) = \int\limits_{(2\pi)} B\left(\frac{\underline{r}_1 + \underline{r}_2}{2}, \underline{s}\right)$$

$$\cdot e^{ik\underline{s}\cdot(\underline{r}_2 - \underline{r}_1)} d\Omega$$
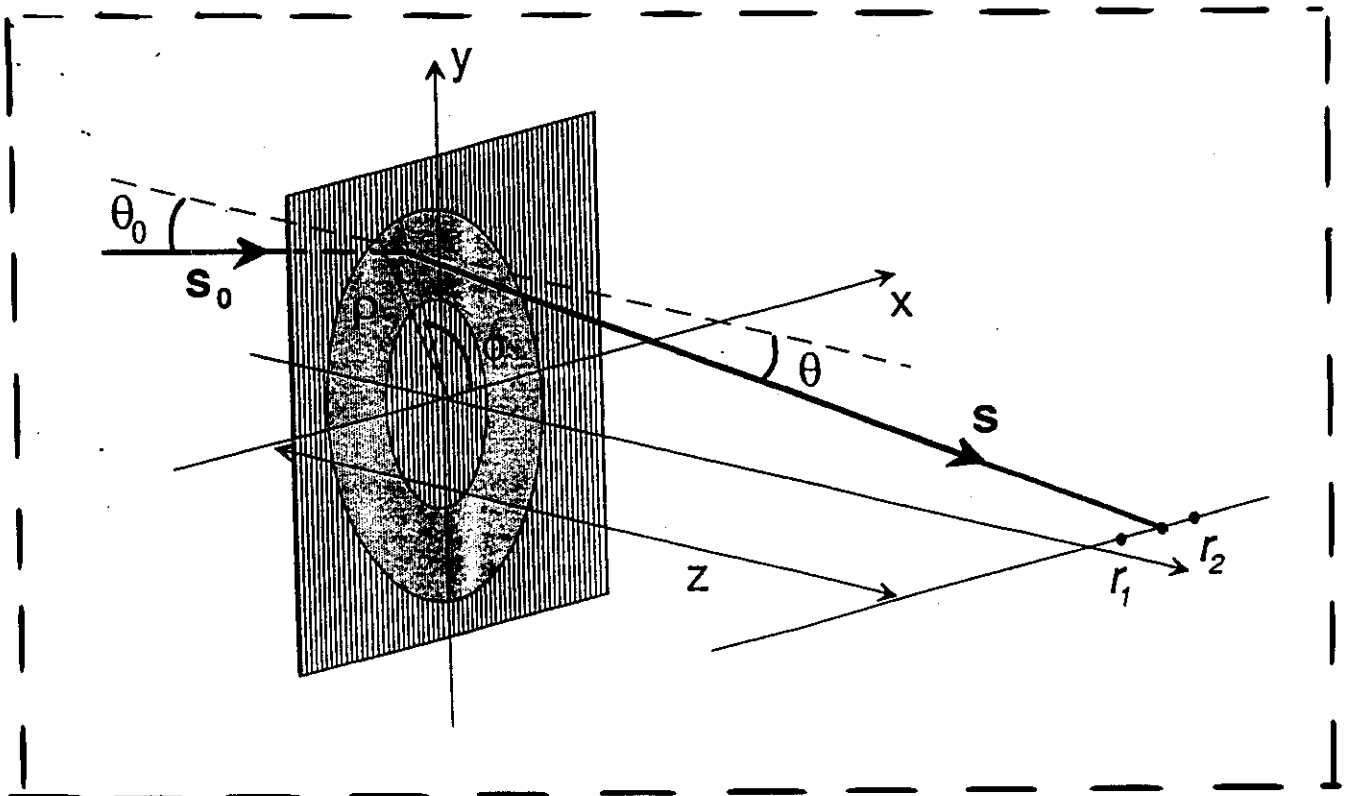
- rectilinear propagation of $B(\underline{r}, \underline{s})$

- diffractive ray-tracing at $z = 0$

$$\underline{s}_\perp = \underline{s}_{0\perp} - \nabla \varphi(\underline{\rho})$$

AXICON LINE IMAGE

● uniform, Gaussian correlated input
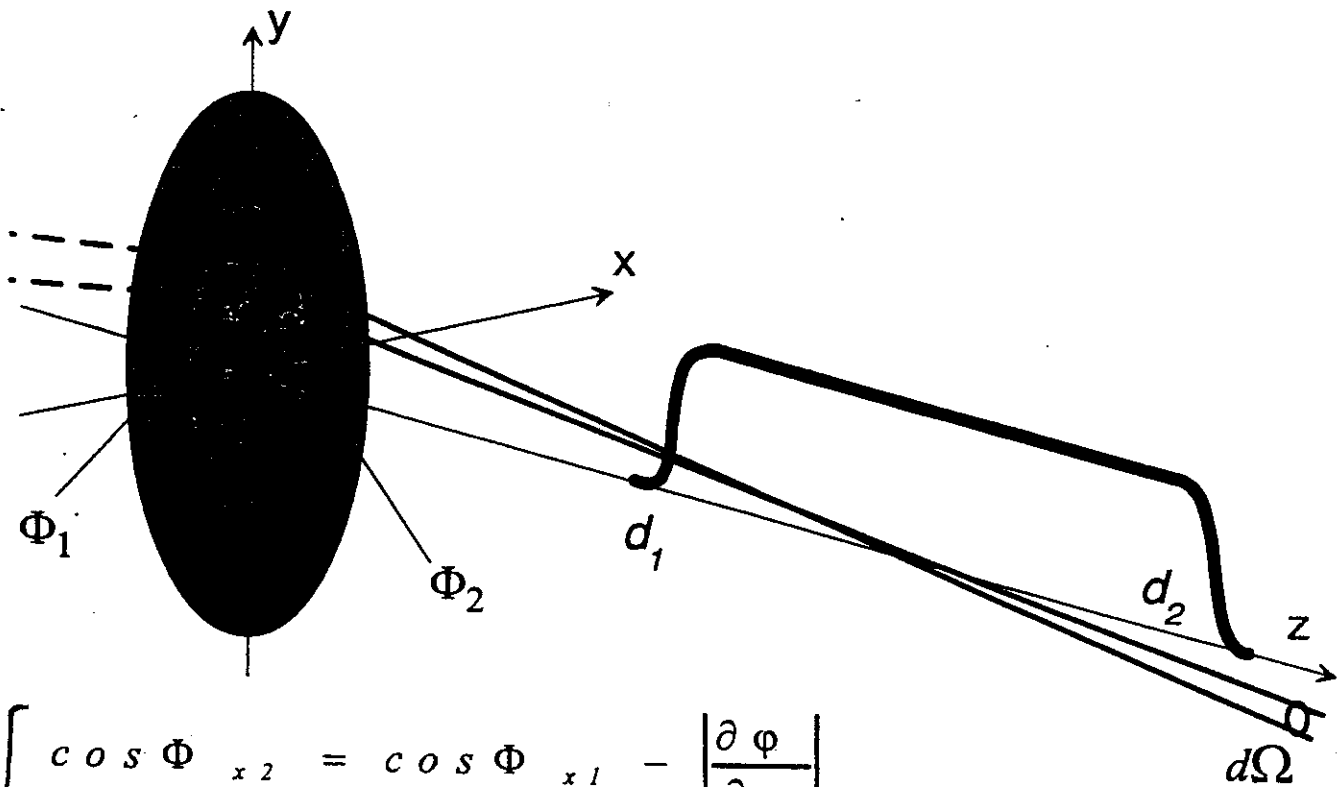
$$\begin{cases} \cos\Phi_{x2} = \cos\Phi_{x1} - \left|\dfrac{\partial\varphi}{\partial x}\right| \\[3mm] \cos\Phi_{y2} = \cos\Phi_{y1} - \left|\dfrac{\partial\varphi}{\partial y}\right| \end{cases}$$

$$I = \int_{\Omega} B(\vec{\rho}, z, \vec{s})\, d\Omega$$

$$B_0(\vec{\rho}, \vec{s}) = k^2 \cos\theta\; I_0(\rho)\left(\frac{\sigma_g^2}{2\pi}\right) e^{-\frac{1}{2}(k\sigma_g)^2 \vec{s}_\perp^2}$$

$$\varphi(\rho) = -\frac{1}{2} ln\left[d_1 + a(\rho^2 - r^2)\right]$$

- asymptotic as $\lambda \to 0$
- rectilinear propagation of B
- includes coherence effects

(30)

WAVE MODEL
AXICON LINE IMAGE

annular radii
$R_1 = 2.5$ mm
$R_2 = 5.0$ mm
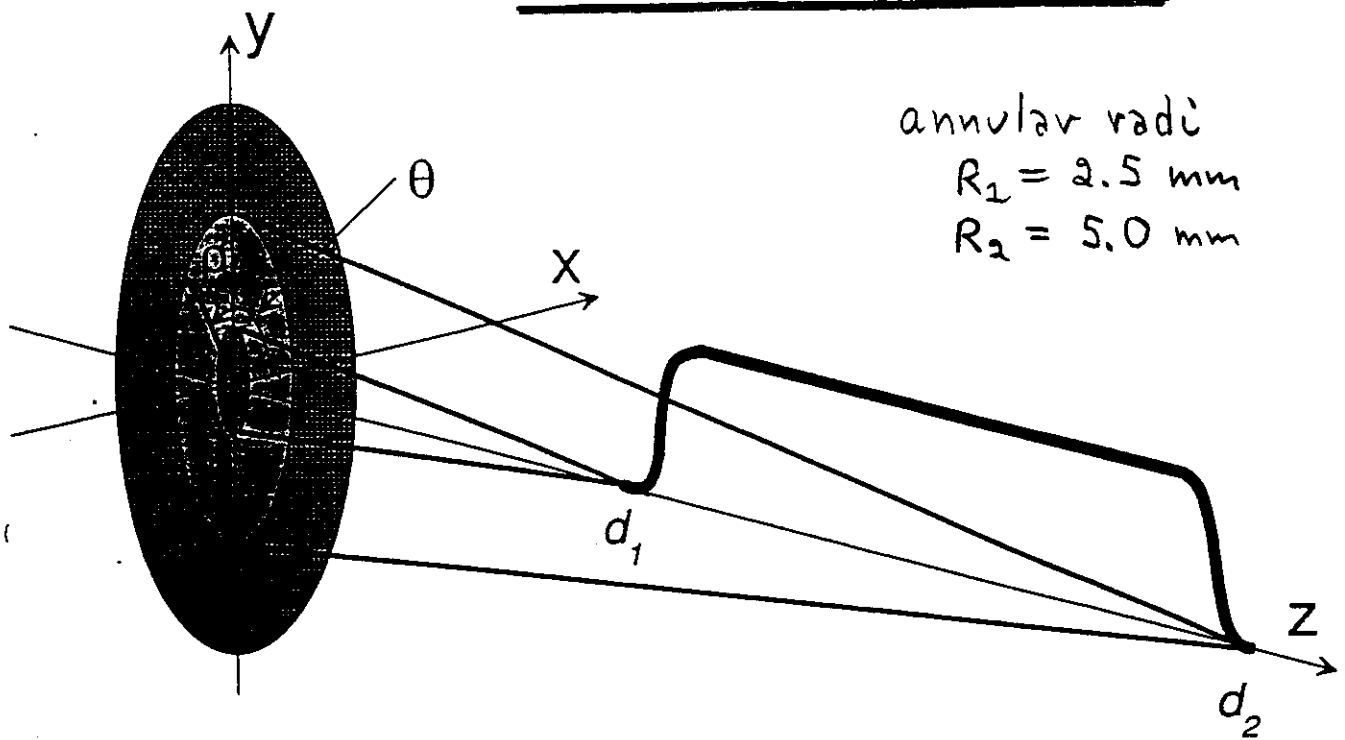
$$U(\vec{\rho}, z) = -\frac{i}{\lambda z} e^{ikz} \iint U_0\, e^{i\frac{k}{2z}(\vec{\rho} - \vec{\rho}')^2}\, d^2\vec{\rho}'$$

$$U_0 = e^{ik\varphi(\rho)} \qquad \varphi(\rho) = -\tfrac{1}{2} ln\left[d_1 + a(\rho^2 - r^2)\right]$$

$\Rightarrow$

$$I(\rho, z) = \left(\frac{k}{2\pi z}\right)^2 \iint \left[I_a(\rho_1) I_a(\rho_2)\right]^{1/2} C(\rho_1, \rho_2; \rho, z; \sigma_g) e^{-\frac{(\rho_1^2 + \rho_2^2)}{2\,\sigma_g^2}}$$

$$\times e^{-ik\frac{(\rho_1^2 - \rho_2^2)}{2z}}\, e^{-ik\left[\varphi(\rho_1) - \varphi(\rho_2)\right]} \rho_1 \rho_2 d\rho_1 d\rho_2$$

where

$$C(\rho_1, \rho_2; \rho, z; \sigma_g) = \iint e^{\frac{(\rho_1 \rho_2 \cos(\theta_1 - \theta_2))}{\sigma_g^2}}\, e^{-ik\rho\frac{(\rho_1 \cos\theta_1 - \rho_2 \cos\theta_2)}{z}}\, d\theta_1 d\theta_2$$

$\left(34\right)$

Optical Intensity

- **annular aperture** $R_1 = 2.5$ mm
  $R_2 = 5.0$ mm

* Longitudinal, transverse, and 3D image profiles by radiometry
* Calculations are <u>fast</u> and <u>accurate</u> even at low coherence levels
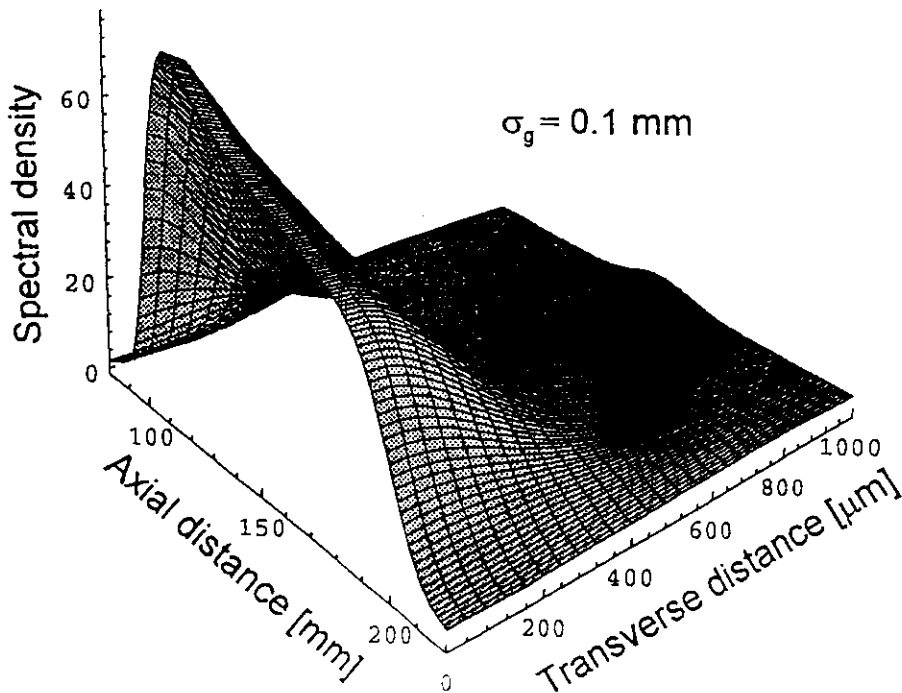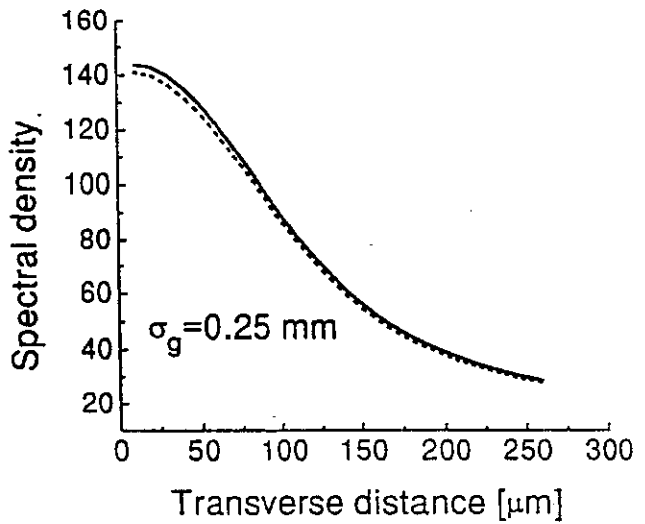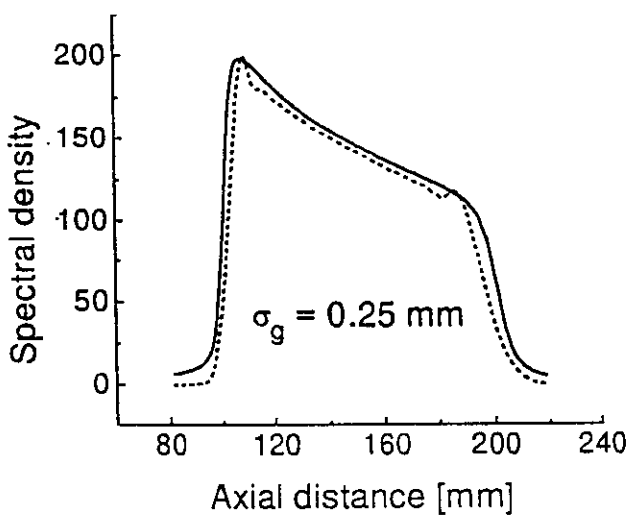
Spatial Coherence
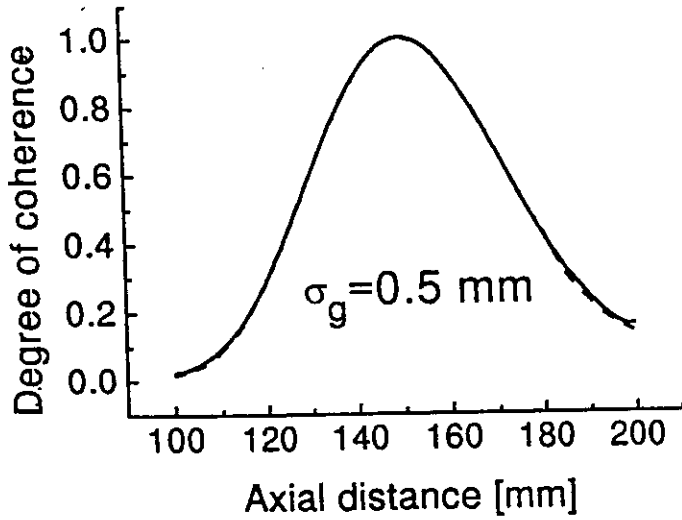
Complex Degree of Spectral Coherence

$$\mu(r_1, r_2) = \frac{W(r_1, r_2)}{[S(r_1)S(r_2)]^{1/2}}$$

$\sigma_g = 0.5$ mm

Axial distance [mm]

Degree of coherence

Transverse Distributions at $z = 150$ mm

$\sigma_g = 0.5$ mm

Transverse distance [μm]
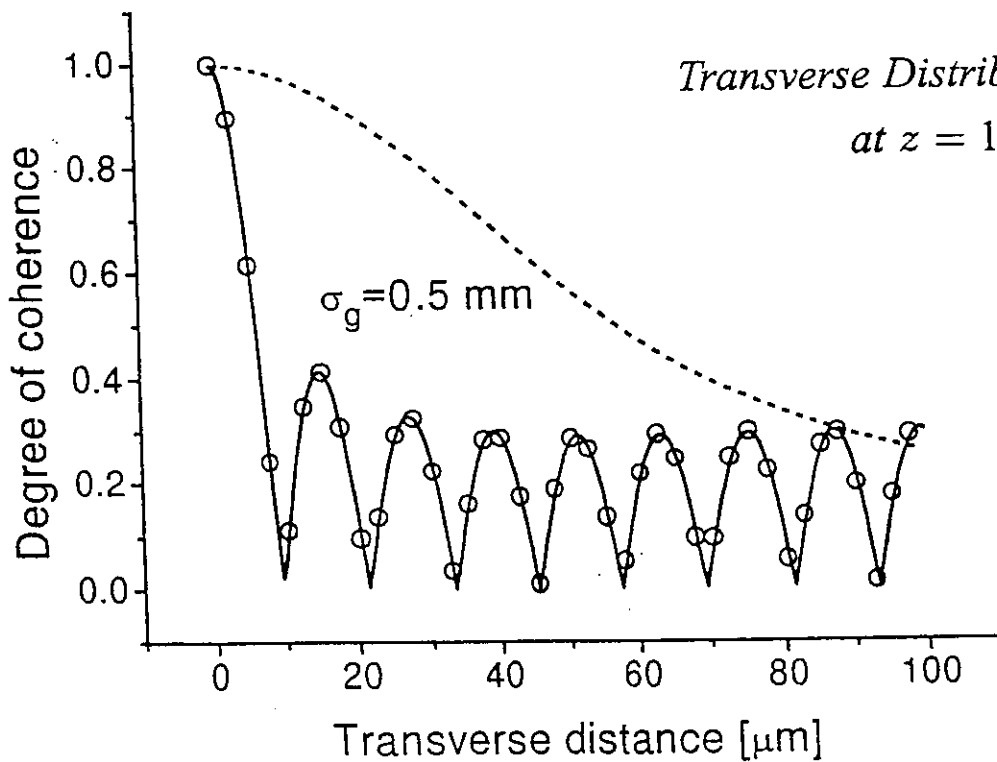
* Radiometric and wave-theoretic results are indistinguishable!

33

Illustration: (a) Lambertian
(b) Gaussian correlation

(a)
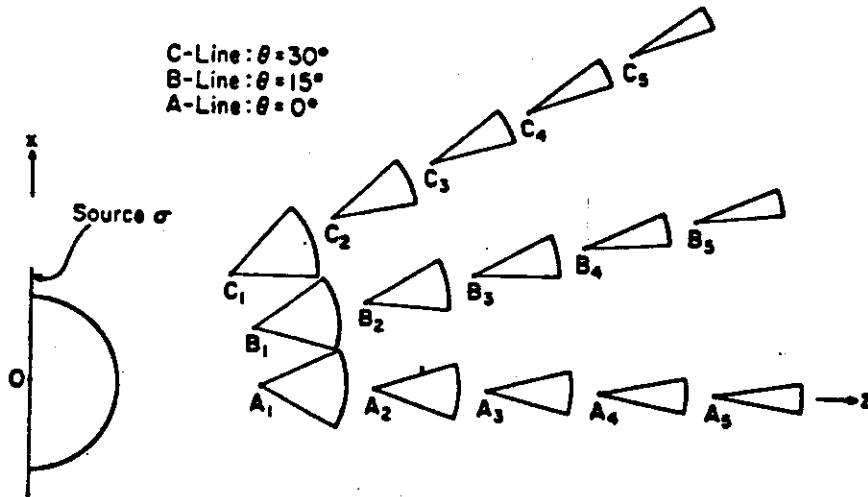
(b)
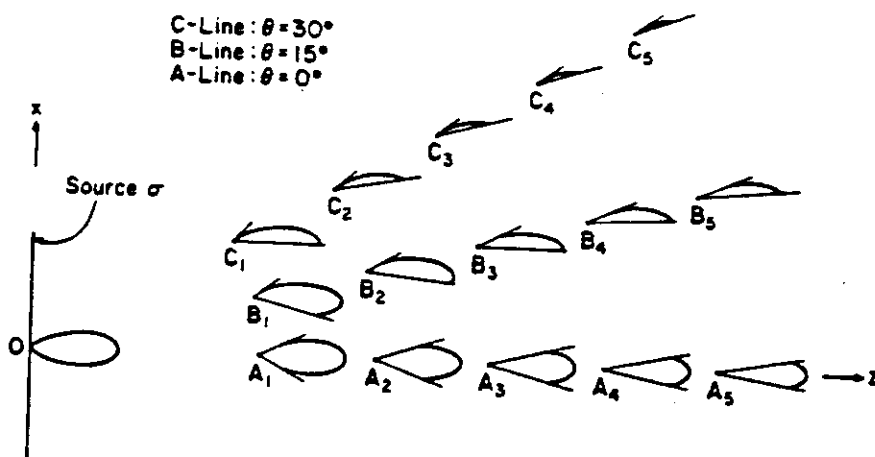
Fig. 2. Polar diagrams, calculated from Eq. (10), of the spectral radiance at different points in the x,y-plane, generated by some planar, secondary, quasi-homogeneous sources. The points with subscripts 1, 2, 3, 4 and 5 are at distances r = 4 cm, 6 cm, 8 cm, 10 cm and 12 cm respectively from the center) at the source. (a) From an uniform, circular, quasi-homogeneous, lambertian source, $\left\{\mu^{(0)}(r') = \left[\sin(kr')/kr'\right]\right\}$, of radius a = 2 cm. (b) From an uniform, circular, quasi-homogeneous, Gaussian-correlated source, $\left\{\mu^{(0)}(r') = \exp\left[(-r'^2/2\sigma_\mu^2)\right]\right\}$, of radius a = 2 cm and with $\sigma_\mu = 0.5\lambda$ [After J. T. Foley and E. Wolf, ref. 7].

34

LITERATURE

Textbooks on Conventional Radiometry:

R.B. Boyd, *Radiometry and the Detection of Optical Radiation*, John Wiley & Sons, New York, 1983.

W.L. Wolfe, *Introduction to Radiometry*, Volume TT 29, SPIE, Bellingham, WA, 1998 (tutorial text).

Reviews of Generalized Radiometry and Radiative Transfer:

E. Wolf, "Coherence and radiometry", J. Opt. Soc. Am. **68**, 7-17 (1978).

A.T. Friberg, "Phase-space methods for partially coherent wavefields", in *Optics in Four Dimensinon - 1980*, eds. M.A. Machado and L.M. Narducci, Conference Proceedings No. 65, American Institute of Physics, New York, 1981, pp. 313-331.

A.T. Friberg, ed., *Selected Papers on Coherence and Radiometry*, Volume MS 69, SPIE, Bellingham, WA, 1993 (summary and a collection of papers).

L. Mandel and E. Wolf, *Optical Coherence and Quantum Optics*, Cambridge University Press, Cambridge, UK, 1995, chapter 5.

Yu.A. Kravtsov and L.A. Apresyan, "Radiative transfer: new aspects of the old theory", in *Progress in Optics*, Vol. XXXVI, ed. E. Wolf, Elsevier, Amsterdam, 1996, pp. 179-244.

Operator Approach (Classical Theory):

G.S. Agarwal, J.T. Foley, and E. Wolf, "The radiance and phase-space representations of the cross-spectral density operator", Opt. Commun. **62**, 67-72 (1987).

Asymptotic Radiometry:

M. Nieto-Vesperinas, "Classical radiometry and radiative transfer theory: a short-wavelength limit of a general mapping of cross-spectral densities in second-order coherence theory", J. Opt. Soc. Am. A **3**, 1354-1359 (1986).

J.T. Foley and E. Wolf, "Radiance functions for partially coherent fields", J. Mod. Opt. **38**, 2053-2058 (1991).

A.T. Friberg, G.S. Agarwal, J.T. Foley, and E. Wolf, "Statistical wave-theoretical derivation of the free-space transport equation of radiometry", J. Opt. Soc. Am. B **9**, 1386-1393 (1992).

Coherence Transport:

E. Wolf, "Radiometric model for propagation of coherence", Opt. Lett. **19**, 2024-2026 (1994).

A.T. Friberg and S.Yu. Popov, "Radiometric description of intensity and coherence in generalized holographic axicon images", Appl. Opt. **35**, 3039-3046 (1996).

Optical
Engineering

EFFECTS OF COHERENCE IN RADIOMETRY

Ari T. Friberg*

University of Rochester
The Institute of Optics
Rochester, New York 14627

Effects of coherence in radiometry

Ari T. Friberg*
University of Rochester
The Institute of Optics
Rochester, New York 14627

Abstract. Radiometry evolved over a long period of time around rather incoherent sources of thermal nature. Only during the last few years have the effects of coherence begun to be taken into account in radiometric considerations of light sources. In this review article the fundamental concepts of conventional radiometry and of the theory of partial coherence will be first briefly recalled. The basic radiometric quantities, namely the radiance, the radiant emittance, and the radiant intensity, associated with a planar source of any state of coherence will then be introduced. It will be pointed out that the radiant intensity, representing the primary measurable quantity, obeys in all circumstances the usual postulates of conventional radiometry, whereas the radiance and the radiant emittance turn out to be much more elusive concepts. The radiometric characteristics of light from incoherent and coherent sources as well as from a certain type of partially coherent source, viz., the so-called quasihomogeneous source, will be analyzed. Quasihomogeneous sources are useful models for radiation sources that are usually found in nature. Lambertian sources will be discussed as examples.

Keywords: partial coherence; radiometry; radiance; diffraction; energy transfer; quasihomogeneity.

Optical Engineering 21(5), 927-936 (September/October 1982).

CONTENTS

1. INTRODUCTION

Radiometry, being one of the oldest branches of optics, has undergone extensive development and refinement over a period of several hundreds of years. The earliest notions of radiometry originated in the studies of Bouguer and Lambert, who in the eighteenth century formulated some empirical laws of optics.[1] Radiometry was subsequently developed in connection with the investigation of energy transfer by heat radiation. Notable contributions are especially the introduction of the concept of blackbody by Kirchhoff and Stewart and the discovery, in 1900, of the spectral

distribution of blackbody radiation by Planck.[2] In its conventional form radiometry appears to have been systematized around this time, the turn of the twentieth century.

Conventional radiometry describes the transfer of radiant energy on a phenomenological basis involving intuitive notions such as tubes of light rays. In that form it has been applied to a wide variety of problems both in physics and in engineering. Yet it does not seem to be generally realized that the fundamental concepts and laws of conventional radiometry have never been derived from the presently accepted basic theories of light. Only relatively recently the accuracy and the range of validity of conventional radiometry have come under closer examination.

It is sometimes asserted that conventional radiometry describes, in some unspecified approximation, light fields generated by incoherent sources and that incoherent sources are Lambertian. Experimental evidence indicates that light sources under thermal equilibrium conditions, such as blackbody sources, radiate in accordance with Lambert's law. This fact would imply that blackbody radiation sources are incoherent, an assertion which is in disagreement with recent researches in coherence theory. Moreover, even the fields emitted by incoherent sources do not remain incoherent but instead, according to the famous van Cittert-Zernike theorem, gain coherence by the mere process of propagation. This results in a great variety of radiation patterns that can be found in nature but cannot be explained on the basis of conventional radiometry with incoherent sources. The above observations serve to illustrate the connection that must exist between the radiometric and the coherence properties of a light source.

The first attempt to incorporate the coherence properties of a light source into its radiometric description was made by Walther[3] in 1968. Considering a planar source of any state of coherence, he constructed a function that possesses several of the properties normally attributed to the radiance in conventional radiometry. This paper has become the cornerstone of virtually all of the subsequent research on the relationship between the radiometric properties of a source and its coherence properties. Other major contributions include an investigation by Marchand and Wolf[4] generalizing the
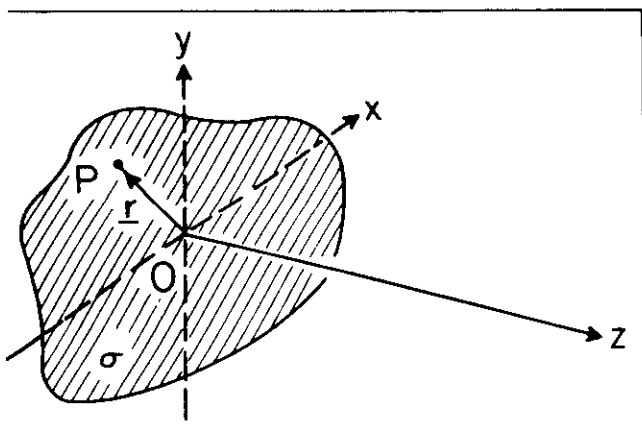
1. A planar source σ occupying a portion of the plane z = 0 radiating into the half space z > 0.

2. Illustration of the notation relating to the traditional defini- of radiance.

ic concepts of conventional radiometry to fields generated by steady-state planar source (including fully coherent sources h as lasers), and a study by Carter and Wolf[5] on the coherence perties of Lambertian as well as non-Lambertian sources. Of at importance also is a recent investigation by Carter and Wolf,[6] which they introduce and study a model that can be used to resent true natural radiation sources.

n the present article we will review some of the more important cts that recent research on radiometry with partially coherent t has revealed. In order to bring out the essence of these nomena, we will make a number of simplifying assumptions. t of all, the quantum nature of light will be entirely ignored. We also neglect all polarization effects and hence take the light d to be represented by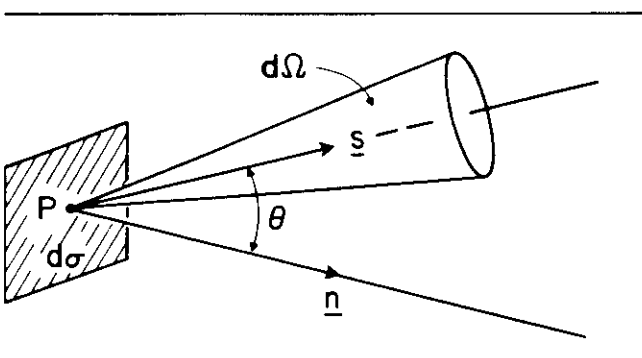 a (fluctuating) complex scalar function. thermore, we will consider only fields generated by two-lensional (planar) radiation sources.

SOME FUNDAMENTAL CONCEPTS

ore discussing in some detail the major effects that the lerence properties of a light source have on its radiometric racteristics, it will be convenient first to recall briefly the basic cepts and laws of conventional radiometry and of classical ory of partial coherence.

. Conventional radiometry

his article we are mainly concerned with the light energy emerg-into the half space z > 0 from a planar source σ located in the ne z = 0 (Fig. 1). The central quantity in the traditional iometric description of such a source is the radiance (also own as the brightness or the specific intensity). It is defined in following way[7]: Let dΦ_ω represent the power, per unit frequen-

cy interval centered at frequency ω, radiated by a source element dσ surrounding a point P into a solid angle dΩ around a direction specified by a unit vector s (Fig. 2). Then, the formula

$$d\Phi_\omega = B_\omega(r,s)\cos\theta d\Omega d\sigma \,, \tag{1}$$

where r denotes the position vector of the source point P and θ is the angle between the s direction and the normal n to the source, defines the radiance $B_\omega(r,s)$ at frequency ω, at the point P(r), in the s direction. The radiance $B_\omega(r,s)$, which is simultaneously a func-tion of both position and direction, thus represents the power (at frequency ω) radiated by the source per unit solid angle and per unit projected source area, the projection being onto a plane perpen-dicular to the s direction.

The fundamental relationship expressed by Eq. (1) can be used to obtain expressions for the other radiometric quantities. The radiant emittance, denoted by $E_\omega(r)$, is defined as the power (at frequency ω) radiated by the source per unit area around the point P(r). In view of Eq. (1), it may be written as

$$E_\omega(r) = \int_{(2\pi)} B_\omega(r,s)\cos\theta d\Omega \,, \tag{2}$$

where the integration extends over the 2π solid angle formed by all the possible s directions. The radiant intensity, denoted by $J_\omega(s)$, is defined, on the other hand, as the power (at frequency ω) radiated by the source per unit solid angle around the s direction. Using Eq. (1), it can be expressed in terms of the radiance as

$$J_\omega(s) = \cos\theta \int_\sigma B_\omega(r,s)d\sigma \,, \tag{3}$$

where the integration extends over the source area σ. If the source is of infinite extent, the integration is to be carried over the entire source plane.

It is obvious from the definitions of the radiant emittance and the radiant intensity that the total power (at frequency ω) radiated by the source σ into the half space z > 0, denoted by Φ_ω, is obtained from either one of the following two formulas:

$$\Phi_\omega = \int_\sigma E_\omega(r)d\sigma = \int_{(2\pi)} J_\omega(s)d\Omega \,. \tag{4}$$

In terms of the radiance $B_\omega(r,s)$, an expression for the total power Φ_ω would, of course, involve a double integration over the source area σ and over the solid angle 2π.

The three basic radiometric quantities defined above, namely, the radiance $B_\omega(r,s)$, the radiant emittance $E_\omega(r)$, and the radiant intensity $J_\omega(s)$, have certain characteristic properties by virtue of their physical significance. In particular, they are always non-negative for all possible values of their arguments. Moreover, $B_\omega(r,s)$ and $E_\omega(r)$ assume a zero value whenever the vector r represents a point located in the source plane outside the source area σ (if the source is of finite extent). To these properties we must add still a further requirement on the radiance $B_\omega(r,s)$ in the half space z > 0. For this purpose we first need to generalize slightly the definition (Eq. (1)) of $B_\omega(r,s)$, where we assumed that the point P(r) is located in the source plane z = 0. We will now allow the vector r to represent a point in any plane z = z_1 with z_1 ≥ 0. Hence, Eq. (1) then defines the radiance $B_\omega(r,s)$ at a point P(r) in the plane z = z_1. The unit vector s specifies a direction towards z > z_1. The dependence of $B_\omega(r,s)$ on z is left implicit for simplicity. It is nor-mally assumed in conventional radiometry that the radiance $B_\omega(r,s)$, with s fixed, remains constant along the line through the point P(r) in the direction of the fixed s vector. With the above generalized notation, this requirement may be expressed as[8]

$$\frac{d}{ds} B_\omega(r,s) = 0 \,. \tag{5}$$

where d/ds denotes the directional derivative with respect to the spatial variables ($\underline{r}$ and implicit z) in the $\underline{s}$ direction. Equation (5) is known as the equation of radiative transfer in free space. It expresses the notion, tantamount to conventional radiometry, that in free space energy is propagated along straight lines.

To conclude this brief review we wish to emphasize four aspects of traditional radiometry which are evident from the above discussion. First, the radiance, the radiant emittance, and the radiant intensity are conventionally defined at a single temporal frequency of the optical field. Second, the three radiometric quantities are regarded as measurable in principle. Third, a simple additive superposition of energy from the various parts of the source is assumed to hold. And fourth, any effects due to diffraction are neglected. As we will see shortly, most of these presumptions of conventional radiometry have to be relaxed when considering partially coherent fields with diffraction and interference taking place.

2.2. Theory of partial coherence

A proper accounting for the diffraction and interference of light requires the introduction of the notion of coherence of the light field. This concept is closely related to the more or less irregular fluctuations that every practical optical field undergoes. In general, the fluctuations are much too rapid to be directly measurable by means of the usual types of detectors. However, it is often the correlations between the fluctuations rather than the fluctuations themselves which are of principal physical importance.

Let us therefore briefly discuss how the correlations of the fluctuations may be mathematically represented in a form suitable for our present purposes. It will be sufficient to consider only correlations up to the second order in the optical field variable. Let V(r,t) be the complex analytic signal[9] that represents the optical field at a point P specified by the vector $\underline{r}$, at a time instant t. For simplicity V(r,t) is taken to be a scalar. We assume also that the field V(r,t) is statistically stationary in time. For such fields the most common quantity in the analysis of coherence effects is the so-called mutual coherence function. It is normally defined in terms of a long time average (Ref. 7, Sec. 10.3.1). In recent years it has become customary, however, to define the mutual coherence function in a more general manner by means of an average over a suitable ensemble of realizations characterizing the statistical properties of the field V(r,t). If the field is not only stationary but also ergodic, then such an ensemble averaging yields the same result as the time averaging. Since most optical fields of practical interest are stationary and ergodic, we will consider only such fields from now on. We may then define the mutual coherence function by the formula

$$\Gamma(\underline{r}_1,\underline{r}_2;\tau) = \langle V(\underline{r}_1,t + \tau)V^*(\underline{r}_2,t) \rangle , \tag{6}$$

where the brackets denote either the time average or the ensemble average and the asterisk denotes the complex conjugate. Despite the appearance of the variable t on the right-hand side of Eq. (6), $\Gamma(\underline{r}_1,\underline{r}_2;\tau)$ is independent of t because of the assumed stationarity. The mutual coherence function $\Gamma(\underline{r}_1,\underline{r}_2;\tau)$ characterizes the second-order field correlations at the points specified by the vectors $\underline{r}_1$ and $\underline{r}_2$, at instants of time separated by τ.

The transfer of radiant energy from partially coherent sources is, however, more naturally described in the space-frequency rather than the space-time domain. This circumstance is a consequence of the fact that the different temporal frequency components of a statistically stationary field are uncorrelated. To obtain a measure of the optical field correlations in the space-frequency domain, we recall first that the cross-spectral density function (also known as the cross-power spectrum), denoted by $W(\underline{r}_1,\underline{r}_2;\omega)$, and the mutual coherence function $\Gamma(\underline{r}_1,\underline{r}_2;\tau)$ are related by the formula

$$W(\underline{r}_1,\underline{r}_2;\omega) = \frac{1}{2\pi} \int_{-\infty}^{\infty} \Gamma(\underline{r}_1,\underline{r}_2;\tau)e^{i\omega\tau}d\tau . \tag{7}$$

The Fourier transform relationship expressed by Eq. (7) is, of course, an optical analog of the well-known Wiener-Khintchine theorem for stationary random processes. The cross-spectral density function $W(\underline{r}_1,\underline{r}_2;\omega)$ characterizes the correlations of the optical field at frequency ω, at the two points $P(\underline{r}_1)$ and $P(\underline{r}_2)$. Further properties of $W(\underline{r}_1,\underline{r}_2;\omega)$ are discussed in a paper by Mandel and Wolf.[10]

In terms of the cross-spectral density function $W(r_1,r_2;\omega)$, one may define the quantity[10]

$$\mu(\underline{r}_1,\underline{r}_2;\omega) = \frac{W(\underline{r}_1,\underline{r}_2;\omega)}{[I(\underline{r}_1,\omega) I(\underline{r}_2,\omega)]^{1/2}} , \tag{8}$$

where

$$I(\underline{r},\omega) = W(\underline{r},\underline{r};\omega) \tag{9}$$

represents the averaged optical intensity at frequency ω, at the point $P(\underline{r})$. It can be shown that $\mu(\underline{r}_1,\underline{r}_2;\omega)$ is normalized so that for all values of $\underline{r}_1$, $\underline{r}_2$, and ω

$$0 \leq |\mu(\underline{r}_1,\underline{r}_2;\omega)| \leq 1 . \tag{10}$$

The quantity $\mu(\underline{r}_1,\underline{r}_2;\omega)$, defined by Eq. (8), is called the complex degree of spatial coherence of the light fluctuations at frequency ω, at the points $P(\underline{r}_1)$ and $P(\underline{r}_2)$. The limiting values 1 and 0 in Eq. (10) indicate that the light fluctuations at frequency ω at the points $P(\underline{r}_1)$ and $P(\underline{r}_2)$ are completely correlated or uncorrelated, respectively. If $|\mu(\underline{r}_1,\underline{r}_2;\omega)| = 1$ for all values of $\underline{r}_1$ and $\underline{r}_2$, then the optical field (at frequency ω) is said to be completely spatially coherent. On the other hand if $|\mu(\underline{r}_1,\underline{r}_2;\omega)| = 0$ for all $\underline{r}_1 \neq \underline{r}_2$, then the optical field (at frequency ω) is said to be completely spatially incoherent. These limiting cases should be regarded only as convenient mathematical idealizations rather than real physical conditions actually observed in nature. No practical optical field can be spatially incoherent in the sense defined above. A more realistic model for spatial incoherence will be introduced later.

3. RADIOMETRY WITH PLANAR SOURCES OF ANY STATE OF COHERENCE

In this section we will first obtain expressions for the basic radiometric quantities [cf. Eqs. (1)–(3)] associated with a planar source of arbitrary state of coherence, located in the plane z = 0. The source can be either a true primary source or a secondary one, such as an optical image for example.[11,12] In either case, there will be some field distribution across the plane z = 0. This distribution, occupying an area σ (which may be infinite), is what in the following will be referred to as the source σ (Fig. 1). It gives rise, by the process of optical wave propagation, to the field distribution in the half space z > 0. The state of coherence of the source is specified in terms of the cross-spectral density function $W^{(0)}(\underline{r}_1,\underline{r}_2;\omega)$, where $\underline{r}_1$ and $\underline{r}_2$ are the position vectors of two typical points in the plane z = 0 (indicated by the superscript 0), and ω denotes the temporal frequency under consideration. The resulting formulas for the radiometric quantities are consequently expressed in terms of the function $W^{(0)}(\underline{r}_1,\underline{r}_2;\omega)$. Some features of these radiometric expressions associated with a partially coherent source will be discussed and contrasted with the corresponding properties postulated in conventional radiometry.

3.1. Expressions for radiometric quantities

In order to determine the radiometric quantities associated with a partially coherent planar source, we need to consider the energy flow in the far zone of the source. This situation is a consequence of the fact that only sufficiently far away from the source can the behavior of the energy flow be unambiguously described. Let us denote by $\underline{F}(r,\omega)$ the energy flow vector associated with the optical field at the point $P(\underline{r})$. Then it can be shown that in the far zone of
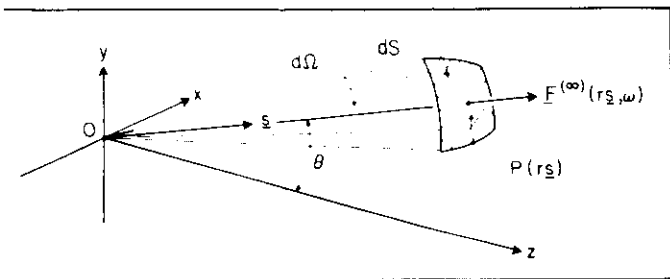
Fig. 3. Energy flow in the far zone of the source.

The source $\underline{F}(\underline{r},\omega)$ always points radially outwards from the source and that it is proportional to the optical intensity.[13] Hence, in a suitable system of units,

$$\underline{F}^{(\infty)}(r\underline{s},\omega) = I^{(\infty)}(r\underline{s},\omega)\underline{s}, \tag{11}$$

where $\underline{s}$ is a three-dimensional unit vector pointing to the point $P(\underline{r})$ (i.e., $\underline{s} = \underline{r}/r$ with $r = |\underline{r}|$), and the superscript ∞ indicates that the quantity has been evaluated in the far zone of the source (i.e., as $kr \to \infty$ with $k = \omega/c$, c being the speed of light in free space) (Fig. 3). The quantity $\underline{s} \cdot \underline{F}^{(\infty)}(r\underline{s},\omega)$ represents the rate per unit area, located in the direction specified by the unit vector $\underline{s}$, at which energy traverses a surface element dS on a large sphere of radius r centered at the origin. If we let $d\Omega$ denote the solid angle that dS subtends at the origin, then, in view of the relation

$$dS = r^2 d\Omega, \tag{12}$$

the radiant intensity $J_\omega(\underline{s})$ and the far-field flux vector $\underline{F}^{(\infty)}(r\underline{s},\omega)$ are clearly related by the formula

$$J_\omega(\underline{s}) = r^2 \underline{s} \cdot \underline{F}^{(\infty)}(r\underline{s},\omega). \tag{13}$$

On substituting from Eq. (11), we obtain

$$J_\omega(\underline{s}) = r^2 I^{(\infty)}(r\underline{s},\omega). \tag{14}$$

The right-hand side of Eq. (14) is to be considered in the limit $kr \to \infty$, and hence it is independent of r.

The next task is to express the far-zone optical intensity $I^{(\infty)}(r\underline{s},\omega)$ in terms of the cross-spectral density function $W^{(0)}(\underline{r}_1,\underline{r}_2,\omega)$ across the source. This can be accomplished by first considering the propagation of the cross-spectral density function into the far zone and then using Eq. (9) to find the optical intensity. The cross-spectral density function is known to obey a pair of Helmholtz equations in free space. Using standard mathematical techniques, such as Green's functions or the angular spectrum method, one can show that[14]

$$I^{(\infty)}(r\underline{s},\omega) = (2\pi k)^2 \cos^2\theta \frac{1}{r^2} \widetilde{W}^{(0)}(k\underline{s}_\perp,-k\underline{s}_\perp;\omega), \tag{15}$$

where $\widetilde{W}^{(0)}(\underline{f}_1,\underline{f}_2;\omega)$ is the four-dimensional spatial Fourier transform of $W^{(0)}(\underline{r}_1,\underline{r}_2;\omega)$, defined by

$$\widetilde{W}^{(0)}(\underline{f}_1,\underline{f}_2;\omega) = \frac{1}{(2\pi)^4} \int_{-\infty}^{\infty}\int_{-\infty}^{\infty} W^{(0)}(\underline{r}_1,\underline{r}_2;\omega)$$

$$\cdot e^{-i(\underline{f}_1 \cdot \underline{r}_1 + \underline{f}_2 \cdot \underline{r}_2)} d^2r_1 d^2r_2. \tag{16}$$

In Eq. (15), θ is the angle between the $\underline{s}$ direction and the normal to the source (i.e., the positive z axis), and $\underline{s}_\perp$ is the two-dimensional

vector obtained by projecting the unit vector $\underline{s}$ onto the source plane $z = 0$.

On substituting from Eq. (15) into Eq. (14), we find the following important expression for the radiant intensity[4,13]:

$$J_\omega(\underline{s}) = (2\pi k)^2 \cos^2\theta \widetilde{W}^{(0)}(k\underline{s}_\perp,-k\underline{s}_\perp;\omega). \tag{17}$$

The formula (17), in its various forms, forms the basis for the discussion of radiation from partially coherent sources. It also represents the starting point in an effort to define the radiance and the radiant emittance associated with a partially coherent planar source. This can be seen more clearly if Eq. (17) is first rewritten, with the help of Eq. (16), in the form

$$J_\omega(\underline{s}) = \left(\frac{k}{2\pi}\right)^2 \cos^2\theta \int_{-\infty}^{\infty}\int_{-\infty}^{\infty} W^{(0)}(\underline{r}_1,\underline{r}_2;\omega)$$

$$\cdot e^{-ik\underline{s}_\perp \cdot (\underline{r}_1-\underline{r}_2)} d^2r_1 d^2r_2. \tag{18}$$

Then, introducing the difference and average coordinates

$$\underline{r}' = \underline{r}_1 - \underline{r}_2; \quad \underline{r} = \frac{1}{2}(\underline{r}_1 + \underline{r}_2) \tag{19}$$

as new integration variables, the expression (18) for the radiant intensity becomes

$$J_\omega(\underline{s}) = \left(\frac{k}{2\pi}\right)^2 \cos^2\theta \int_{-\infty}^{\infty}\int_{-\infty}^{\infty} W^{(0)}(\underline{r} + \frac{1}{2}\underline{r}', \underline{r} - \frac{1}{2}\underline{r}';\omega)$$

$$\cdot e^{-ik\underline{s}_\perp \cdot \underline{r}'} d^2r d^2r'. \tag{20}$$

The integration is to be taken twice independently over the entire source plane, once with respect to $\underline{r}'$ and a second time with respect to $\underline{r}$.

Comparison of Eqs. (3) and (20) suggests that the radiance $B_\omega(\underline{r},\underline{s})$ associated with a partially coherent planar source might be given by[3,4]

$$B_\omega(\underline{r},\underline{s}) = \left(\frac{k}{2\pi}\right)^2 \cos\theta \int_{-\infty}^{\infty} W^{(0)}(\underline{r} + \frac{1}{2}\underline{r}', \underline{r} - \frac{1}{2}\underline{r}';\omega)$$

$$\cdot e^{-ik\underline{s}_\perp \cdot \underline{r}'} d^2r'. \tag{21}$$

This expression for the radiance was first introduced by Walther[3] in 1968. The radiant emittance $E_\omega(\underline{r})$, obtained by substituting from Eq. (21) into Eq. (2), can then be written as[4]

$$E_\omega(\underline{r}) = \int_{-\infty}^{\infty} W^{(0)}(\underline{r} + \frac{1}{2}\underline{r}', \underline{r} - \frac{1}{2}\underline{r}';\omega) K_\omega(\underline{r}') d^2r', \tag{22}$$

where

$$K_\omega(\underline{r}') = \left(\frac{k}{2\pi}\right)^2 \int_{(2\pi)} \cos^2\theta e^{-ik\underline{s}_\perp \cdot \underline{r}'} d\Omega. \tag{23}$$

The integration in Eq. (23) may be carried out to yield[4]

$$K_\omega(\underline{r}') = \frac{k^2}{2\sqrt{2\pi}} \frac{J_{3/2}(kr')}{(kr')^{3/2}}. \tag{24}$$

where $r' = |\underline{r}'|$ and $J_{3/2}(x)$ is the Bessel function of the first kind and order $3/2$. It can be represented in terms of trigonometric functions as

$$J_{3/2}(x) = \sqrt{\frac{2}{\pi x}} \left[\frac{\sin x}{x} - \cos x \right].$$ (25)

We have thus established expressions for the basic radiometric quantities associated with a planar source of any arbitrary state of coherence. The radiance $B_\omega(\underline{r},s)$ is given by Eq. (21), the radiant emittance $E_\omega(\underline{r})$ by Eq. (22), and the radiant intensity $J_\omega(s)$ by Eq. (20). The coherence properties of the source are embodied into the cross-spectral density function $W^{(0)}(\underline{r}_1,\underline{r}_2;\omega)$ entering each of these expressions.

3.2. Properties of radiometric quantities

Equations (20)–(22) appear at first sight as the complete solution to the problem of specifying the basic radiometric quantities associated with partially coherent planar sources. Closer examination reveals, however, that some problems still remain concerning this radiometric description. It has been shown[4] that both the radiance $B_\omega(\underline{r},\underline{s})$ and the radiant emittance $E_\omega(\underline{r})$ occasionally assume negative values and that they do not necessarily always vanish outside the source area σ in the source plane. Moreover, there is no reason to expect that the radiance $B_\omega(\underline{r},\underline{s})$ would, under all circumstances, obey the equation (5) of radiative transfer in the half space $z > 0$ [cf. Ref. 3, Sec. III]. For these reasons the radiance $B_\omega(\underline{r},\underline{s})$ and the radiant emittance $E_\omega(\underline{r})$, given by Eqs. (21) and (22) respectively, cannot strictly speaking be regarded as true measures of energy flow in the traditional sense. The radiant intensity $J_\omega(s)$, given by Eq. (20), on the other hand always correctly represents the power per unit solid angle as in conventional radiometry.

Another problem associated with the radiance $B_\omega(\underline{r},s)$ is that the procedure by which it was derived above does not specify it uniquely. It is easy to find other nonequivalent expressions for the radiance such that, when substituted into Eq. (3) with the integration extending over the whole source plane (rather than just over the source area σ), they would lead to the correct expression (20) for the radiant intensity $J_\omega(s)$. One such expression was actually proposed by Walther[15] in 1973. Its derivation was originally based on a local energy balance argument involving an energy flux vector $\underline{F}(r,\omega)$ associated with the optical field. It was later rederived[16] in an interesting way by means of a set of constraints posed on the radiance $B_\omega(\underline{r},s)$. However, because of the inherent ambiguity of an energy flux vector in the near field of a source, that expression cannot be regarded as any more correct than the expression in Eq. (21). It does not possess all the features of the radiance in conventional radiometry. In particular, it too can occasionally take on negative values.[17]

In view of the fact that there are several possible definitions for the radiance function associated with a partially coherent planar source, one cannot avoid asking the following question: is it possible to find amongst all these definitions one that would satisfy all the requirements normally postulated for the radiance in conventional radiometry? It has been shown by Friberg[18,19] that no such definition, assumed to be linear in the source cross-spectral density function, can be given with sources of all states of coherence. This result has its root in the fact that the radiance $B_\omega(\underline{r},s)$ is simultaneously a function of both r and s, which are essentially Fourier conjugate variables of each other. In analogy with the principles of quantum mechanics, this result also suggests that the radiance no longer can be regarded as a measurable quantity.[18,20] In fact, the basic measurable quantity associated with radiation from partially coherent sources is the distribution of the radiant intensity $J_\omega(s)$.

In spite of the above somewhat disconcerting comments made about the radiance and the radiant emittance associated with a partially coherent source, they can nevertheless be used successfully in

calculating values of truly measurable quantities. As we shall see later, in most practical cases they behave much in the same way as the radiance and the radiant emittance in conventional radiometry and provide a great deal of insight into the manner in which energy is radiated by partially coherent sources.

4. LIMITING CASES OF COHERENCE

As special cases of the general formulas (20)–(22) for the radiometric quantities, let us consider the two limiting cases when the planar source is either completely spatially incoherent or completely spatially coherent. Even though these two limits must be regarded as pure mathematical idealizations, they nonetheless provide useful information about the properties of several types of sources. A more realistic model representing a true natural source will be discussed in the next section.

4.1. Incoherent sources

In an earlier section we already encountered a definition of spatial incoherence in terms of the cross-spectral density function. For most practical purposes it is, however, more convenient to represent the cross-spectral density function of a completely spatially incoherent source in the form [Ref. 9, Sec. 4.4]

$$W^{(0)}(\underline{r}_1,\underline{r}_2;\omega) = i^{(0)}(\underline{r}_1,\omega)\delta(\underline{r}_1-\underline{r}_2),$$ (26)

where $\delta(\underline{r}')$ is the two-dimensional Dirac delta function, and $i^{(0)}(\underline{r},\omega) \geqq 0$ with $i^{(0)}(\underline{r},\omega) = 0$ for points located outside the source area σ. The quantity $\overline{i}^{(0)}(\underline{r},\omega)$ may be loosely identified with the optical intensity distribution across the source.

Because of the delta function appearing in Eq. (26), some of the integrations in the expressions for the radiometric quantities can now be readily carried out. On substituting from Eq. (26) into Eqs. (21), (22), and (20), we find for the radiance, the radiant emittance, and the radiant intensity, respectively,[4]

$$B_\omega(\underline{r},\underline{s}) = \left(\frac{k}{2\pi} \right)^2 \cos\theta \, i^{(0)}(\underline{r},\omega),$$ (27)

$$E_\omega(\underline{r}) = \frac{k^2}{6\pi} i^{(0)}(\underline{r},\omega),$$ (28)

and

$$J_\omega(\underline{s}) = \left(\frac{k}{2\pi} \right)^2 \cos^2\theta \int_\sigma i^{(0)}(r,\omega)d\sigma.$$ (29)

In Eq. (29) we have used the fact that $i^{(0)}(\underline{r},\omega)$ is assumed to vanish outside the source area σ. It is observed from Eqs. (27) and (28) that for a spatially completely incoherent planar source the radiance and the radiant emittance are non-negative quantities and, moreover, that they assume zero values in the source plane outside the source area σ. These results indicate that in the limit of spatial incoherence there is no disagreement with conventional radiometry (except that the equation of radiative transfer may not be rigorously satisfied in the field generated by an incoherent source).

Another interesting feature is seen from Eq. (29). Denoting the radiant intensity in the forward direction (i.e., in the direction with $\theta = 0$) by $J_{\omega,o}$, Eq. (29) may be rewritten as

$$J_\omega(\underline{s}) = J_{\omega,o}\cos^2\theta.$$ (30)

This shows that the radiant intensity from a completely spatially incoherent source decreases, regardless of its optical intensity

distribution, in proportion to $\cos^2\theta$ and not to $\cos\theta$ as is typical of a Lambertian source.[21] In view of this result, a blackbody radiation source, whose radiant intensity distribution is well known to follow a $\cos\theta$ law, must possess some degree of spatial coherence. Recent researches have shown, indeed, that a blackbody source exhibits field correlations over distances of the order of the mean wavelength of the radiation.

4.2. Coherent sources

In the idealized case when the source is completely spatially coherent, its cross-spectral density function may be factored in the form[22]

$$W^{(0)}(\underline{r}_1,\underline{r}_2;\omega) = v^{(0)}(\underline{r}_1,\omega)v^{(0)*}(\underline{r}_2,\omega) . \tag{31}$$

Here $v^{(0)}(\underline{r},\omega)$ may be identified as the optical field distribution across the source. Naturally, $v^{(0)}(\underline{r},\omega)$ vanishes whenever $\underline{r}$ represents a point outside the source area σ.

With the cross-spectral density function of the source being represented by Eq. (31), the radiance, the radiant emittance, and the radiant intensity, given by Eqs. (21), (22), and (20) respectively, may be written as[4]

$$B_\omega(\underline{r},s) = \left(\frac{k}{2\pi}\right)^2 \cos\theta \int_{-\infty}^{\infty} v^{(0)}(\underline{r} + \frac{1}{2}\underline{r}',\omega)$$

$$\cdot v^{(0)*}(\underline{r} - \frac{1}{2}\underline{r}',\omega)e^{-iks_\perp \cdot \underline{r}'} d^2r' , \tag{32}$$

$$E_\omega(\underline{r}) = \frac{k^2}{2\sqrt{2\pi}} \int_{-\infty}^{\infty} v^{(0)}(\underline{r} + \frac{1}{2}\underline{r}',\omega)v^{(0)*}(\underline{r} - \frac{1}{2}\underline{r}',\omega)$$

$$\cdot \frac{J_{3/2}(kr')}{(kr')^{3/2}} d^2r' , \tag{33}$$

and

$$I_\omega(s) = (2\pi k)^2 \cos^2\theta \, |\widetilde{v}^{(0)}(ks_\perp,\omega)|^2 , \tag{34}$$

where $\widetilde{v}^{(0)}(\underline{f},\omega)$ is the two-dimensional spatial Fourier transform of $v^{(0)}(\underline{r},\omega)$, defined by

$$\widetilde{v}^{(0)}(\underline{f}) = \frac{1}{(2\pi)^2} \int_{-\infty}^{\infty} v^{(0)}(\underline{r},\omega)e^{-i\underline{f}\cdot\underline{r}}d^2r . \tag{35}$$

The best way to illustrate the predictions of Eqs. (32)-(34) is to consider a simple example.

Example. Let us consider a cophasal planar source with Gaussian optical intensity distribution

$$I^{(0)}(\underline{r},\omega) = I_0 e^{-r^2/2\sigma_I^2} , \tag{36}$$

where I_0 and σ_I are positive parameters (Fig. 4). The optical field distribution across the source can then be written as

$$v^{(0)}(\underline{r},\omega) = \sqrt{I_0} \, e^{-r^2/4\sigma_I^2} . \tag{37}$$
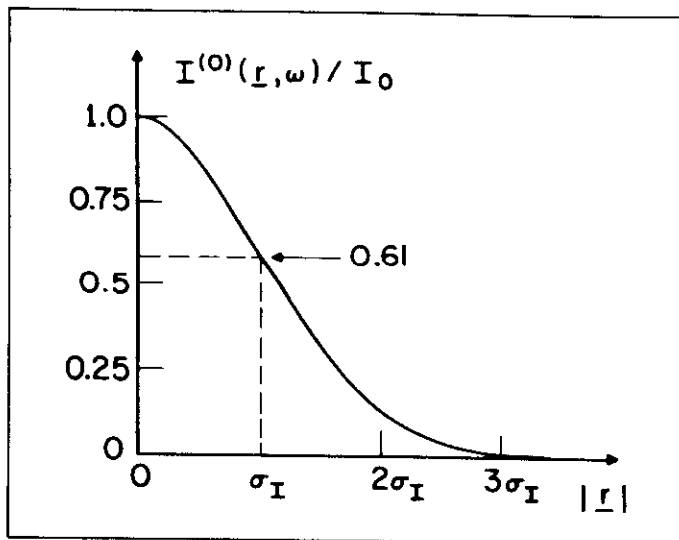
Fig. 4. Gaussian distribution of optical intensity.

Fig. 5. Angular distribution of the normalized radiance associated with a fully coherent and cophasal planar source with Gaussian optical intensity distribution.

The waist of a fully coherent laser beam, for example, is a practical realization of the type of source represented by Eq. (37).

On substituting from Eq. (37) into Eq. (32), we find for the radiance

$$B_\omega(\underline{r},s) = B_{\omega,0}(\underline{r})\cos\theta \, e^{-2(k\sigma_I)^2\sin^2\theta} , \tag{38}$$

where

$$B_{\omega,0}(\underline{r}) = \frac{2}{\pi} (k\sigma_I)^2 I^{(0)}(\underline{r},\omega) . \tag{39}$$

In deriving Eq. (38) we made use of the identity $s_\perp^2 = \sin^2\theta$. The radiance at any given source point is seen to be proportional to the optical intensity at that point. The graphs in Fig. 5, calculated from Eq. (38), illustrate the dependence of the radiance $B_\omega(\underline{r},s)$ on the angle θ for several values of the parameter $k\sigma_I$.

On substituting from Eq. (37) into Eqs. (35) and (34), the radiant intensity is readily found to be

$$I_\omega(s) = I_{\omega,0}\cos^2\theta \, e^{-2(k\sigma_I)^2\sin^2\theta} , \tag{40}$$

where

$$I_{\omega,0} = (2k\sigma_I^2)^2 I_0 . \tag{41}$$
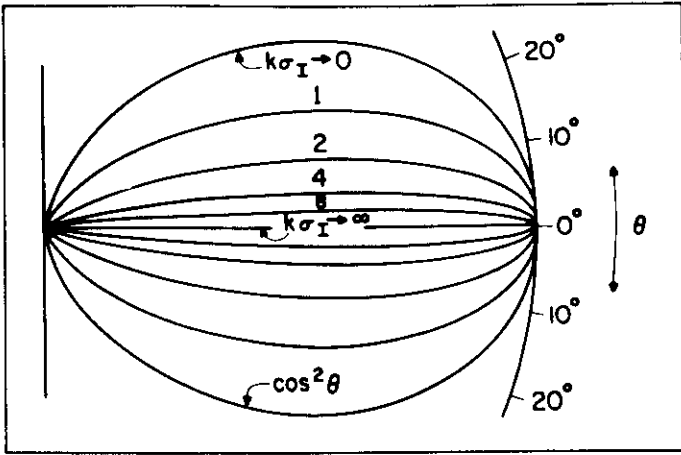
Fig. 6. Polar diagram of the normalized radiant intensity from a fully coherent and cophasal planar source with Gaussian optical intensity distribution.

Figure 6 illustrates, in the form of polar diagrams, the dependence of the radiant intensity $J_\omega(s)$ on the angle θ for several values of $k\sigma_I$. These graphs, computed according to Eq. (40), differ from the graphs in Fig. 5 by a multiplicative factor of $\cos\theta$. With a suitable value for $k\sigma_I$, Eq. (40) represents the radiant intensity generated by a fully coherent laser operating in its lowest transverse mode. For typical lasers $k\sigma_I \gg 1$, and thus the radiant intensity distribution is highly directional, centered in the forward direction. One may then approximate $\cos\theta \approx 1$ and $\sin\theta \approx \theta$. For instance, for a He-Ne laser with $\lambda = 6328\,\text{Å}$ and $\sigma_I = 1$ mm, the parameter $k\sigma_I = 0.99 \cdot 10^4$, and the radiant intensity $J_\omega(s)$ drops to e^{-2} times its value in the forward direction when $\theta = 1.01 \cdot 10^{-4}$ radians.
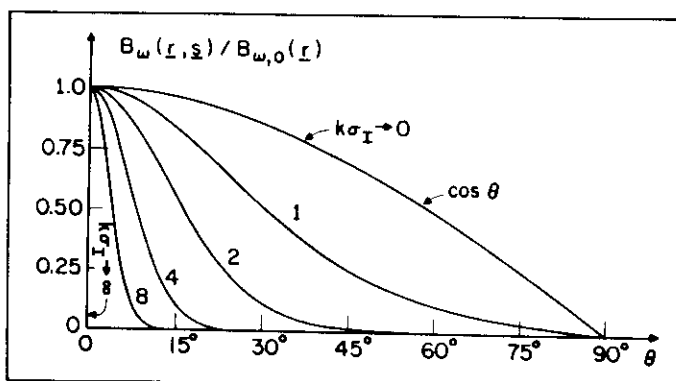
The radiant emittance $E_\omega(r)$ associated with the fully coherent and cophasal planar source with Gaussian intensity distribution can be obtained by substituting Eq. (37) into Eq. (33). After some algebra, the result is found to be

$$E_\omega(r) = \left[1 - \frac{F(a)}{a} \right] I^{(0)}(r,\omega) , \tag{42}$$

where

$$a = \sqrt{2}\,(k\sigma_I) , \tag{43}$$

and

$$F(a) = e^{-a^2} \int_0^a e^{u^2}\,du . \tag{44}$$

The quantity $F(a)$, defined by Eq. (44), is the so-called Dawson integral whose values can be found tabulated in the literature.[23] The radiant emittance is seen to be proportional to the distribution of the optical intensity across the source.

In an effort to describe the radiation characteristics of a source, it will be convenient to let

$$N_\omega = \int_{-\infty}^{\infty} I^{(0)}(r,\omega)\,d^2r \tag{45}$$

denote the integrated optical intensity across the source. Then the ratio

$$C_\omega = \Phi_\omega/N_\omega . \tag{46}$$
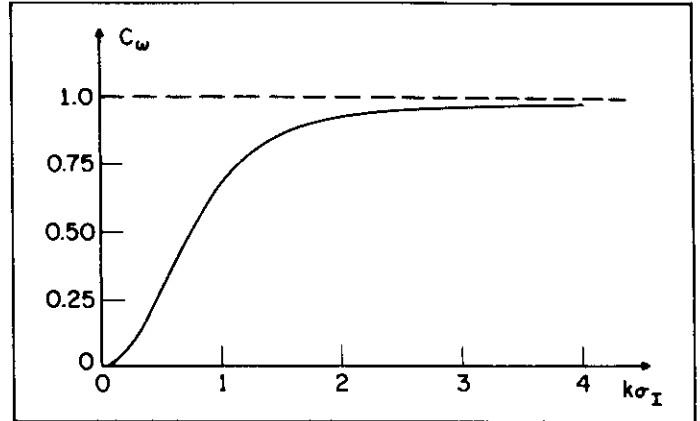
Fig. 7. Radiation efficiency of a fully coherent and cophasal planar source with Gaussian optical intensity distribution.

where Φ_ω is the total radiated power given by Eq. (4), may be called the radiation efficiency of the source at frequency ω. It can be shown that regardless of the state of coherence of the source, the radiation efficiency satisfies the inequality

$$0 \leq C_\omega \leq 1 . \tag{47}$$

The radiation efficiency C_ω may be smaller than unity for two reasons: first, a substantial amount of the radiation may be converted into evanescent waves which do not carry energy into the far zone. And second, the source may be only partially spatially coherent.

The radiation efficiency C_ω of the fully coherent and cophasal planar source with Gaussian optical intensity distribution (Eq. (36)) is seen from Eqs. (46), (45), and (42) to be

$$C_\omega = 1 - \frac{F[\sqrt{2}\,(k\sigma_I)]}{\sqrt{2}\,(k\sigma_I)} , \tag{48}$$

where $F(a)$ is the Dawson integral defined by Eq. (44). Figure 7 illustrates the dependence of C_ω on the parameter $k\sigma_I$. Since the source under consideration is completely spatially coherent, the less than perfect radiation efficiency is entirely due to the evanescent waves. However, for a typical laser source $C_\omega \approx 1$, as is evident from Fig. 7. Later we shall encounter sources where the loss of radiation efficiency is due to the imperfect coherence properties. One such example will be the class of the so-called quasihomogeneous sources discussed in the next section. In fact, in that case the loss due to the evanescent waves is entirely negligible when compared to the loss caused by partial spatial coherence.

Let us finally briefly examine the limiting case as $k\sigma_I \to \infty$. In this limit Eqs. (38), (40), (42), and (48) reduce to

$$\frac{B_\omega(r,s)}{B_{\omega,0}(r)} \to \frac{J_\omega(s)}{J_{\omega,0}} \to \begin{cases} 1, & \theta = 0, \\ 0, & \theta \neq 0, \end{cases} \tag{49}$$

$$E_\omega(r) \to I^{(0)}(r,\omega) , \tag{50}$$

and

$$C_\omega \to 1 . \tag{51}$$

It is apparent that in this limit the source approaches a homogeneous plane wave, giving rise to a perfect unidirectional light beam undergoing no diffraction at all.

Fig. 8. Schematic illustration of the intensity and coherence variations across a quasihomogeneous source.

5. RADIOMETRY WITH QUASIHOMOGENEOUS PLANAR SOURCES

A quasihomogeneous planar source is characterized by a cross-spectral density function of the form[6]

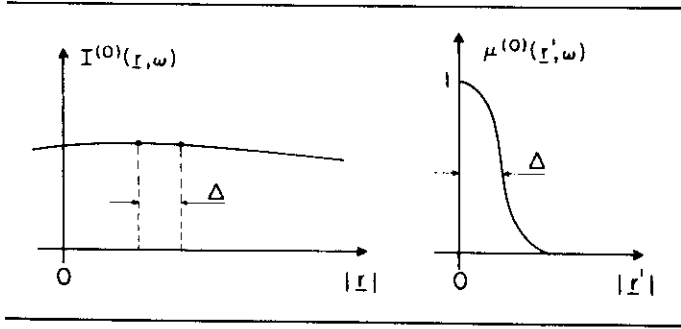$$W^{(0)}(\underline{r}_1,\underline{r}_2;\omega) = I^{(0)}\left[\frac{1}{2}(\underline{r}_1 + \underline{r}_2),\omega\right]\mu^{(0)}(\underline{r}_1 - \underline{r}_2;\omega),\tag{52}$$

where $I^{(0)}(\underline{r},\omega)$ represents the optical intensity distribution across the source, and $\mu^{(0)}(\underline{r}';\omega)$ is the complex degree of spatial coherence [cf. Eq. (8)], assumed to depend only on the difference $\underline{r}' = \underline{r}_1 - \underline{r}_2$. It is assumed that the intensity distribution $I^{(0)}(\underline{r},\omega)$ varies with $\underline{r}$ much more slowly than the complex degree of spatial coherence $\mu^{(0)}(\underline{r}',\omega)$ varies with $\underline{r}'$ (Fig. 8). Furthermore, it is assumed that the linear dimensions of the source are large compared with the wavelength of the light and that $|\mu^{(0)}(\underline{r}',\omega)|$ is substantially different from zero only within an $\underline{r}'$ domain that is small compared to the size of the source. The quasihomogeneous model, unlike the strictly homogeneous one, can be used to represent radiation sources of finite size frequently encountered in practice.

The radiometric quantities associated with a quasihomogeneous planar source can be readily found by substituting from Eq. (52) into the general expressions (20)–(22). The results are[6]

$$B_\omega(\underline{r},\underline{s}) = \left(\frac{k}{2\pi}\right)^2 \cos\theta I^{(0)}(\underline{r},\omega)\int_{-\infty}^{\infty}\mu^{(0)}(\underline{r}',\omega)\,e^{-ik\underline{s}_\perp\cdot\underline{r}'}\,d^2r',\tag{53}$$

$$\Xi_\omega(\underline{r}) = I^{(0)}(\underline{r},\omega)\int_{-\infty}^{\infty}\mu^{(0)}(\underline{r}',\omega)K_\omega(\underline{r}')d^2r',\tag{54}$$

and

$$J_\omega(\underline{s}) = k^2\cos^2\theta\tilde{I}^{(0)}(0,\omega)\int_{-\infty}^{\infty}\mu^{(0)}(\underline{r}',\omega)\,e^{-ik\underline{s}_\perp\cdot\underline{r}'}\,d^2r',\tag{55}$$

where $K_\omega(\underline{r}')$ is given by Eq. (24), and $\tilde{I}^{(0)}(0,\omega)$ is the value, at the origin $\underline{f} = 0$, of the two-dimensional spatial Fourier transform of the source intensity distribution, defined by

$$\tilde{I}^{(0)}(\underline{f},\omega) = \frac{1}{(2\pi)^2}\int_{-\infty}^{\infty}I^{(0)}(\underline{r},\omega)e^{-i\underline{f}\cdot\underline{r}}\,d^2r.\tag{56}$$

It is seen from Eq. (53) that the radiance $B_\omega(\underline{r},\underline{s})$ is proportional to the optical intensity $I^{(0)}(\underline{r},\omega)$ and to the two-dimensional spatial Fourier transform of the complex degree of spatial coherence $\mu^{(0)}(\underline{r},\omega)$ of the light across the source. Because $\mu^{(0)}(\underline{r},\omega)$ is a nonnegative definite quantity,[10] its Fourier transform is always nonnegative by the classic theorem of Bochner.[24] Hence, the radiance

$B_\omega(\underline{r},\underline{s})$ associated with a quasihomogeneous planar source is a nonnegative quantity that vanishes outside the source area. Moreover, it can be shown[25] that the radiance $B_\omega(\underline{r},\underline{s})$, given by Eq. (53), remains essentially constant along any given $\underline{s}$ direction over a distance ℓ that satisfies the condition

$$\ell \ll \left(\frac{2\cos^4\theta}{\sin\theta}\right)\left(\frac{k}{|f|_{max}}\right)^3\lambda.\tag{57}$$

Here θ is the angle that the $\underline{s}$ direction makes with the positive z axis, $k = 2\pi/\lambda$, and $|f|_{max}$ is, roughly speaking, the magnitude of the largest spatial frequencies of the source intensity distribution [cf. Eq. (56)]. Since the optical intensity across a quasihomogeneous source varies very little over distances of the order of wavelength, the ratio $k/|f|_{max}$ is large compared to unity. Consequently, the radiance associated with a quasihomogeneous source satisfies the equation (5) of radiative transfer to a good approximation. In the limits as the source approaches a strictly homogeneous source or the angle $\theta \rightarrow 0$, the upper bound for ℓ set by Eq. (57) approaches infinity, indicating that in these cases the equation of radiative transfer is rigorously obeyed.[25]

Comparing the expression (54) for the radiant emittance $E_\omega(\underline{r})$ to the definition (46) of the radiation efficiency C_ω, one sees that[6,26]

$$E_\omega(\underline{r}) = C_\omega I^{(0)}(\underline{r},\omega),\tag{58}$$

where

$$C_\omega = \int_{-\infty}^{\infty}\mu^{(0)}(\underline{r}',\omega)K_\omega(\underline{r}')d^2r'.\tag{59}$$

Hence, the radiant emittance $E_\omega(\underline{r})$ associated with a quasihomogeneous planar source is proportional to the source intensity distribution, with the proportionality factor being determined by the complex degree of spatial coherence $\mu^{(0)}(\underline{r}',\omega)$. In view of Eq. (47), the radiant emittance $E_\omega(\underline{r})$ never exceeds the value of the optical intensity $I^{(0)}(\underline{r},\omega)$.

An interesting result[6] is readily seen from Eq. (55): the angular distribution of the radiant intensity $J_\omega(\underline{s})$ is proportional to the two-dimensional spatial Fourier transform of the complex degree of spatial coherence of the light across the source and to the square of the cosine of the angle that the $\underline{s}$ direction makes with the positive z axis. Thus, the coherence properties of a quasihomogeneous source completely determine the angular distribution of the radiant intensity generated by the source. This important result is one part of a remarkable reciprocity theorem,[6] the other part of which asserts that the complex degree of spatial coherence of the light in the far zone of a quasihomogeneous source is, apart from a simple geometrical factor, equal to the normalized spatial Fourier transform of the optical intensity across the source. This second part of the theorem can be regarded as a generalization of the famous van Cittert-Zernike theorem to quasihomogeneous planar sources.

5.1. Examples of quasihomogeneous planar sources

We will illustrate the general expressions (53)–(55) of the radiometric quantities pertaining to quasihomogeneous planar sources by several examples.

5.1.1. Gaussian correlated source

Let us assume that the complex degree of spatial coherence of the light in the source plane is given by

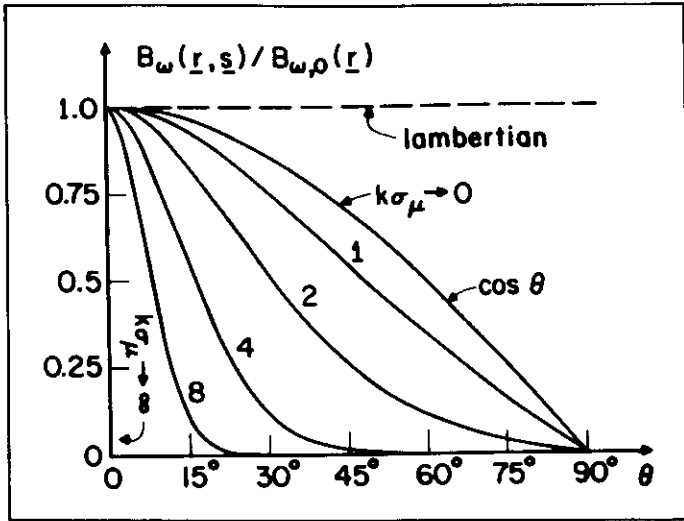$$\mu^{(0)}(\underline{r}',\omega) = e^{-r'^2/2\sigma_\mu^2},\tag{60}$$

Fig. 9. Angular distribution of the normalized radiance from a Gaussian correlated quasihomogeneous planar source.

Fig. 10. Polar diagram of the normalized radiant intensity from a Gaussian correlated quasihomogeneous planar source [after Carter and Wolf[6]].

where σ_μ is a positive parameter. The exact form of the optical intensity distribution $I^{(0)}(r,\omega)$ across the source is of no consequence as long as it meets the requirements stated at the beginning of this section. On substituting from Eq. (60) into Eq. (53), we find for the radiance

$$B_\omega(r,s) = B_{\omega,0}(r)\cos\theta e^{-\frac{1}{2}(k\sigma_\mu)^2\sin^2\theta} , \qquad (61)$$

where

$$B_{\omega,0}(r) = \frac{(k\sigma_\mu)^2}{2\pi} I^{(0)}(r,\omega) . \qquad (62)$$

The graphs in Fig. 9, computed from Eq. (61), illustrate the dependence of $B_\omega(r,s)$ on the angle θ for several values of the parameter $k\sigma_\mu$. It is observed that the larger the effective coherence area of the source is, the more directional the radiance $B_\omega(r,s)$ becomes. The broken line corresponds to a Lambertian source. Substitution from Eq. (60) into Eq. (55) yields for the radiant intensity[6,27]

$$J_\omega(s) = J_{\omega,0}\cos^2\theta e^{-\frac{1}{2}(k\sigma_\mu)^2\sin^2\theta} , \qquad (63)$$

where

$$J_{\omega,0} = 2\pi(k\sigma_\mu)^2 \tilde{I}^{(0)}(0,\omega) . \qquad (64)$$

Here, $\tilde{I}^{(0)}(0,\omega)$ is given by Eq. (56) with $f = 0$. Figure 10 illustrates, in the form of polar diagrams calculated according to Eq. (63), the distribution of the radiant intensity $J_\omega(s)$ as a function of the angle θ for several values of $k\sigma_\mu$. It is evident from these graphs that there is a profound modification in the directionality of the radiant intensity when the correlation distance σ_μ is increased from zero to a value of about a wavelength.[27] The broken line corresponding to the radiant intensity from a Lambertian source is included for comparison.

The radiation efficiency of a Gaussian correlated quasihomogeneous planar source is found by substituting from Eq. (60) into Eq. (59). The result is[6]

$$C_\omega = 1 - \frac{F[k\sigma_\mu/\sqrt{2}]}{k\sigma_\mu/\sqrt{2}} , \qquad (65)$$
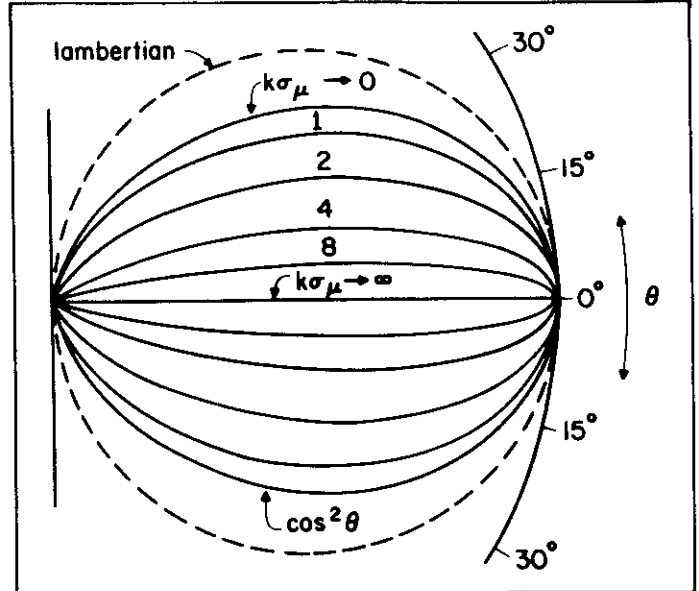
where F(a) is the Dawson integral defined by Eq. (44). The radiation efficiency C_ω, calculated from Eq. (65), is presented in Fig. 11 as a function of $k\sigma_\mu$. It is seen to increase monotonically from a value zero, when $k\sigma_\mu = 0$ (incoherent source), to its maximum value unity, when $k\sigma_\mu = \infty$ (coherent source). Hence, the loss in radiation efficiency is due to imperfect spatial coherence properties of the light across the source.

5.1.2. Blackbody source

Consider an opening of area A made into one of the walls of a cavity inside which optical radiation is at thermal equilibrium. We assume that the linear dimensions of the opening are large compared to the mean wavelength of the radiation field. The opening can be regarded as a planar source within which the optical intensity (at frequency ω) is a constant, denoted by $I_{\omega,0}$, and the complex degree of spatial coherence is[5]

$$\mu^{(0)}(r',\omega) = \frac{\sin kr'}{kr'} , \qquad (66)$$

where $r' = |r'|$. For such a source, which is a special case of the so-called Bessel correlated sources,[28] Eqs. (53) and (55) yield for the radiance and the radiant intensity

$$B_\omega(r,s) = \frac{1}{2\pi} I_{\omega,0} , \qquad (67)$$

and

$$J_\omega(s) = \frac{A}{2\pi} I_{\omega,0}\cos\theta , \qquad (68)$$

respectively. The radiation efficiency is found[26] to be $C_\omega = 1/2$. Equations (67) and (68) show that the radiance is a constant within the source area and that the radiant intensity follows a $\cos\theta$ law. Both these features are characteristic of a Lambertian source. This result then indicates that a Lambertian source is not completely spatially incoherent but exhibits, according to Eq. (66), field correlations over distances of the order of the wavelength of the light.

6. SUMMARY AND DISCUSSION

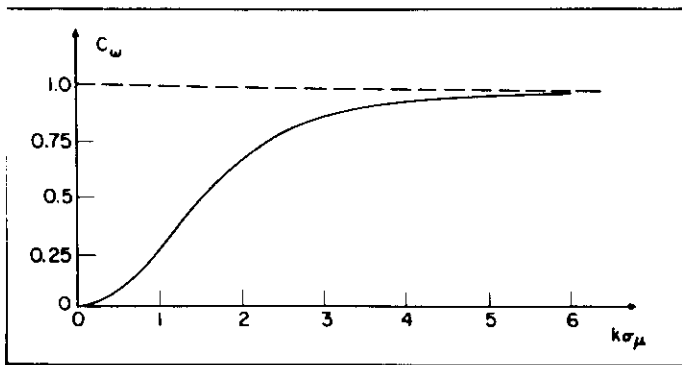In this article we have reviewed some of the more important

Fig. 11. Radiation efficiency of a Gaussian correlated quasihomogeneous planar source [after Carter and Wolf[6]].

features of radiation emanating from planar sources of any prescribed state of coherence. It is evident from the discussion that the coherence properties of a source play an essential role in determining its radiation characteristics. When comparing radiometry of partially coherent light with conventional radiometry, it is observed that in both cases energy transfer is naturally treated frequency by frequency. However, many other aspects of conventional radiometry cannot directly be taken over into the generalized radiometry. In particular, the radiance and the radiant emittance can no longer be considered as measurable quantities with their intuitive physical interpretations postulated in conventional radiometry. The primary measurable quantity associated with radiation from partially coherent sources is the angular distribution of the radiant intensity.

We have discussed the radiometric description of planar sources of any state of coherence and analyzed in some detail the limiting cases of spatially completely incoherent and spatially completely coherent sources. We have also presented, with illustrative examples, the radiometric characteristics of a source model, the so-called quasihomogeneous model, that can be used in many instances to represent true natural sources. Still more refined source models, which we have not been able to touch upon in this article, have been proposed in the literature. One example is the so-called Schell model source,[29-31] which represents a broader class of radiation sources than does the quasihomogeneous model. When the area occupied by the source is sufficiently large and the intensity variation across the source sufficiently slow, the predictions based on the Schell model are essentially the same as those obtained from the quasihomogeneous model. Further details and relevant references can be found in some recent related review articles.[20,32,33]

All throughout this article we have been concerned with the determination of the radiometric characteristics of a source assuming that its coherence properties are known. The inverse problem, i.e., determining the distributions of the optical intensity and the complex degree of spatial coherence across the source from the measured radiation data and especially from the angular distribution of the radiant intensity, has recently acquired increased atten-

tion.[5,33-35] The solution of the inverse problem is important both from a practical point of view and from a mathematical point of view, but it does not fall into the category of topics to be covered under the present title. In Ref. 36 some aspects of the uniqueness of the relationship between the cross-spectral density function across a planar source and the angular distribution of the radiant intensity will be considered.

7. ACKNOWLEDGMENTS

8. REFERENCES

1. Geist, J., Opt. Eng. 15(6), 537 (1976).
2. Planck, M., *The Theory of Heat Radiation*, Dover, New York (1959).
3. Walther, A., J. Opt. Soc. Am. 58, 1256 (1968).
4. Marchand, E. W. and Wolf, E., J. Opt. Soc. Am. 64, 1219 (1974).
5. Carter, W. H. and Wolf, E., J. Opt. Soc. Am. 65, 1067 (1975).
6. Carter, W. H. and Wolf, E., J. Opt. Soc. Am. 67, 785 (1977).
7. Born, M. and Wolf, E., *Principles of Optics*, fifth edition, Sec. 4.8.1., Pergamon, Oxford and New York (1975).
8. Chandrasekhar, S., *Radiative Transfer*, Chap. 1, Eq. (47), Dover, New York (1960).
9. Beran, M. J. and Parrent, G. B., Jr., *Theory of Partial Coherence*, Sec. 2.1., Society of Photo-Optical Instrumentation Engineers, Bellingham, WA (1974).
10. Mandel, L. and Wolf, E., J. Opt. Soc. Am. 66, 529 (1976).
11. Wolf, E. and Carter, W. H., J. Opt. Soc. Am. 68, 953 (1978).
12. Carter, W. H. and Wolf, E., Opt. Commun. 25, 288 (1978).
13. Wolf, E., J. Opt. Soc. Am. 68, 1597 (1978).
14. Marchand, E. W. and Wolf, E., J. Opt. Soc. Am. 62, 379 (1972).
15. Walther, A., J. Opt. Soc. Am. 63, 1622 (1973).
16. Walther, A., Opt. Lett. 3, 127 (1978).
17. Marchand, E. W. and Wolf, E., J. Opt. Soc. Am. 64, 1273 (1974).
18. Friberg, A. T., in *Coherence and Quantum Optics IV*, ed. Mandel, L. and Wolf, E., Plenum, New York (1978).
19. Friberg, A. T., J. Opt. Soc. Am. 69, 192 (1979).
20. Wolf, E., J. Opt. Soc. Am. 68, 6 (1978).
21. Marchand, E. W. and Wolf, E., Opt. Commun. 6, 305 (1972).
22. Perina, J., *Coherence of Light*, Sec. 4.2., Van Nostrand, London (1971).
23. Abramowitz, M. and Stegun, I.A., *Handbook of Mathematical Functions*, p. 319, Dover, New York (1965).
24. Goldberg, R. R., *Fourier Transforms*, Chap. 5, Cambridge University Press, Cambridge, England (1965).
25. Friberg, A. T., Opt. Acta 28, 261 (1981).
26. Wolf, E. and Carter, W. H., in *Coherence and Quantum Optics IV*, ed. Mandel, L. and Wolf, E., Plenum, New York (1978).
27. Wolf, E. and Carter, W. H., Opt. Commun. 13, 205 (1975).
28. Baltes, H. P., Steinle, B., and Antes, G., Opt. Commun. 18, 242 (1976).
29. Schell, A. C., "The Multiple Plate Antenna," Doctoral Dissertation, Sec. 7.5., Massachusetts Institute of Technology (1971).
30. Baltes, H. P., Steinle, B. and Antes, G., in *Coherence and Quantum Optics IV*, ed. Mandel, L. and Wolf, E., Plenum, New York (1978).
31. Baltes, H. P. and Steinle, B., Nuovo Cimento B 41, 428 (1977).
32. Baltes, H. P., Appl. Phys. 12, 221 (1977).
33. Baltes, H. P., Geist, J., and Walther, A., in *Inverse Source Problems in Optics*, ed. Baltes, H. P., Springer, New York and Berlin (1978).
34. Baltes, H. P. and Steinle, B., Lett. Nuovo Cimento 18, 313 (1977).
35. McGuire, D., Opt. Commun. 29, 17 (1979).
36. Friberg, A. T., Proc. SPIE 194, 71 (1979). A revised version of this paper appears in Opt. Eng. 21(2), 362 (1982).

Optical Engineering

RADIATION FROM PARTIALLY COHERENT SOURCES

Ari T. Friberg*

Pellila
SF-31600
Jakioinen, Finland

*Present address: Department of Physics and Astronomy,
University of Rochester, Rochester, New York 14627

Radiation from partially coherent sources

Ari T. Friberg*
Pellila
SF-31600
Jakioinen, Finland

Abstract. Although the theory of partial coherence was formulated in a reasonably general form about a quarter of a century ago, it was not until a few years ago that this theory began to be applied to problems of radiation from partially coherent sources. In this review article, the properties of the radiant intensity generated by a planar source of any state of coherence will be discussed. It will be first recalled that the radiant intensity can be expressed as a two-dimensional spatial Fourier transform of a correlation function of the field in the source plane, averaged over the source area. The characteristics of the radiation from several model sources will then be analyzed. With the help of these results, certain equivalence theorems relating to the radiant intensity from planar sources of entirely different degrees of spatial coherence will be reviewed and the underlying physical principles will be elucidated. A number of illustrative examples will also be given. Finally some very recent work, which has led to the construction of planar sources with controllable degrees of spatial coherence, will be described. Experiments carried out with these sources will be discussed; they verify the main relationships between the coherence properties of the source and the directionality of the light it generates.

CONTENTS

1. INTRODUCTION

In an earlier article,[1] we have reviewed some of the more important effects that have been discovered during the last ten years or so in connection with the studies of radiometry with partially coherent light. In that article we presented expressions for the basic radiometric quantities associated with a planar source of arbitrary state of coherence and discussed, with illustrative examples, the limiting cases of completely coherent and incoherent sources as well as some partially coherent model sources that have been proposed in the literature. We noted that the angular distribution of the radiant intensity is the primary measurable quantity pertaining to radiation from par-

tially coherent sources. In the present article, we will pursue further the considerations of the radiation characteristics of steady-state planar sources; in particular, we will analyze more deeply the properties of the radiant intensity generated by a planar source of any state coherence. Some very recent experiments aimed at testing the theoretical predictions will also be briefly discussed.

To get some insight as to the type of phenomena we will be talking about in this paper, let us consider a simple example.[2] Suppose one compares the radiation generated, on one hand, by a thermal light source and, on the other hand, by a typical gas laser (Fig. 1). The angular distribution of the radiant intensity from a thermal source is well known to follow Lambert's law, whereas the distribution of the radiant intensity from a typical laser is quite different, being sharply peaked in the forward direction. Now, a thermal source is spatially almost completely incoherent, and a laser is, of course, spatially highly coherent. Hence, this example seems to indicate that there is a close relationship between the state of coherence of the source and the directionality of the light it generates. This, indeed, is the case, as recent researches on radiation from partially coherent sources have shown.

Illustrative as the above example may be, it does not fully clarify the matter. One might be tempted to conclude from it that complete spatial coherence is a sufficient condition for the generation of highly directional light beams. This is obviously incorrect, as can be easily seen by considering the diffraction of an expanded laser beam from a circular opening.[3] If the radius of the opening is of the order of the wavelength, the resulting radiant intensity distribution—the classic Airy pattern—shows a substantial divergency angle. More surprising, however, is the fact that not only is complete spatial coherence not a sufficient condition, but it is not even a necessary condition for the attainment of high directionality. This result was recently demonstrated by Collett and Wolf,[4,5] who describe several planar sources which are rather incoherent in the global sense and yet generate precisely the same angular distribution of the radiant intensity as a fully coherent laser. This research has also led to the novel concept of partially coherent light beams.[6]
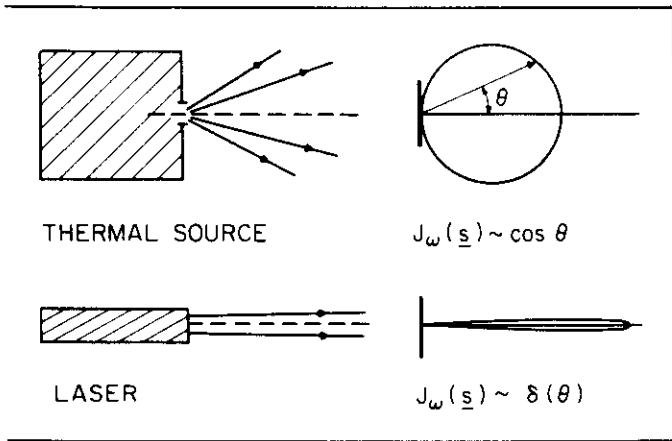
Fig. 1. Schematic illustration of the angular distribution of the radiant intensity from a thermal light source and from a typical laser.

Fig. 2. Illustration of the notation relating to radiation from partially coherent planar sources.

In the present article, we continue to use the same notation as in the previous article.[1] We consider a planar source, either a primary or a secondary one, occupying an area σ (which may be infinite) in the plane $z = 0$ and radiating into the half-space $z > 0$ (Fig. 2). The light generated by the source is represented by a fluctuating complex analytic signal, taken to be a scalar function of position and time and assumed to be stationary and ergodic. Because the different temporal frequency components of a stationary random function are uncorrelated,[7] it is sufficient to consider the transfer of energy at a single temporal frequency, ω say, of the optical field. The state of coherence of the radiation source is therefore conveniently specified by the cross-spectral density function[7] $W^{(0)}(\underline{r}_1, \underline{r}_2; \omega)$ of the light across the plane $z = 0$. The vectors $\underline{r}_1$ and $\underline{r}_2$ represent a typical pair of points in the source plane $z = 0$ (indicated by the superscript 0). Equivalently, the coherence properties of the source may be expressed in terms of the complex degree of spatial coherence $\mu^{(0)}(\underline{r}_1, \underline{r}_2; \omega)$ and the optical intensity $I^{(0)}(\underline{r}, \omega)$ of the light across the plane $z = 0$. They are related to the cross-spectral density function $W^{(0)}(\underline{r}_1, \underline{r}_2; \omega)$ by the following formulas:[7]

$$I^{(0)}(\underline{r}, \omega) = W^{(0)}(\underline{r}, \underline{r}; \omega) , \tag{1}$$

$$\mu^{(0)}(\underline{r}_1, \underline{r}_2; \omega) = \frac{W^{(0)}(\underline{r}_1, \underline{r}_2; \omega)}{\left[I^{(0)}(\underline{r}_1, \omega) \, I^{(0)}(\underline{r}_2, \omega) \right]^{1/2}} . \tag{2}$$

Several properties of these functions as well as their relationship to some of the more commonly known quantities in the theory of partial coherence, such as the mutual coherence function and the complex degree of coherence, are discussed in Ref. 7.

The primary object of interest in this paper is the angular distribution of the radiant intensity generated by the planar source σ. The radiant intensity, denoted by $J_\omega(\underline{s})$, is defined as the power (at frequency ω) radiated by the source per unit solid angle around a direction specified by the unit vector $\underline{s}$ (Fig. 2). The total power (at frequency ω) radiated by the planar source σ into the half-space $z > 0$ may thus be obtained from

$$\Phi_\omega = \int_{(2\pi)} J_\omega(\underline{s}) d\Omega , \tag{3}$$

here the integration extends over the 2π solid angle formed by all the directions pointing into the half-space $z > 0$. Denoting, moreover, by
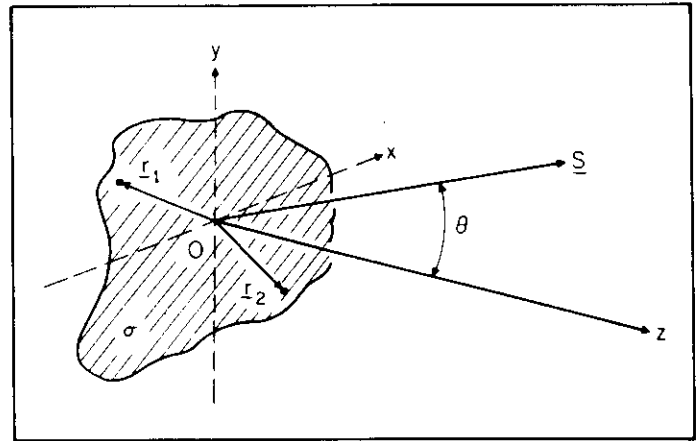
$$N_\omega = \int_{-\infty}^{\infty} I^{(0)}(\underline{r}, \omega) d^2 r \tag{4}$$

the integrated optical intensity (at frequency ω) across the source, one may define the ratio

$$C_\omega = \Phi_\omega \cdot N_\omega \tag{5}$$

as the radiation efficiency of the source at frequency ω. Irrespective of the state of coherence of the source, it can be shown to satisfy the inequality $0 \leq C_\omega \leq 1$.

2. RADIANT INTENSITY FROM PLANAR SOURCES OF ANY STATE OF COHERENCE

In this section we will first present several different formulas expressing the radiant intensity generated by the planar source σ described in the introduction (Fig. 2). The state of coherence of the source, which may be quite arbitrary, is specified by the cross-spectral density function $W^{(0)}(\underline{r}_1, \underline{r}_2; \omega)$ of the light across the source plane $z = 0$. The different formulas for the radiant intensity, each having their own distinct advantages, will then be used to elucidate various aspects of radiation from partially coherent planar sources.

2.1. Expressions for the radiant intensity

The radiant intensity $J_\omega(\underline{s})$ generated by a planar source in the direction specified by a unit vector $\underline{s}$ (Fig. 2) has been shown to be given by[1,8,9]

$$J_\omega(\underline{s}) = (2\pi k)^2 \cos^2\theta \, \tilde{W}^{(0)}(k\underline{s}_\perp, -k\underline{s}_\perp; \omega) , \tag{6}$$

where $k = \omega/c$, with c being the speed of light in free space, and $\tilde{W}^{(0)}(\underline{f}_1, \underline{f}_2; \omega)$ is the four-dimensional spatial Fourier transform of $W^{(0)}(\underline{r}_1, \underline{r}_2; \omega)$, defined by

$$\tilde{W}^{(0)}(\underline{f}_1, \underline{f}_2; \omega) = \frac{1}{(2\pi)^4} \int_{-\infty}^{\infty} \int_{-\infty}^{\infty} W^{(0)}(\underline{r}_1, \underline{r}_2; \omega)$$
$$\cdot e^{-i(\underline{f}_1 \cdot \underline{r}_1 + \underline{f}_2 \cdot \underline{r}_2)} d^2 r_1 d^2 r_2 . \tag{7}$$

Moreover, in Eq. (6), θ is the angle that the unit vector $\underline{s}$ makes with the positive z-axis, and $\underline{s}_\perp$ denotes the two-dimensional vector obtained by projecting $\underline{s}$ onto the source plane $z = 0$.

On substituting from Eq. (7) into Eq. (6), we obtain

$$J_\omega(\underline{s}) = \left(\frac{k}{2\pi} \right)^2 \cos^2\theta \int_{-\infty}^{\infty} \int_{-\infty}^{\infty} W^{(0)}(\underline{r}_1, \underline{r}_2; \omega)$$
$$\cdot e^{-ik\underline{s}_\perp \cdot (\underline{r}_1 - \underline{r}_2)} d^2 r_1 d^2 r_2 . \tag{8}$$

Let us next introduce the difference and average coordinates

$$\underline{r}' = \underline{r}_1 - \underline{r}_2; \quad \underline{r} = \frac{1}{2}(\underline{r}_1 + \underline{r}_2) \tag{9}$$

and define

$$C_v(\underline{r}',\omega) = \int_{-\infty}^{\infty} W^{(0)}\left(\underline{r} + \frac{1}{2}\underline{r}'.\underline{r} - \frac{1}{2}\underline{r}';\omega\right) d^2r . \tag{10}$$

where the integration extends throughout the source plane $z = 0$. With this notation, Eq. (8) may be rewritten as[9,10]

$$J_\omega(\underline{s}) = k^2\cos^2\theta\widetilde{C}_v(k\underline{s}_\perp,\omega) , \tag{11}$$

where $\widetilde{C}_v(\underline{f},\omega)$ is the two-dimensional spatial Fourier transform of $C_v(\underline{r}',\omega)$, namely,

$$\widetilde{C}_v(\underline{f},\omega) = \frac{1}{(2\pi)^2} \int_{-\infty}^{\infty} C_v(\underline{r}',\omega) e^{-i\underline{f}\cdot\underline{r}'} d^2r' . \tag{12}$$

The quantity $C_v(\underline{r}',\omega)$, defined by Eq. (10), is called the source-averaged cross-spectral density function of the light in the source plane. In view of the physical significance of $W^{(0)}(\underline{r}_1,\underline{r}_2;\omega)$, the function $C_v(\underline{r}',\omega)$ is clearly proportional to the average value of the correlations of the light fluctuations at frequency ω for all pairs of points $\underline{r}_1$ and $\underline{r}_2$ in the source plane whose relative "separation" is $\underline{r}' = \underline{r}_1 - \underline{r}_2$, the average being taken over the whole source.

It will be convenient to introduce still a third expression for the radiant intensity. For that purpose, let us define the quantity

$$\eta^{(0)}(\underline{r}',\omega) = \frac{C_v(\underline{r}',\omega)}{C_v(0,\omega)} = \frac{C_v(\underline{r}',\omega)}{N_\omega} . \tag{13}$$

where the second equality follows the Eqs. (10), (1), and (4). It can be shown that $\eta^{(0)}(\underline{r}',\omega)$ satisfies the conditions[11]

$$\eta^{(0)}(0,\omega) = 1; \quad \left|\eta^{(0)}(\underline{r}',\omega)\right| \leq 1 , \tag{14}$$

regardless of the state of coherence of the source. Substitution from Eq. (13) into Eq. (11) yields for the radiant intensity

$$J_\omega(\underline{s}) = k^2\cos^2\theta N_\omega\widetilde{\eta}^{(0)}(k\underline{s}_\perp,\omega) , \tag{15}$$

where $\widetilde{\eta}^{(0)}(\underline{f},\omega)$ is, of course, the two-dimensional spatial Fourier transform of $\eta^{(0)}(\underline{r}',\omega)$ [cf. Eq. (12)]. With Eqs. (14) and (15) in mind, it is natural to call the quantity $\eta^{(0)}(\underline{r}',\omega)$ the coefficient of directionality[11] of the planar source at frequency ω.

We have thus three formally different expressions for the radiant intensity from a planar source, namely those given by Eqs. (6), (11), and (15). The formulas in Eqs. (6) and (15) are useful when describing certain recent equivalence theorems[4,11] which imply that sources of entirely different states of coherence may nonetheless produce exactly the same distributions of the radiant intensity. A consequence of such an equivalence is, for example, that sources which are far from being spatially completely coherent generate light beams that are just as directional as a Gaussian laser beam.[5] The expression in Eq. (11), on the other hand, turns out to be very convenient when discussing the implications of the analytic properties of the radiant intensity.

2.2. Implications of the expressions for the radiant intensity

Let us consider, first, Eq. (6). According to that formula, only those spatial frequencies of $W^{(0)}(\underline{r}_1,\underline{r}_2;\omega)$, which obey the constraints $\underline{f}_1 = -\underline{f}_2 = k\underline{s}_\perp$, contribute to the radiant intensity. Such a pair $(\underline{f},-\underline{f})$ is commonly called an antidiagonal pair of spatial frequencies, and the corresponding spatial Fourier component $\widetilde{W}^{(0)}(\underline{f},-\underline{f};\omega)$ is referred

to as an antidiagonal element of $\widetilde{W}^{(0)}(\underline{f}_1,\underline{f}_2;\omega)$. Moreover, since $|k\underline{s}_\perp| \leq |k\underline{s}| = k$, only spatial frequencies for which $|\underline{f}| \leq k$, the so-called low spatial frequencies, appear in the expression (6) for the radiant intensity. With this terminology we may thus say that the radiant intensity from a planar source is uniquely determined by the low-frequency antidiagonal elements of the four-dimensional spatial Fourier transform of the cross-spectral density function $\widetilde{W}^{(0)}(\underline{r}_1,\underline{r}_2;\omega)$ of the light across the source plane.[4]

An interesting conclusion may be immediately drawn from the above result: any two planar sources, whose cross-spectral density functions are such that their four-dimensional spatial Fourier transforms have identical low-frequency antidiagonal elements, will generate identical distributions of the radiant intensity. This is the original form of the equivalence theorem, formulated by Collett and Wolf,[4] pertaining to planar sources of arbitrary states of coherence. Such equivalent sources will, of course, in general generate fields with entirely different far-zone coherence properties, because the far-field coherence is determined by all the low-frequency elements of $\widetilde{W}^{(0)}(\underline{f}_1,\underline{f}_2;\omega)$, not just by the antidiagonal ones.[12]

Let us now turn our attention to Eq. (15) and reformulate the above equivalence theorem in a manner that affords a simple and intuitive explanation of the underlying physical reasons for the equivalence. The following result is seen at once from Eq. (15): any two planar sources, which have the same coefficients of directionality $\eta^{(0)}(\underline{r}',\omega)$ and whose integrated optical intensities N_ω are the same, will generate identical distributions of the radiant intensity. This new version of the equivalence theorem, with some additional mathematical refinements, was formulated by Collett and Wolf.[11] To fully appreciate the physical insight provided by this new formulation, let us express the coefficient of directionality $\eta^{(0)}(\underline{r}',\omega)$ in terms of the complex degree of spatial coherence $^{(0)}(\underline{r}_1,\underline{r}_2;\omega)$ and the optical intensity $I^{(0)}(\underline{r},\omega)$. By substituting from Eq. (2) into Eq. (10) and using the result in Eq. (13), the following expression is obtained:

$$\eta^{(0)}(\underline{r}',\omega) = \frac{1}{N_\omega} \int_{-\infty}^{\infty} \mu^{(0)}\left(\underline{r} + \frac{1}{2}\underline{r}'.\underline{r} - \frac{1}{2}\underline{r}',\omega\right)$$

$$\left[I^{(0)}\left(\underline{r} + \frac{1}{2}\underline{r}',\omega\right) I^{(0)}\left(\underline{r} - \frac{1}{2}\underline{r}',\omega\right)\right]^{1/2} d^2r . \tag{16}$$

This formula shows that the coefficient of directionality depends not only on the distribution of the complex degree of spatial coherence, but also on the optical intensity distribution of the light across the source. The coefficient of directionality may be thought of as being obtained by means of an integral of the complex degree of spatial coherence, appropriately weighting each contribution to the integral by an intensity-dependent factor. For instance, two planar sources with the same integrated optical intensities N_ω may have quite different distributions of the complex degree of spatial coherence $\mu^{(0)}(\underline{r}_1,\underline{r}_2;\omega)$ and of the optical intensity $I^{(0)}(\underline{r},\omega)$, and yet they generate the same distributions of the radiant intensity, provided only that for each $\underline{r}'$ the integral in Eq. (16) is the same for both of them. In such a case, the differences in the complex degrees of spatial coherence are compensated by the differences in the optical intensities. Concrete illustrations of these remarks will be provided shortly.

Finally, let us briefly consider the implications of Eq. (11). It shows that the radiant intensity (at frequency ω) produced by a planar source of any state of coherence is proportional to the product of $\cos^2\theta$ and the two-dimensional spatial Fourier transform of the source-averaged cross-spectral density function $C_v(\underline{r}',\omega)$ of the field in the source plane. Since $k = \omega c = 2\pi \lambda$, where λ is the wavelength corresponding to the frequency ω, the radiant intensity is also inversely proportional to the square of the wavelength of the light. If the planar source σ under consideration is of finite extent, the source-averaged cross-spectral density function $C_v(\underline{r}',\omega)$, in view of

Eq. (10), obviously vanishes identically outside some finite $\underline{r}'$ domain. According to some theorems on Fourier transforms, the function $\tilde{C}_v(\underline{f}, \omega)$ in such a case possesses certain unique analytic properties. Without going into the details of the mathematics, we will mention a few conclusions that can be drawn by such analytic considerations. In the first place, it can be shown that[5]

$$J_\omega(\underline{s}) \to 0, \quad \text{as} \quad \theta \to \pi/2 , \tag{17}$$

to at least the second order in $\cos\theta$. Hence a finite planar source does not radiate in any direction parallel to the source plane. This result also implies that, strictly speaking, no *finite* planar source radiating in accordance with Lambert's law can exist. However, many light sources encountered in practice are Lambertian to a good approximation.

Another important conclusion that follows immediately from the analytic properties of the radiant intensity produced by a finite planar source is related to the inverse problem of determining the source coherence properties from the measurements of the radiant intensity. The following very strong theorem has been proven by Wolf:[9] the exact knowledge of the radiant intensity for all $\underline{s}$ directions filling any finite solid angle, however small, uniquely determines the complete source-averaged cross-spectral density function $C_v(\underline{r}', \omega)$ of the light in the source plane. According to Eq. (13), the coefficient of directionality $\eta^{(0)}(\underline{r}', \omega)$ and the integrated optical intensity N_ω of the planar source are readily obtained once $C_v(\underline{r}', \omega)$ is known. In particular, one can take the finite solid angle appearing in the above theorem to be the whole 2π solid angle formed by all the possible $\underline{s}$ directions. These results then imply that the quantities $C_v(\underline{r}', \omega)$, $\eta^{(0)}(\underline{r}', \omega)$, and N_ω associated with a planar source giving rise to any prescribed distribution of the radiant intensity $J_\omega(\underline{s})$ (assumed to have been produced by some *finite* planar source) can be uniquely specified.

It should be noted that even though the radiant intensity $J_\omega(\underline{s})$ uniquely determines the source-averaged cross-spectral density function $C_v(\underline{r}', \omega)$, the cross-spectral density function $W^{(0)}(\underline{r}_1, \underline{r}_2; \omega)$ itself is not necessarily unique across the source. This remark is in keeping with the earlier observations that planar sources of entirely different states of coherence may generate identical distributions of the radiant intensity. However, it can be shown that in the special case of a nonradiating finite planar source (i.e., a source for which $J_\omega(\underline{s})$ has a zero value for all the possible $\underline{s}$ directions), the cross-spectral density function $W^{(0)}(\underline{r}_1, \underline{r}_2; \omega)$ must vanish whenever $\underline{r}_1 \neq \underline{r}_2$. Hence every *finite* planar source, other than a strictly spatially incoherent one, necessarily radiates. This result also implies that a finite planar source cannot generate a field that consists of a pure surface wave. Analogous considerations pertaining to true primary planar sources were presented by Friberg.[13]

3. QUASIHOMOGENEOUS SOURCE THAT GENERATES A KNOWN DISTRIBUTION OF RADIANT INTENSITY

As an application of the general discussion presented in the previous section, we will consider here the following two related problems:[11] first, how to specify a quasihomogeneous planar source that will produce the same radiant intensity as any given planar source,[14] and, second, how to specify a quasihomogeneous planar source that will generate any prescribed distribution of the radiant intensity, assuming that the radiant intensity was produced by some finite planar source.

For that purpose, we first recall that a quasihomogeneous planar source is characterized by a cross-spectral density function of the form[1,15]

$$W^{(0)}(\underline{r}_1, \underline{r}_2; \omega) = I^{(0)}\left[\frac{1}{2}(\underline{r}_1 + \underline{r}_2), \omega\right] \mu^{(0)}(\underline{r}_1 - \underline{r}_2; \omega), \tag{18}$$

where $I^{(0)}(\underline{r}, \omega)$ is the optical intensity distribution, and $\mu^{(0)}(\underline{r}', \omega)$, assumed to depend only on the difference $\underline{r}' = \underline{r}_1 - \underline{r}_2$, is the com-

plex degree of spatial coherence of the light in the source plane. It is assumed, moreover, that $I^{(0)}(\underline{r}, \omega)$ varies with $\underline{r}$ much more slowly than $\mu^{(0)}(\underline{r}', \omega)$ varies with $\underline{r}'$, and that the linear dimensions of the source are large compared to both the wavelength of the light and the effective coherence interval of the light across the source. On substituting from Eq. (18) into Eq. (16), the coefficient of directionality of a quasihomogeneous planar source (denoted by subscript Q) is readily found to be

$$\eta_Q^{(0)}(\underline{r}', \omega) = \mu_Q^{(0)}(\underline{r}', \omega) , \tag{19}$$

where use was made of the result

$$N_{\omega, Q} = \int_{-\infty}^{\infty} I_Q^{(0)}(\underline{r}, \omega) d^2r , \tag{20}$$

with $I_Q^{(0)}(\underline{r}, \omega)$ being the optical intensity distribution of the quasihomogeneous source. Eq. (19) shows that the coefficient of directionality of a quasihomogeneous planar source is precisely equal to its complex degree of spatial coherence.

Consider now some given planar source σ of any state of coherence whatever. Its coefficient of directionality, denoted by $\eta_\sigma^{(0)}(\underline{r}', \omega)$, may be computed from Eq. (16), and its integrated optical intensity, denoted by $N_{\omega, \sigma}$, is readily obtained from Eq. (4). The radiant intensity distribution produced by this source is therefore known, it being given by Eq. (15). Now, according to the equivalence theorem discussed earlier, a quasihomogeneous planar source whose coefficient of directionality $\eta_Q^{(0)}(\underline{r}', \omega)$ and integrated optical intensity $N_{\omega, Q}$ satisfy the conditions

$$\eta_Q^{(0)}(\underline{r}', \omega) = \eta_\sigma^{(0)}(\underline{r}', \omega); \quad N_{\omega, Q} = N_{\omega, \sigma} , \tag{21}$$

will generate precisely the same distribution of the radiant intensity as the given planar source σ. With the help of Eqs. (19) and (20), these conditions take the form[11]

$$\mu_Q^{(0)}(\underline{r}', \omega) = \eta_\sigma^{(0)}(\underline{r}', \omega); \quad \int_{-\infty}^{\infty} I_Q^{(0)}(\underline{r}, \omega) d^2r = N_{\omega, \sigma} . \tag{22}$$

These results show that there is, in fact, an infinite number of quasihomogeneous sources that produce the same radiant intensity as any given source. They all have the same complex degree of spatial coherence, uniquely specified by the first condition in Eq. (22), but their optical intensity distributions may differ, provided that they are sufficiently smooth and satisfy the second condition in Eq. (22).

To illustrate the above comments, let us determine a quasihomogeneous source that will produce the same radiant intensity as a completely coherent and cophasal square source of uniform intensity I_0. Taking the sides to be of length 2ℓ, one easily finds for such a source

$$\eta_\sigma^{(0)}(\underline{r}', \omega) = \begin{cases} (1 - |x'|/2\ell)(1 - |y'|/2\ell), & \text{if } |x'| \leq 2\ell \text{ and } |y'| \leq 2\ell , \\ 0, & \text{otherwise} , \end{cases} \tag{23}$$

where $\underline{r}' = (x', y')$. The integrated optical intensity $N_{\omega, \sigma}$ is, of course, equal to $4\ell^2 I_0$. The radiant intensity distribution generated by the source under consideration is known to be

$$J_\omega(\underline{s}) = \left(\frac{k}{2\pi}\right)^2 (4\ell^2)^2 I_0 \cos^2\theta \left(\frac{\sin k s_x \ell}{k s_x \ell}\right)^2 \left(\frac{\sin k s_y \ell}{k s_y \ell}\right)^2 , \tag{24}$$

where $\underline{s} = (s_x, s_y, s_z)$ with $s_z = \cos\theta$. Now, according to Eq. (22), a quasihomogeneous planar source, whose complex degree of spatial coherence is given by the right-hand side of Eq. (23), will also give rise to the radiant intensity of Eq. (24). The complex degree of spatial coherence $\mu_Q^{(0)}(\underline{r}', \omega)$ of the quasihomogeneous source, with $y' = 0$,
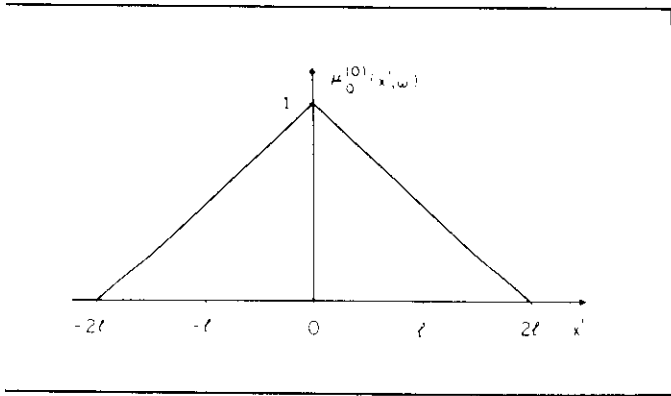
g. 3. The complex degree of spatial coherence, with y' = 0, of a quasi-ɔmogeneous planar source that produces the same distribution of the diant intensity as a uniform, completely coherent, and cophasal square ɔurce of sides 2ℓ.
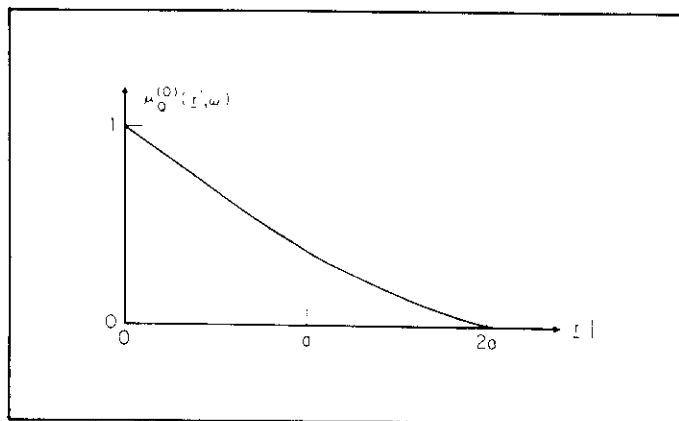

Fig. 4. The complex degree of spatial coherence of a quasihomogeneous planar source that produces the classic Airy pattern of the radiant intensity (after Collett and Wolf[11]).

illustrated in Fig. 3. The actual shape of the optical intensity istribution across this equivalent source is irrelevant, as long as it ieets the requirements of quasihomogeneity and integrates to $4\ell^2 I_0$. quivalent quasihomogeneous sources corresponding to more ɔmplicated examples, possibly illuminated with partially coherent ght, can be specified in a similar manner.

Let us now turn our attention to the second problem stated at the ɛginning of this section. As we have already explained, a prescribed stribution of the radiant intensity (assumed to have been generated / some finite source σ) uniquely determines the source-averaged oss-spectral density function, denoted here by $C_{v,\sigma}(\underline{r}',\omega)$ for ɔnvenience. According to Eq. (13), this in turn uniquely determines ie coefficient of directionality $\eta_q^{(0)}(\underline{r}',\omega)$ and the integrated optical tensity $N_{\omega,\sigma}$ of the source. Now, by substituting these on the ght-hand side of the conditions in Eq. (22), we obtain a quasihomo-ɛneous source that also will produce the prescribed distribution of ɛ radiant intensity. As before, the complex degree of spatial coher-ɪce of such a quasihomogeneous source is unique, but its optical tensity distribution may vary.

As an example, we will take the prescribed distribution of the diant intensity to be the famous Airy pattern

$$J(\underline{s}) = \left(\frac{k}{2\pi}\right)^2 (\pi a^2)^2 I_0 \cos^2\theta \left[\frac{2J_1(ka\sin\theta)}{ka\sin\theta}\right]^2 , \quad (25)$$

here $J_1(x)$ is the Bessel function of the first kind and first order. The ιantities a and I_0 are positive parameters. A quasihomogeneous anar source producing the radiant intensity, given by Eq. (25), can ɛ shown[11] to have a complex degree of spatial coherence

$$\mu^{(0)}(\underline{r}',\omega) = \begin{cases} \frac{2}{\pi}\left[\cos^{-1}\left(\frac{r'}{2a}\right) - \left(\frac{r'}{2a}\right)\sqrt{1-\left(\frac{r'}{2a}\right)^2}\right], & \text{if } r' \leq 2a , \\ 0, & \text{otherwise} . \end{cases} \quad (26)$$

here $r'=|\underline{r}'|$. Its optical intensity distribution must have an integral ɛr the entire source equal to $(\pi a^2)I_0$. The complex degree of atial coherence, given by Eq. (26), is illustrated in Fig. 4.

MODEL SOURCES

ɔ become more familiar with the various concepts introduced rlier in this article, we will now discuss several partially coherent ɔdel sources. In addition to the quasihomogeneous sources,[15] we II also consider the so-called Schell model sources.[16,17] A Schell

model source is characterized by a cross-spectral density function of the form

$$W^{(0)}(\underline{r}_1,\underline{r}_2;\omega) = \left[I^{(0)}(\underline{r}_1,\omega)\, I^{(0)}(\underline{r}_2,\omega)\right]^{1/2} \mu^{(0)}(\underline{r}_1-\underline{r}_2;\omega) . \quad (27)$$

Here $I^{(0)}(\underline{r},\omega)$ is the optical intensity distribution, and $\mu^{(0)}(\underline{r}',\omega)$, assumed to depend only on the difference $\underline{r}' = \underline{r}_1 - \underline{r}_2$, is the com-plex degree of spatial coherence of the light in the source plane. The Schell model sources, like the quasihomogeneous ones, are a gener-alization of the statistically homogeneous sources. If the optical intensity distribution across the source varies sufficiently slowly from point to point, as is the case with many natural radiation sources, the Schell model sources become essentially quasihomogeneous.

We will consider three types of quasihomogeneous sources and one type of Schell model source. The quasihomogeneous sources are taken to have a distribution of the complex degree of spatial coherence, which is either of Gaussian or of exponential form, or it is specified in terms of Bessel functions. These distributions are, respectively,

$$\mu^{(0)}(\underline{r}',\omega) = e^{-\underline{r}'^2/2\sigma_\mu^2} , \quad (28)$$

$$\mu^{(0)}(\underline{r}',\omega) = e^{-|\underline{r}'|/D} , \quad (29)$$

$$\mu^{(0)}(\underline{r}',\omega) = \frac{2}{\sqrt{\pi}}\Gamma\left(\nu+\frac{3}{2}\right)\frac{j_\nu(k|\underline{r}'|)}{\left(\frac{1}{2}k|\underline{r}'|\right)^\nu} \quad (30)$$

Here σ_μ and D are positive parameters, $\Gamma(x)$ denotes the gamma function, and $j_\nu(x)$ is the spherical Bessel function of the first kind and of order ν, with $\nu \geq -1/2$. The exact forms of the optical intensity distributions $I^{(0)}(\underline{r},\omega)$ across these sources are of no impor-tance in the present context, as long as they meet the requirements of quasihomogeneity. The Schell model source, on the other hand, is taken to have both its complex degree of spatial coherence and its optical intensity of Gaussian form; i.e., $\mu^{(0)}(\underline{r}',\omega)$ is the same as Eq. (28), and $I^{(0)}(\underline{r},\omega)$ is given by

$$I^{(0)}(\underline{r},\omega) = I_0 e^{-\underline{r}^2/2\sigma_I^2} , \quad (31)$$

where I_0 and σ_I are positive parameters.

We will determine the coefficient of directionality $\eta^{(0)}(\underline{r}',\omega)$, the distribution of the radiant intensity $J_\omega(\underline{s})$, and the radiation effi-ciency C_ω associated with these four model sources. The results, some of which can be found in Refs. 1, 5, 11, 15, 18, 22, and some of which are new, are given in tabulated form (Table I).

A few comments are perhaps in order regarding the entries in Table I. In the first place, if $\sigma_I \gg \sigma_\mu$ then $\Delta \rightarrow \sigma_\mu$, and the Gaussian Schell model source reduces to a Gaussian correlated quasihomo-

TABLE I. Radiation from Partially Coherent Model Sources.

MODEL	QUASIHOMOGENEOUS			SCHELL
INTENSITY	NOT RELEVANT			GAUSSIAN
COHERENCE	GAUSSIAN	EXPONENTIAL	BESSEL	GAUSSIAN
COEFFICIENT OF DIRECTIONALITY	$e^{-r'^2/2\sigma_\mu^2}$	$e^{-\lvert r'\rvert/D}$	$\frac{2}{\sqrt{\pi}}\,\Gamma(v+\frac{3}{2})\frac{J_v(k\lvert r'\rvert)}{(\frac{1}{2}k\lvert r'\rvert)^v}$	$e^{-r'^2/2\Delta^2}$ $\frac{1}{\Delta^2}=\frac{1}{\sigma_\mu^2}+\frac{1}{(2\sigma_I)^2}$
RADIANT INTENSITY	$J_{\omega,0}\cos^2\theta\, e^{-\frac{1}{2}(k\sigma_\mu)^2\sin^2\theta}$ $J_{\omega,0}=\frac{(k\sigma_\mu)^2}{2\pi}\int I^{(0)}(r,\omega)d^2r$	$J_{\omega,0}\cos^2\theta[1+(kD)^2\sin^2\theta]^{-\frac{3}{2}}$ $J_{\omega,0}=\frac{(kD)^2}{2\pi}\int I^{(0)}(r,\omega)d^2r$	$J_{\omega,0}\cos^{2v+1}\theta$ $J_{\omega,0}=\frac{1}{\pi}(v+\frac{1}{2})\int I^{(0)}(r,\omega)d^2r$	$J_{\omega,0}\cos^2\theta\, e^{-\frac{1}{2}(k\Delta)^2\sin^2\theta}$ $J_{\omega,0}=(k\Delta\sigma_I)^2 I_0$
RADIATION EFFICIENCY	$1-\dfrac{F(k\sigma_\mu/\sqrt{2})}{k\sigma_\mu/\sqrt{2}}$ $F(a)=e^{-a^2}\int_0^a e^{u^2}du$	$1-\dfrac{1}{(kD)}\sin^{-1}\!\left(\dfrac{kD}{\sqrt{1+(kD)^2}}\right)$	$\dfrac{2v+1}{2v+2}$	$1-\dfrac{F(k\Delta/\sqrt{2})}{k\Delta/\sqrt{2}}$ $F(a)=e^{-a^2}\int_0^a e^{u^2}du$

geneous source. On the other hand, if $\sigma_\mu \to \infty$, then it represents a completely coherent and cophasal planar source with Gaussian optical intensity distribution. In that case, $\Delta \to 2\sigma_I$, and the results are found to be identical to those given in Refs. 1, 4, and 11. If, moreover, $k\sigma_I \gg 1$, then such a source represents a Gaussian laser, and one may, of course, approximate $\cos\theta \approx 1$ and $\sin\theta \approx \theta$. Several special cases of the Bessel correlated quasihomogeneous sources are also of interest. For $v = -1/2$, the complex degree of spatial coherence is found from Eq. (30) to be $J_0(kr')$, where $r' = \lvert r'\rvert$ and $J_0(x)$ is the Bessel function of the first kind and order zero. Hence the source exhibits a finite (non-zero) correlation distance, and yet its radiation efficiency is seen to be zero. At first sight this appears to contradict our earlier remark that every finite planar source (other than a strictly spatially incoherent one) necessarily radiates.[13] The resolution of this dilemma is, of course, that the Bessel correlated quasihomogeneous source with $v = -1/2$ is of infinite extent. For $v = 0$, the right-hand side of Eq. (30) reduces to $\sin kr'/kr'$, leading to a Lambertian planar source.[1,23] For $v = 1/2$, Eq. (30) gives, on the other hand, a complex degree of spatial coherence of the form $2J_1(kr')/kr'$, where $J_1(x)$ is the Bessel function of the first kind and order one. The radiant intensity from such a source is seen to follow a $\cos^2\theta$-law, identical to that from a spatially incoherent source (when spatial incoherence is defined in terms of the non-normalizable Dirac delta function).[1,8,23]

5. PARTIALLY COHERENT SOURCES THAT PRODUCE THE SAME RADIANT INTENSITY AS A LASER

We have already described a procedure by which one can specify the characteristics of a quasihomogeneous planar source that will generate the same distribution of the radiant intensity as any given planar source. We illustrated this procedure by determining a quasihomogeneous source which produces the same radiant intensity as a uniform, fully coherent, and cophasal square source. In this section, we will discuss a broader class of partially coherent sources, each with a different coherence area and a different optical intensity distribution, giving rise to a radiant intensity distribution identical to that of a fully coherent Gaussian laser beam.[5]

Let us first compute the radiant intensity distribution generated

by a laser source with a flat output mirror, operating in its lowest-order transverse mode. Neglecting the diffraction effects caused by the edges of the output mirror, the radiant intensity may be found from Table I by setting $\sigma_\mu = \infty$ for the Gaussian Schell model source. Writing σ_L and I_L in place of σ_I and I_0 to indicate that these quantities pertain to the laser. the optical intensity distribution across the output mirror is

$$I_L^{(0)}(r,\omega) = I_L e^{-r^2/2\sigma_L^2},\qquad(32)$$

and the resulting radiant intensity distribution is readily found to be[1,4,5]

$$J_{\omega,L}(s) = (2k\sigma_L^2)^2 I_L\cos^2\theta\, e^{-2(k\sigma_L)^2\sin^2\theta}.\qquad(33)$$

By comparing the formula of Eq. (33) to the expression of the radiant intensity given in Table I for the Gaussian Schell model source, the following important theorem follows at once:[5] any Schell model source, whose optical intensity distribution and complex degree of spatial coherence are both Gaussian and whose parameters σ_μ, σ_I, and I_0 satisfy the conditions

$$\frac{1}{\sigma_\mu^2}+\frac{1}{(2\sigma_I)^2}=\frac{1}{(2\sigma_L)^2};\quad I_0=\left(\frac{\sigma_L}{\sigma_I}\right)^2 I_L,\qquad(34)$$

will generate precisely the same distribution of the radiant intensity, namely that of Eq. (33), as a fully coherent and cophasal planar laser source with the Gaussian optical intensity distribution of Eq. (32). Even though all sources satisfying the conditions (34) will generate the same radiant intensity distributions, their far-field coherence properties will, as we have discussed earlier, in general be different.

It is evident from the first condition of Eq. (34) that the parameters σ_μ and σ_I of any Gaussian Schell model source producing the radiant intensity of Eq. (33) must satisfy the inequalities $\sigma_I \geq \sigma_L$ and $\sigma_\mu \geq 2\sigma_I$. Hence the width of the optical intensity distribution across any such Schell model source can be no smaller than the width of the laser intensity distribution. and the width of the complex degree of spatial coherence must be at least twice the width of the laser intensity.
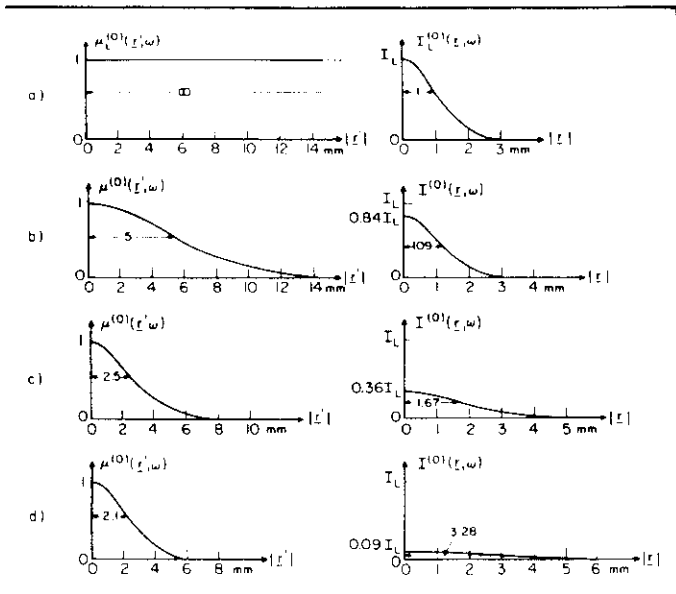
Fig. 5. Illustrating the coherence and intensity distributions across partially coherent Gaussian Schell model sources (b, c, and d) giving rise to the same radiant intensity distribution as a fully coherent laser source (a). The radiant intensity is given by Eq. (33) with $\sigma_L = 1$ mm and I_L arbitrary (after Wolf and Collett[5]).
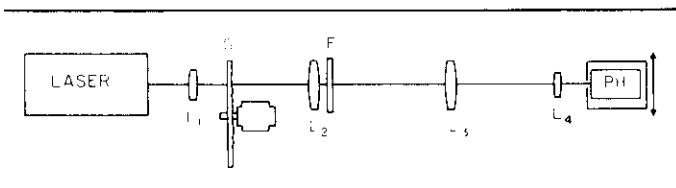

Fig. 6. Schematic illustration of the Gori system (after De Santis, Gori, Guattari, and Palma[27]).

Choosing $\sigma_\mu \approx 2\sigma_I$ and $\sigma_I \gg \sigma_\mu$, the resulting Schell model source is essentially quasihomogeneous.[4] This source is precisely the one which would have been obtained by using the procedure, described earlier, of specifying equivalent quasihomogeneous planar sources.

In Fig. 5, we present the distributions of the optical intensity and the complex degree of spatial coherence of the light across several different Gaussian Schell model sources, each source generating the same radiant intensity as a fully coherent Gaussian laser source. The graphs clearly illustrate the trade-off taking place between the source coherence and the source intensity, so as to produce identical distributions of the radiant intensity.

6. SOURCES WITH CONTROLLABLE DISTRIBUTIONS OF INTENSITY AND COHERENCE

Even though the properties of radiation from partially coherent sources have been the subject of active research for more than ten years, experimental investigations as to the practical realization of such sources and the testing of the theoretical predictions have only very recently begun. Among the suggested ways of producing a controllable partially coherent source are, for example, a suitable superposition of independent laser beams[24] and the scattering of light by a liquid crystal under the application of a dc electric field.[21,25,26] Most of the experimental effort so far has concentrated on direct verification of the predicted relationship between the coherence properties of a source and the directionality of the light it generates. The first experimental results, supporting the equivalence theorem which implies that certain partially coherent planar sources may produce light fields just as directional as a laser beam, were obtained by DeSantis, Gori, Guattari, and Palma[27] using an optical

system resembling an ordinary collimator. Because of the importance of the results and the ingenuity of the device, we will briefly describe the experiment carried out by Gori and his coworkers.

The Gori system is illustrated in Fig. 6. G is a rotating ground glass, F is a Gaussian amplitude filter, and L_1-L_4 are simple lenses. Consider first the ground glass G and the amplitude filter F removed. The field, originating in the laser, can be made to emerge from the lens L_2 with no phase curvature and with a Gaussian optical intensity distribution, if the focal lengths f_1 and f_2 of the lenses L_1 and L_2 as well as their separation are chosen properly. Hence, in this case, the lens L_2 realizes a fully coherent Gaussian planar source. Its optical intensity distribution may thus be represented by Eq. (32), with the constants I_I and σ_I being determined by the system parameters. The lens L_3 produces in its back focal plane the far-field distribution of the coherent field emerging from the lens L_2, and the lens L_4 forms an enlarged image of that distribution on the photodetector PH. The intensity profile scanned along a line perpendicular to the optical axis in the far-field distribution of the coherent Gaussian source (i.e., the plane of the lens L_2) is presented in Fig. 7.

After examining the coherent case, the rotating ground glass G and the Gaussian amplitude filter F are reinserted. A Gaussian spot of laser light is produced on the ground glass by the lens L_1. If the spot diameter is large compared to the inhomogeneity scale of the glass, it can be considered as a spatially incoherent planar source with a Gaussian intensity distribution.[28] Let us denote the value of the intensity on the optical axis by I_S and the rms width of the intensity distribution by σ_S. The lens L_2 is placed a distance f_2, i.e., the focal length of L_2, from the ground glass G, and the filter F, with a field transmission function of rms width σ_F, is adjacent to the lens L_2. Using the van Cittert-Zernike theorem and the usual optical propagation laws, the cross-spectral density function of the field emerging from the filter F can be shown to be[27]

$$W^{(0)}(\underline{r}_1,\underline{r}_2;\omega) = \frac{I_S(k\sigma_S)^2}{4\pi f_2^2} e^{-(k\sigma_S/2f_2)^2(\underline{r}_1-\underline{r}_2)^2}$$
$$e^{-(\underline{r}_1^2+\underline{r}_2^2)/2\sigma_F^2} \qquad (35)$$

This formula implies that the plane of the filter F acts as a Gaussian Schell model source. Its complex degree of spatial coherence is given by Eq. (28), and its optical intensity is given by Eq. (31), with the constants I_0, σ_I, and σ_μ being related to the system parameters I_S, σ_S, f_2, and σ_F by the formulas

$$I_0 = \frac{I_S(k\sigma_S)^2}{4\pi f_2^2} \ ; \ \sigma_I = \frac{\sigma_F}{\sqrt{2}} \ ; \ \sigma_\mu = \frac{\sqrt{2}f_2}{k\sigma_S} \ . \qquad (36)$$
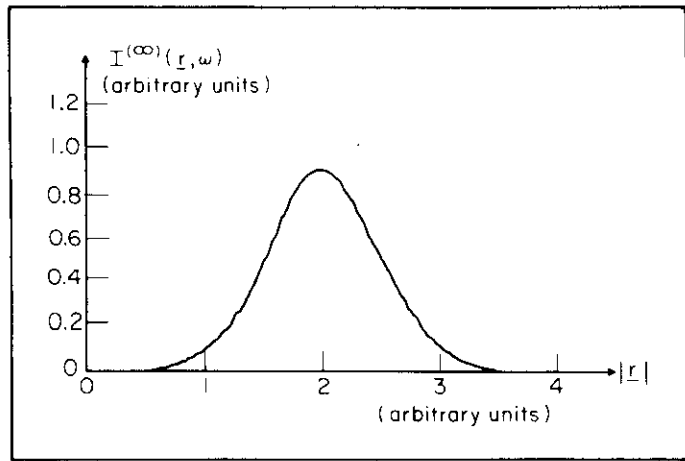

Fig. 7. Recording of the optical intensity distribution in the far field of a fully coherent Gaussian laser source (after De Santis, Gori, Guattari, and Palma[27]).
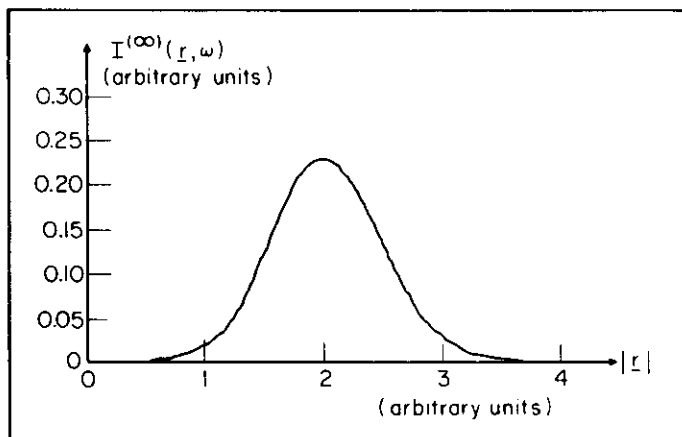
Fig. 8. Recording of the optical intensity distribution in the far field of a Gaussian Schell model source realized by means of the Gori system (after De Santis, Gori, Guattari, and Palma[27]).

Now, according to the discussion in the previous section, if the parameters I_0, σ_1, and σ_μ associated with the light emerging from the filter F satisfy the conditions (34), then such a source produces exactly the same far-field intensity distribution as the fully coherent Gaussian source characterized by the parameters I_L and σ_L. The intensity profile scanned along a line perpendicular to the optical axis in the far field produced by a source of this type (i.e., the field emerging from the filter F) with suitably chosen system parameters is shown in Fig. 8. The arbitrary units used for the intensity and for the distance from the optical axis are the same in both Figs. 7 and 8. It is observed that the measured far-field intensity distributions presented in these figures show a remarkable similarity, thus providing evidence in support of the theoretical predictions.

It is of interest to note that the Gori system described above can be used to produce a whole class of partially coherent sources with controllable distributions of intensity and spatial coherence. By varying the system parameters I_S, σ_S, f_2, and σ_F, the constants I_0, σ_1, and σ_μ may be altered thus changing the spatial coherence and intensity profiles of the Gaussian Schell model source, located in the plane of the filter F. An additional degree of freedom could be provided by using, in place of the laser illuminated rotating ground glass G, some partially coherent light source with known spatial coherence and intensity properties.

Further experimental studies with regard to the highly directional character of the radiation patterns produced by certain types of quasihomogeneous sources have been carried out by Farina, Narducci, and Collett.[29] Their interest has been to investigate the problem with a minimum number of optical elements, so as to reduce extraneous effects and the possibility of experimental error. Using phase screens illuminated by a collimated laser light as quasi-homogeneous sources, they have observed that the radiated fields are very directional, as predicted by the theory, in spite of the globally incoherent character of the light in the source plane. They have also observed that changing the intensity distribution across the source plane does not essentially alter the radiation pattern, as long as the intensity distribution meets the requirements of quasi-homogeneity. Some preliminary measurements concerning the reciprocity theorem[1,15] pertaining to quasihomogeneous planar sources were also made.

7. SUMMARY AND DISCUSSION

In this review article we have discussed various aspects of the radiant intensity generated by a planar source of any state of coherence. Among the more important results mentioned is an equivalence

theorem which implies that sources with entirely different coherence properties may, nevertheless, produce identical distributions of the radiant intensity. This theorem was illustrated by means of several examples, including a class of partially coherent sources which give rise to a radiation field that is just as directional as a fully coherent laser beam. Several model sources were analyzed in terms of convenient new concepts, such as the coefficient of directionality and the radiation efficiency. Finally, some experimental work, aimed at the practical realization of partially coherent sources with controllable coherence and intensity properties and at the testing of the theoretical predictions regarding their radiation characteristics, was briefly described.

Even though the number of experimental results regarding radiation from partially coherent sources is still rather limited, it appears safe to say that such measurements have verified the main relationships between the coherence properties of a source and the directionality of the light it generates. In particular, the fact that complete spatial coherence is not a necessary requirement for the generation of highly directional light beams has been experimentally confirmed. However, to obtain convincing experimental evidence about many other phenomena predicted by the theory, a subtantial amount of further effort is required.

As is well known, fully coherent laser beams give rise to pronounced speckle effects that are often very disturbing. In many applications, a very directional light beam with low spatial coherence would have several advantages over the fully coherent laser beam. For these reasons, especially after it was shown that a globally rather incoherent source may produce a light beam which is just as directional as a laser beam, highly directional partially coherent light beams appear to be likely subjects of future research.

8. ACKNOWLEDGMENTS

9. REFERENCES

1. Friberg, A. T., Proc. SPIE 194, 55(1979).
2. Wolf, E., J. Opt. Soc. Am. 68, 6(1978).
3. Parrent, G. B., Jr. and Thompson, B. J., *Physical Optics Notebook*, SPIE, Bellingham, WA (1969).
4. Collett, E. and Wolf, E., Opt. Lett. 2, 27(1978).
5. Wolf, E. and Collett, E., Opt. Commun. 25, 293(1978).
6. Foley, J. T. and Zubairy, M. S., Opt. Commun. 26, 297(1978).
7. Mandel, L. and Wolf, E., J. Opt. Soc. Am. 66, 529(1976).
8. Marchand, E. W. and Wolf, E., J. Opt. Soc. Am. 64, 1219(1974).
9. Wolf, E., J. Opt. Soc. Am. 68, 1597(1978).
10. Carter, W. H., Opt. Commun. 26, 1(1978).
11. Collett, E. and Wolf, E., J. Opt. Soc. Am. 69, 942(1979).
12. Marchand, E. W. and Wolf, E., J. Opt. Soc. Am. 62, 379(1972).
13. Friberg, A. T., J. Opt. Soc. Am. 68, 1281(1978).
14. De Santis, P., Gori, F. and Palma, C., Opt. Commun. 28, 151(1979).
15. Carter, W. H. and Wolf, E., J. Opt. Soc. Am. 67, 785(1977).
16. Schell, A. C., "The multiple plate antenna." Doctoral Dissertation, Massachusetts Institute of Technology (1971), Section 7.5.
17. Steinle, B. and Baltes, H. P., J. Opt. Soc. Am. 67, 241(1977).
18. Baltes, H. P., Steinle, B. and Antes, G., Opt. Commun. 18, 242(1976).
19. Antes, G., Baltes, H. P., and Steinle, B., Helv. Phys. Acta 49, 759(1976).
20. Baltes, H. P. and Steinle, B., Nuovo Cimento B, 41, 428(1977).
21. Carter, W. H. and Bertolotti, M., J. Opt. Soc. Am. 68, 329(1978).
22. Baltes, H. P., Steinle, B. and Antes, G., "Radiometric and correlation properties of bounded planar sources," in *Coherence and Quantum Optics IV*, eds. Mandel, L. and Wolf, E., Plenum, New York (1978).
23. Carter, W. H. and Wolf, E., J. Opt. Soc. Am. 65, 1067(1975).
24. Gori, F. and Palma, C., Opt. Commun. 27, 185(1978).
25. Scudieri, F., Bertolotti, M. and Bartolino, R., Appl. Opt. 13, 181(1974).
26. Bertolotti, M., Scudieri, F. and Verginelli, S., Appl. Opt. 15, 1842(1976).
27. De Santis, P., Gori, F., Guattari, G. and Palma, C., Opt. Commun. 29, 256 (1979).
28. Martienssen, W. and Spiller, E., Am. J. Phys. 32, 919(1964).
29. Farina, J. D., Narducci, L. M. and Collett, E., Opt. Commun. 32, 203(1980).

RADIOMETRIC MODEL FOR HOLOGRAPHIC AXICONS
IN PARTIALLY COHERENT LIGHT

S.Yu. Popov and A.T. Friberg
Materials Physics Laboratory, Helsinki University of Technology
Rakentajanaukio 2 C, FIN-02150 Espoo, FINLAND
phone: +358 (0) 451 3163   fax: +358 (0) 451 3164

Abstract

A radiometric model for the computer simulation of the light intensity distribution formed by a holographic axicon is presented. This model leads to a considerable simplification (in comparison with rigorous wave theory) in the assessment of the axicon performance for producing a desired space energy distribution. It is shown, moreover, that the radiometric model can be successfully used also for the computation of the spatial coherence properties of the light in the axicon image region. The comparison of the radiometric simulation results with those obtained by diffractive wave theory demonstrates the applicability and excellent accuracy of the present radiometric approach under conditions of partially coherent radiation.

Introduction

Axicons producing axially prolonged light intensity distributions were introduced into optics by McLeod[1] for the first time in 1954. Because of their unique properties, generalized axicons have found several novel and potential uses both in research and commercial applications.[2] Recent fast developments in diffractive and micro-optical technologies have provided a basis for the penetration of generalized axicons into the field of holographic and computer simulated image processing devices. Holographic axicons have a number of attractive features, e.g. compact size, simplicity of fabrication, high efficiency of energy transformation (up to 90% for well designed multistep phase relief), that make these optical components promising for a variety of applications.

As a computer simulated diffractive optical element, a generalized axicon involves the calculation of multidimensional Fresnel integrals. In most cases the complexity of the integrand functions makes it impossible to perform the integrations analytically. Basically, one of the main properties of generalized axicons is their rotational symmetry, and this simplifies the numerical computation techniques to some extent. However, even so most currently applied simulation methods are fairly time consuming on computer and sometimes the calculation of the axicon image profiles becomes simply a formidable task. The difficulties grow especially with the decrease of the light coherence level. A classical radiometric approach using quite simple notions and expressions enables to overcome most of these difficulties, providing an efficient solution. The accuracy of the method increases when approaching natural (nearly incoherent) light. With partially coherent sources the radiometric model can be used to calculate both the intensity and spatial coherence distributions of the axicon images. The method is an asymptotic technique that relies on diffractive ray tracing and on rectilinear propagation of the generalized radiance.

Axicon design and radiometric model with partially coherent light

Traditionally the concept of a radiance function is formulated and applied for dealing with essentially noncoherent radiative transfer phenomena. Recently, however, it was demonstrated that the radiometric approach can be utilized also in the calculation of coherence propagation.[3] We use this method for the simulation of both the light intensity and the coherence degree distribution.

The generalized holographic axicon to be discussed is a rotationally symmetric synthetic hologram with a blocked central part. We consider a holographic axicon, designed to produce an axially uniform intensity distribution within

the region $d_1 < z < d_2$ (Fig. 1). The amplitude transmission function, providing the necessary phase shift of the incoming field, is described as

$$h(\rho) = t(\rho)\exp[ik\varphi(\rho)] , \qquad (1)$$

where k is the wave number and the phase function $\varphi(\rho)$ is expressed in the form of the logarithmic dependence[4]

$$\varphi(\rho) = -\tfrac{1}{2a}\log[d_1 + a(\rho^2 - R_1^2)] ; \qquad (2)$$

here $a = (d_2 - d_1)/(R_2^2 - R_1^2)$, and R_1 and R_2 are the radii of the aperture annulus. Actually, owing to the ripples originating from the axicon edges, the intensity distribution would not be uniform. To prevent these undesirable axial intensity perturbations we use an appropriate apodization function, given as follows:

$$t(\rho) = \{0.5 + \arctan[\Delta(R_2 - \rho)]/\pi\}\{0.5 + \arctan[\Delta(\rho - R_1)]/\pi\} , \qquad (3)$$

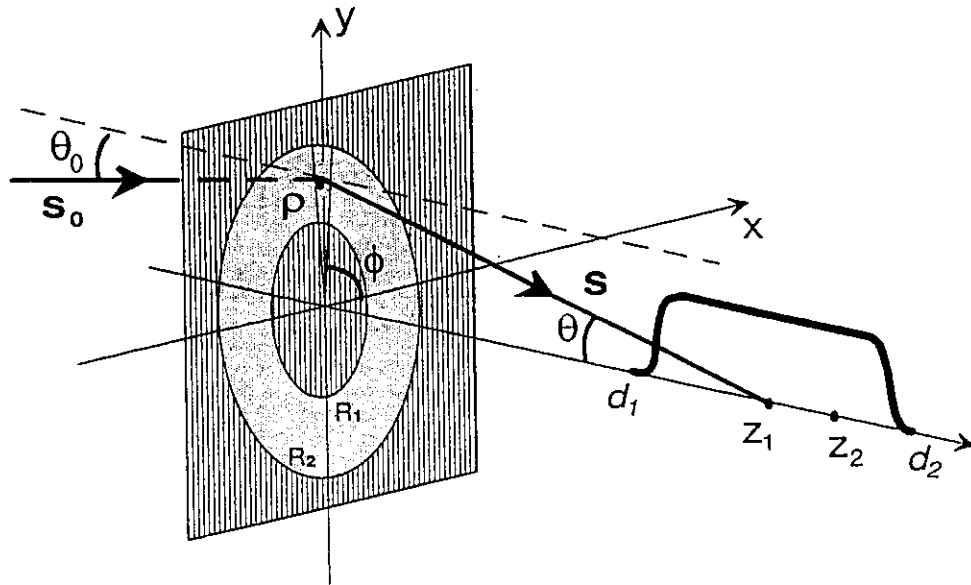with Δ being a suitable (dimensional) constant.

Fig. 1 Illustration of the geometry and notations associated with axial line-image
formation by an annular-apertured axicon.

Using the concept of generalized radiance[5] $B(r,s)$, the cross-spectral density of a fluctuating, statistically stationary, wavefield in the half-space $z > 0$ can be expressed as[3]

$$W(r_1, r_2) = \int B\left(\tfrac{r_1 + r_2}{2}, s\right)\exp[iks(r_2 - r_1)]d\Omega , \qquad (4)$$

where $s = (s_\perp, s_z)$ denotes a directional unit vector and the integration is over the 2π solid angle formed by all the directions such that $s_z > 0$. The optical intensity distribution at a point r can be calculated as the diagonal element of the cross-spectral density evaluated at r. It has been shown that in the asymptotic short-wavelength limit as $k = 2\pi/\lambda \to \infty$, the generalized radiance $B(r,s)$ obeys in free space the conventional equation of radiative transfer.[6]

Making use of this result the generalized radiance in Eq. (4) may then be replaced, within the asymptotic approximation, by

$$B\left(\frac{r_1+r_2}{2}, s\right) = B^{(0)}[\rho - (s_\perp z)/s_z, s] , \tag{5}$$

where the superscript (0) indicates the plane $z = 0$ and, physically, the spatial argument on the right-hand side is the projection onto this plane of the point $r = (r_1 + r_2)/2 = (\rho, z)$ along the direction s.

To calculate the cross-spectral density $W(r_1, r_2)$, we need to take into account the illumination and the operation of the holographic axicon. The general ray-tracing equations for a planar diffractive element characterized by a phase function $\varphi(\rho)$ are[7]

$$s_x(x, y) = s_{0x}(x, y) - \frac{\partial \varphi(x,y)}{\partial x} ,$$

$$s_y(x, y) = s_{0y}(x, y) - \frac{\partial \varphi(x,y)}{\partial y} , \tag{6}$$

where $s_0 = (s_{0x}, s_{0y}, s_{0z})$ and $s = (s_x, s_y, s_z)$ are unit direction vectors of the incident and diffracted rays at $\rho = (x, y)$, respectively. This procedure corresponds simply to the physical statement that at each point the ray direction is along the wavefront normal. The asymptotic form of the generalized radiance $B(r,s)$ is known to remain invariant along geometrical rays in arbitrary (lossless) paraxial systems, which means, that this relation holds true for the present diffractive axicon. Hence, if $B^{(0)}(\rho,s)$ denotes the asymptotic generalized radiance of the field emerging at $z = 0$ from the axicon, then $B^{(0)}(\rho,s) = B_0(\rho,s_0)$, where $B_0(\rho,s_0)$ is the generalized radiance of the irradiation. Finally, the generalized radiance $B_0(\rho,s_0)$ associated with the illumination, taken to be a homogeneous Gaussian correlated wave, is given by the expression[8]

$$B_0(\rho, s_0) = S_0 \frac{(k\sigma_g)^2}{2\pi} s_{0z} \exp\left[-\frac{1}{2}(k\sigma_g)^2 s_{0\perp}^2\right] , \tag{7}$$

where S_0 is the (constant) intensity of the incident beam, $s_{0z} = \cos\theta_0$ and $|s_{0\perp}| = \sin\theta_0$, and θ_0 is the angle that ray direction s_0 makes with the positive z axis. The parameter σ_g is the rms transverse coherence width of the illumination. The apodization function, mentioned above, can be taken into account simply by multiplying expression (7) by the function $|t(\rho)|^2$ from Eq. (3).

Now, combining all the considered components, we can write down the expression for the calculation of the light intensity (or spectral density) distribution in the form

$$S(r) = \int_\Omega B(\rho, z, s) d\Omega , \tag{8}$$

where $d\Omega$ is the solid angle from the point of observation toward the axicon elementary area of integration. To calculate the spatial coherence distribution we use the same cross-spectral concept [see Eq. (4)], and the general expression for the degree of coherence is as follows:

$$\mu(r_1, r_2) = W(r_1, r_2)/[S(r_1)S(r_2)]^{1/2} , \tag{9}$$

with $S(r)$ being the optical intensity (spectral density).

Results of the simulation of intensity and spatial coherence distributions

The space distribution of energy, as transformed by the axicon, can be calculated directly by using Eqs. (5)-(8). The integration is carried out over the aperture of the axicon. Results of the on-axis distributions of the spectral density based on the radiometric and the wave-theoretic models are illustrated in Fig. 2. We consider a sample uniform-intensity holographic axicon with the design parameters of $d_1 = 100$ mm, $d_2 = 200$ mm, $R_1 = 2.5$ mm, and $R_2 = 5.0$ mm. The wavelength corresponds to He-Ne laser radiation at $\lambda = 0.633$ μm. In fully coherent illumination the spectral density along the central axis of the axicon image is constant in average, but ringing occurs especially near the focal-line ends.
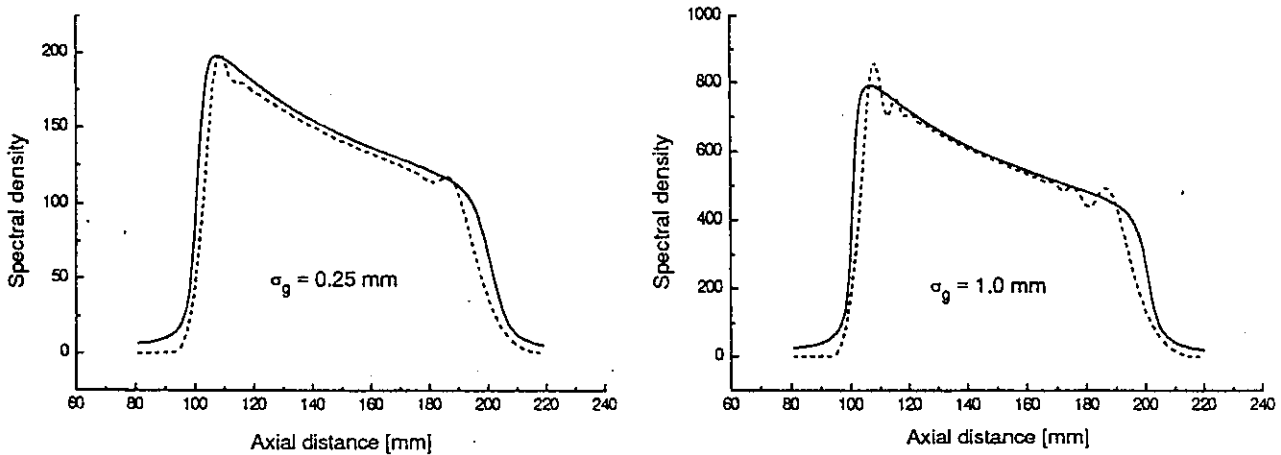

Fig. 2 On-axis spectral density distributions predicted by the radiometric model (solid line)
and the wave-theoretic model (dashed line) for an apodized annular axicon.

This ringing may be suppressed by using an appropriate apodization function on the surface of the axicon, as has been done. For the apodization in Eq. (3), the parameter value $\Delta = 20$ mm^{-1} was chosen. The ringing is also suppressed with the decreasing of the coherence of the illumination, but at the expense of a decrease in intensity. These effects are seen from Fig. 2, where both the wave-theoretic and radiometric results are shown for $\sigma_g = 1.0$ mm and $\sigma_g = 0.25$ mm, respectively. Comparison of the wave theory data with radiometrically obtained spectral density reveals the excellent accuracy of the latter method.
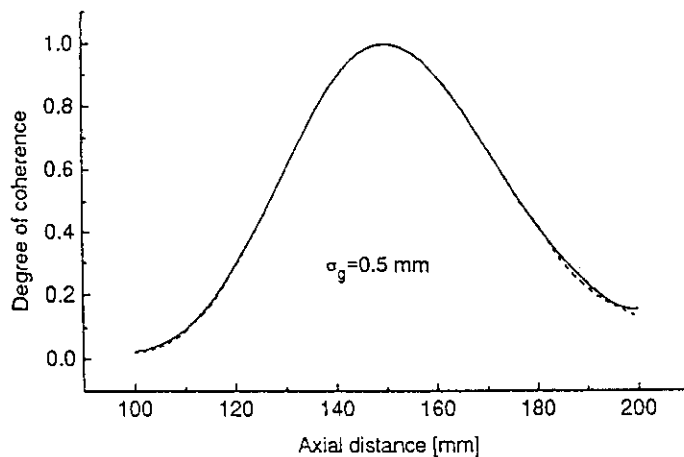

Fig. 3 On-axis distributions of the magnitude of the complex degree of spatial coherence both
for the radiometric (solid line) and the wave-theoretic (dashed line) results,
when one of the field points is located at $z = 150$ mm.

In Fig. 3 the magnitude of the on-axis complex degree of spatial coherence $|\mu(z_1, z_2)|$ is shown for $z_1 = 150$ mm, corresponding to the center of the focal line, while z_2 is varied throughout the image section from 100 mm to 200 mm (Fig. 1). Again, both the radiometric and the wave-theoretic results are plotted, but now for $\sigma_g = 0.5$ mm. Minor differences between the curves are observed at the far ends, but these disappear for smaller values of σ_g. Hence the present results confirm the remarkable accuracy of the radiometric method for axial correlations analysis in the small-coherence limit.
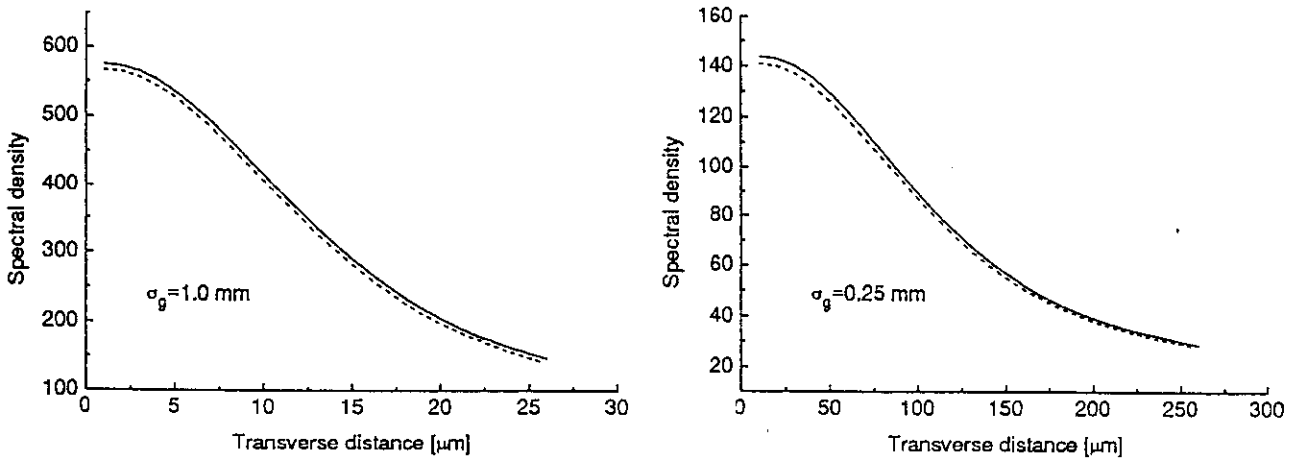

Fig. 4 Transverse distributions of the spectral density in the center of the image line, at z = 150 mm, based on the radiometric (solid line) and the wave-theoretic (dashed line) model.

Some typical results of the spectral density in a transverse plane across the line image produced by the sample logarithmic axicon are displayed in Fig. 4. Both the radiometric distribution and the corresponding wave-theoretic distribution of the spectral density $S(\rho, z)$ in the plane z = 150 mm are shown as a function of the transverse distance ρ. Again, it is seen that the radiometric and diffractive results agree substantially.
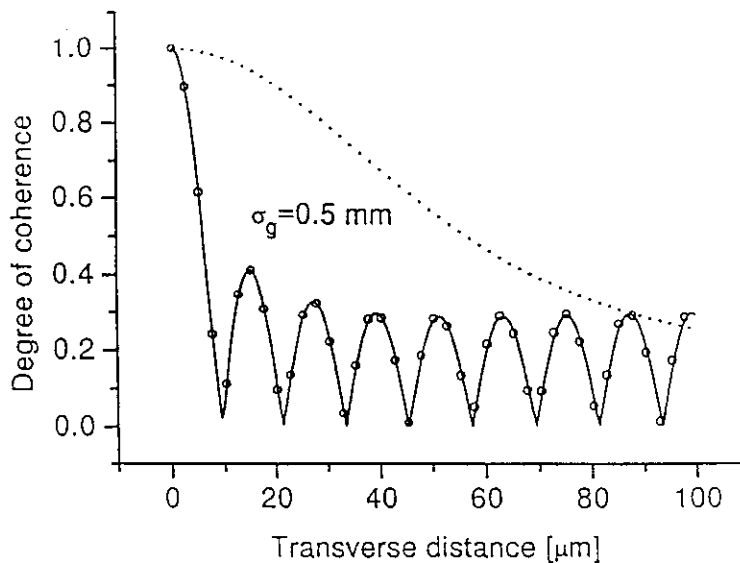

Fig. 5 Transverse distributions of the magnitude of the complex degree of spatial coherence at z = 150 mm, with one point is on the axis and the other varying along a radial direction. Both radiometric (solid line) and wave-theoretic (open circles) results are shown.

The absolute value of the complex degree of spatial coherence $|\mu(\rho_1,\rho_2,z)|$ in a transverse plane, defined in accordance with Eq. (9), is plotted in Fig. 5 again for $\sigma_g = 0.5$ mm, when $z = 150$ mm, $\rho_1 = 0$ (on axis), and ρ_2 is the transverse distance from the axis, that is allowed to vary. It is seen from the graphs that in transverse planes the axicon image is globally fairly incoherent, but as a consequence of the annular aperture the form of the spatial coherence differs markedly from that of the illumination. The degree of transverse coherence contains several sizable oscillations within the image width (shown in dotted line). In any case the radiometrically and wave-theoretically obtained results are found to match almost perfectly.

Conclusions

A simple and physically intuitive radiometric model that includes also the effects of partial coherence was applied to the line-image formation by generalized holographic axicons. The results demonstrate that compared with the usual partially coherent diffraction calculations, the present method provides in normal circumstances considerable simplifications without any sacrifice on the accuracy. The radiometric technique is derived from asymptotic considerations and it involves only a single straightforward integration over the axicon aperture, as opposed to a double integration of strongly oscillating functions in the stochastic wave theory. One of the most important advantages of the suggested radiometric method is the saving of computing time, which is a significant aspect in conditions when the spatial coherence level of the illumination, and of the image, are relatively low. This may correspond to controlled-coherence radiation from thermal sources, high-power laser diodes, or other multi-mode lasers. The graphs presented in the work attest to the nearly immaculate accuracy with which the modified radiometric theory yields the optical intensity and, in particular, the complex degree of spatial coherence characterizing the practical axicon line images at optical wavelengths.

References

1. John H. McLeod, "The axicon: a new type of optical element", *J. Opt. Soc. Am.*, 44(1954), pp. 592-597.
2. L.M. Soroko, "Axicons and meso-optical imaging devices", in *Progress in Optics*, vol. XVIII, ed. E. Wolf (Elsevier, Amsterdam, 1989), pp. 109-160.
3. E. Wolf, "Radiometric model for propagation of coherence", *Opt. Lett.*, 19(1994), pp. 2024-2026.
4. Z. Jaroszewicz, J. Sochacki, A. Kolodziejczyk, and L.R. Staronski, "Apodized annular-aperture logarithmic axicon: smoothness and uniformity of intensity distributions", *Opt. Lett.*, 18(1993), pp. 1893-1895.
5. A. Walther, "Radiometry and coherence", *J. Opt. Soc. Am.*, 58(1968), pp. 1256-1258.
6. K. Kim and E. Wolf, "Propagation law for Walther's first generalized radiance function and its short-wavelength limit with quasihomogeneous sources", *J. Opt. Soc. Am. A*, 4(1987), pp. 1233-1236.
7. R.C. Fairchild and J.R. Fienup, "Computer-originated aspheric holographic optical elements", *Opt. Eng.*, 21(1982), pp. 133-140.
8. J.T. Foley and E. Wolf, "Radiometry with quasihomogeneous sources", *J. Mod. Opt.*, 42(1995), pp. 787-798.

Asymptotic radiometry for spectral density and coherence in gaussian quasihomogeneous beams

Ari T. Friberg*

Technische Universität Berlin, Optisches Institut, Strasse des 17. Juni 135, D-10623, Berlin, Germany

ABSTRACT

The asymptotic radiometric theories formulated recently by Foley and Wolf for the spectral density and (spatial) coherence are applied to the Gaussian Schell-model and quasihomogeneous sources. Since the properties of the beam-like wavefields produced by these sources in free space are known explicitly, this allows for an assessment of the accuracy of the radiometric models. Profiles both along the propagation axis and in planes transverse to the beam are examined in detail. The graphs indicate that already with relatively small sources (beam waists), corresponding to substantial beam divergence, the radiometric models yield highly accurate results. The advantage of the radiometric theory is the (computational) simplicity by which the spectral density and coherence are obtained for fields radiated by arbitrary sources.

1. INTRODUCTION

The so-called Gaussian Schell-model (GSM) beams possess several features that make them appealing to both theoreticians and experimentalists alike [1]. Mathematical analyses associated with these beams can often be carried out explicitly in a closed form and the GSM beam fields are readily generated in the laboratory by a number of techniques. As the degree of spatial coherence is varied, the GSM beams bridge in a continuous manner the gap between the fully coherent Gaussian beams and fully incoherent light described by geometrical optics. Those GSM beams that are spatially relatively incoherent (in relation to the beam width) form the class of

Gaussian quasihomogeneous (GQH) beams [2]. Owing to the many convenient properties, the GSM and GQH beam-like wavefields have been used as test cases and reference yardsticks in a great variety of theoretical and practical situations. The applications of these wavefields include:

- Foundations of radiometry. The GSM sources and beams have served as principal physical models in the elucidations of generalized radiometry with partially coherent wavefields [3,4]. Specific topics have dealt e.g. with radiation directionality [5–7], beam characterization [8, 9], radiation efficiency [10, 11], and second-order radiometry [12].

- Focusing. The effects of partial coherence on the spot size, focal depth, and focus shift have been studied theoretically [13] and experimentally [14] in GSM beam imaging.

- Coherent modes. The GSM beams are one of the few fields for which the so-called coherent-mode decomposition is known explicitly [15, 16].

- Twists. Recently a new phenomenon, viz., a twist induced by partial coherence, was discovered on the GSM beams [17–19]

- Multimode lasers. The GSM beam fields have been applied as characteristic models for (high power) multimode laser radiation [20,21].

- Nonlinear optics and active media. These beams are utilized in studies of the effects of correlations in materials interactions [22,23].

We recall in passing also that an efficient method, based

*Permanent address: Helsinki University of Technology, Department of Technical Physics, FIN-02150 Espoo, Finland

on electronically synthesized acousto-optic holograms, was developed not long ago for a controlled generation of arbitrary GSM beams [24].

In this paper we make use of the spatially partially coherent GSM and GQH beams in yet another application, namely the illustration and assessment of certain radiometric theories that were put forward quite recently by Foley and Wolf [25, 26]. Unlike in the conventional radiation transport, these radiometric models account for the source coherence properties and deal, in the asymptotic short-wavelength limit, not only with the propagation of the spectral density and the energy flux but also with the propagation of the spectral coherence in scalar wavefields produced by (secondary) quasihomogeneous sources. We apply these radiometric descriptions to the GSM beams in the quasihomogeneous regime and show that in a majority of cases they produce with an impeccable accuracy the spectral density and spatial coherence distributions of the wavefields. From these results we may infer that the asymptotic radiometric theories can be usefully applied in practical situations of radiation, scattering, and propagation of optical radiation.

2. RADIOMETRIC MODELS FOR SPECTRAL DENSITY AND COHERENCE

We begin by recalling the main features of the recently proposed asymptotic radiometric models for the propagation of the spectral density and the spatial coherence [25, 26]. For simplicity, we restrict the analysis here to situations in which the evanescent waves involved in the angular-spectrum representations play a negligible role, i.e., effectively to free fields. This assumption is consistent with the beam-like nature of the fields to which the radiometric models are then later applied.

A generalized radiance (at frequency ω) associated with a statistically stationary scalar wavefield can be defined as [26, 27]

$$B(\mathbf{r}, \mathbf{s}) = s_z \int A(\mathbf{s}_\perp - \mathbf{s}_\perp'/2, \mathbf{s}_\perp + \mathbf{s}_\perp'/2)$$
$$\times \exp(iks_\perp' \cdot \mathbf{r}) d^2 s_\perp'. \qquad (1)$$

where $k = \omega/c$ is the (free-space) wave number and $\mathbf{s} = (\mathbf{s}_\perp, s_z)$ is a directional unit vector with $s_z > 0$. The quantity $A(\mathbf{s}_{1\perp}, \mathbf{s}_{2\perp})$ is the angular correlation function that is related to the cross-spectral density $W(\mathbf{r}_1, \mathbf{r}_2)$ of the wavefield through the formula

$$W(\mathbf{r}_1, \mathbf{r}_2) = \iint A(\mathbf{s}_{1\perp}, \mathbf{s}_{2\perp})$$
$$\times \exp[ik(\mathbf{s}_2 \cdot \mathbf{r}_2 - \mathbf{s}_1 \cdot \mathbf{r}_1)]$$
$$\times d^2 s_{1\perp} d^2 s_{2\perp}, \qquad (2$$

where $\mathbf{s}_1$ and $\mathbf{s}_2$ are (real) unit vectors. Since the evanescent waves are neglected, integration is performed only over the domains $|\mathbf{s}_{1\perp}| \leq 1$ and $|\mathbf{s}_{2\perp}| \leq 1$. In terms of the generalized radiance function $B(\mathbf{r}, \mathbf{s})$, the cross-spectral density then becomes [26]

$$W(\mathbf{r}_1, \mathbf{r}_2) = \int B\left(\frac{\mathbf{r}_1 + \mathbf{r}_2}{2}, \mathbf{s}\right)$$
$$\times \exp[iks \cdot (\mathbf{r}_2 - \mathbf{r}_1)] d\Omega, \qquad (.$$

where $d\Omega = d^2 s_\perp / s_z$ is a differential element of the solid angle. From Eq. (3), the spectral density $S(\mathbf{r}) = W(\mathbf{r}_1, \mathbf{r})$ is obtained as [25]

$$S(\mathbf{r}) = \int B(\mathbf{r}, \mathbf{s}) d\Omega, \qquad ($$

which is recognized as the usual expression for the spatial density of radiation in the conventional theory of radiative energy transfer. In Ref. [25] an analogous formula derived also for the average flux vector (using a slightly different generalized radiance function), but in this paper we are not concerned with it.

Equation (3) is the starting point of the present analysis. Let us assume that the field in $z > 0$ is generated by a quasihomogeneous source σ located in the plane $z = 0$. In the asymptotic (short-wavelength) limit as $k = 2\pi/\lambda \to \infty$, the radiance function $B(\mathbf{r}, \mathbf{s})$ obeys the traditional equation of free-space radiative transfer [2], i.e., $(\mathbf{s} \cdot \nabla) B(\mathbf{r}, \mathbf{s}) = 0$. Using this result the function $B(\mathbf{r}, \mathbf{s})$ at an arbitrary point $\mathbf{r}$, in a direction $\mathbf{s}$ such that $s_z > 0$ can readily be projected, as if along a geometrical ray, onto the source plane. More specifically, if we let $\mathbf{r} = (\mathbf{r}_1 + \mathbf{r}_2)/2 = (\rho, z)$, define $\rho_0 = \rho - (\mathbf{s}_\perp z)$ (see Fig. 1), and denote by $B^{(0)}(\rho_0, \mathbf{s})$ the source radiance function, one can readily show that, in the asymptotic limit, the cross-spectral density given by Eq. (3) becomes [26]

$$W(\mathbf{r}_1, \mathbf{r}_2) = \int_\sigma \frac{B^{(0)}(\rho_0, \mathbf{s})}{R^2}\left(\frac{z}{R}\right)$$
$$\times \exp[iks \cdot (\mathbf{r}_2 - \mathbf{r}_1)] d^2 \rho_0.$$

where $\mathbf{R} = \mathbf{r} - \rho_0$, $R = |\mathbf{R}|$, and now $\mathbf{s} = \mathbf{R}/R$.
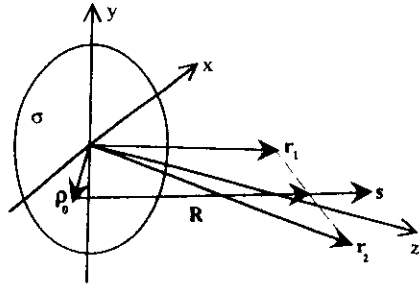
Figure 1. Illustration of the general geometry and notations for a radiometric calculation of the spectral density and the spatial coherence.

asymptotic expression for the spectral density then is [25]

$$S(\mathbf{r}) = \int_\sigma \frac{B^{(0)}(\rho_0,\mathbf{s})}{R^2} \left(\frac{z}{R}\right) d^2\rho_0. \qquad (6)$$

We recall that the radiance function $B^{(0)}(\rho_0,\mathbf{s})$ associated with a quasihomogeneous planar source is known to satisfy all the requirements of conventional radiometry [29]. This property is shared, as is evident from the explicit expression [29], also by the generalized radiance of an arbitrary GSM source. Using Eqs. (5) and (6) the spectral degree of coherence at a pair of field points then is obtained as [30,31]

$$\mu(\mathbf{r}_1,\mathbf{r}_2) = W(\mathbf{r}_1,\mathbf{r}_2)/\sqrt{S(\mathbf{r}_1)S(\mathbf{r}_2)}, \qquad (7)$$

and this quantity is bounded in magnitude between 0 and 1 in the usual way. The limiting values 0 and 1 represent completely incoherent and completely coherent fields (at frequency ω), respectively.

3. GAUSSIAN SCHELL-MODEL AND QUASIHOMOGENEOUS BEAMS

The beam-like wavefields generated by Gaussian quasi-homogeneous sources in accordance with the paraxial wave equation (Fresnel diffraction) constitute the GQH beams. The planar GSM source at $z = 0$ is characterized by Gaussian functions of the spectral density and of the degree of transverse coherence with the rms-widths of σ_S and σ_g, respectively, and in the quasihomogeneous limit $\sigma_S \gg \sigma_g$. Explicit formulas are available in the literature both for the transverse and the longitudinal distributions of the cross-spectral density associated with the GSM beams [2,32].

The cross-spectral density, at points ρ_1 and ρ_2 in a transverse plane $z = $ constant ≥ 0, across a GSM beam is expressible in the form [32]

$$
\begin{aligned}
W_t(\rho_1,\rho_2;z) = \ & \frac{A}{[\Delta(z)]^2} \exp\left\{ -\frac{(\rho_1+\rho_2)^2}{8\sigma_S^2[\Delta(z)]^2} \right\} \\
& \times \ \exp\left\{ -\frac{(\rho_1-\rho_2)^2}{2\sigma_t^2[\Delta(z)]^2} \right\} \\
& \times \ \exp[i\varphi(\rho_1,\rho_2;z)],
\end{aligned}
\qquad (8)
$$

where

$$\Delta(z) = \left[1 + \left(\frac{z}{k\sigma_S\sigma_t}\right)^2 \right]^{1/2}, \qquad (9)$$

$$\varphi(\rho_1,\rho_2;z) = \frac{z}{2k\sigma_S^2\sigma_t^2[\Delta(z)]^2}(\rho_2^2 - \rho_1^2), \qquad (10)$$

and

$$\frac{1}{\sigma_t^2} = \frac{1}{4\sigma_S^2} + \frac{1}{\sigma_g^2}. \qquad (11)$$

Clearly, A is a constant that denotes the spectral density at the origin. When $\sigma_S \gg \sigma_g$, we find from Eq. (11) that $\sigma_t \approx \sigma_g$ and the expression for $W_t(\rho_1,\rho_2;z)$ above then reduces to the result given also in Ref. [2] for GQH beams.

Equations (8)–(11) imply that the beam and its transverse coherence expand on propagation, while the on-axis spectral density decays so that energy is conserved. One can show that in any transverse plane the distributions of the spectral density $S(\rho,z)$ and the magnitude of the complex degree of coherence $|\mu_t(\rho_1,\rho_2;z)| = g(\rho_2 - \rho_1,z)$ are Gaussian functions, and that the ratio of their rms-widths is independent of the propagation distance [32]. Hence in each plane the ratio of the coherence width to the beam width is given by the source-plane value $\alpha = \sigma_g/\sigma_S$, known as the global degree of coherence [2,32].

The cross-spectral density of a GSM beam at equal transverse points ρ but in different planes $z = z_1$ and $z = z_2$ with $z_j \geq 0$ ($j = 1,2$) can be expressed as [32]

$$
\begin{aligned}
W_t(\rho;z_1,z_2) = \ & \frac{A}{[\Delta(z_1,z_2)]^2} \\
& \times \ \exp\left\{ -\left(\frac{1}{2\sigma_S^2} + i\frac{z_2 - z_1}{2k\sigma_S^2\sigma_t^2} \right) \right. \\
& \times \left. \frac{\rho^2}{[\Delta(z_1,z_2)]^2} \right\},
\end{aligned}
\qquad (12)
$$

where

$$\Delta(z_1, z_2) = \left[1 + \frac{z_1 z_2}{(k\sigma_S \sigma_I)^2} + i \left(\frac{z_2 - z_1}{k\sigma_I^2} \right) \right]^{1/2}, \quad (13)$$

$$\frac{1}{\sigma_I^2} = \frac{1}{2\sigma_S^2} + \frac{1}{\sigma_g^2}, \quad (14)$$

and σ_I is given by Eq. (11). The longitudinal coherence properties along the positive z-axis are obtained from Eqs. (12)–(14) by setting $\rho = 0$. We recall that the degree of spatial coherence $|\mu_I(0;0,z)|$, defined in accordance with Eq. (7), between the field fluctuations at the origin and at a positive on-axis point approaches $\sigma_I^2/\sigma_S \sigma_I$ as the distance $z \to \infty$. The behavior of the longitudinal coherence generally is analyzed in detail in Ref. [32].

We note that an interesting formula was recently derived for the axial dependence of the spectral degree of spatial coherence in the case when the planar source is substantially incoherent [33]. Sufficiently far away from the source (so that the paraxial approximation holds), the on-axis cross-spectral density takes on the form

$$W_{\text{inc}}(0; z_1, z_2) \approx \frac{k^2}{8\pi^2 z_1 z_2} e^{ik(z_2 - z_1)}$$

$$\times \int_0^\infty \tilde{S}(\sqrt{\rho}; 0)$$

$$\times \exp\left[i\frac{k}{2} \left(\frac{1}{z_2} - \frac{1}{z_1} \right) \rho \right] d\rho, \quad (15)$$

where

$$\tilde{S}(\sqrt{\rho}; 0) = \int_0^{2\pi} S(\sqrt{\rho}, \theta; 0) \, d\theta, \quad (16)$$

and $S(\sqrt{\rho}, \theta, 0)$ is the source spectral density expressed in polar coordinates $\rho = (\rho, \theta)$, as a function of $\sqrt{\rho}$. For a GSM source we obtain from Eq. (8) simply that

$$\tilde{S}(\sqrt{\rho}; 0) = 2\pi A \exp\left[-\rho/2\sigma_S^2 \right]. \quad (17)$$

It is seen from Eqs. (7) and (15) that the complex degree of spatial coherence $\mu_{\text{inc}}(0; z_1, z_2)$ along the beam propagation axis now is effectively a Fourier transform of the source intensity function $\tilde{S}(\sqrt{\rho}; 0)$, with the transform variable being proportional to $(z_1 - z_2)/z_1 z_2$. The longitudinal coherence can be measured using interferometric systems and it has applications e.g. in spectroscopy and holography [33].

4. RADIOMETRY OF GAUSSIAN QUASIHOMOGENEOUS SOURCES

Now we have an opportunity to make use of results in plied by the general wave-theoretical expressions (8) a (12) to test explicitly the validity of the asymptotic diometric model outlined in Sec. 2. For a GSM pla source located at $z = 0$ the generalized radiance functi $B^{(0)}(\rho_0, s)$ is given by [4]

$$B^{(0)}(\rho_0, s) = \frac{A}{2\pi} k^2 \sigma_I^2 \exp\left[-\frac{\rho_0^2}{2\sigma_S^2} \right]$$

$$\times \cos\theta \exp\left[-\frac{1}{2} k^2 \sigma_I^2 \sin^2\theta \right], \quad ($$

where θ is the angle that vector s makes with the posit z-axis and the parameter σ_I is obtained from Eq. (1 hence the generalized radiance $B^{(0)}(\rho_0, s)$ carries inf mation about the state of coherence of the source. GQH planar sources σ_I assumes the value σ_g, repres ing directly the source's transverse correlation width.

We substitute Eq. (18) into Eqs. (5)–(7), and consi both the spectral density and spatial coherence separat along the beam axis and in planes perpendicular to it

4.1. On-Axis Profiles of Intensity and Coherence

When the observation points r_1 and r_2 are on the b axis, say at z_1 and z_2, respectively, the geometry a ciated with the asymptotic radiometric calculations comes rotationally symmetric (Fig. 2). In this case ply $R = (z^2 + \rho_0^2)^{1/2}$, and on substituting from Eq. to Eq. (5) we find that

$$W_I(0; z_1, z_2) = Ak^2\sigma_I^2 \int \frac{\exp(-\rho_0^2/2\sigma_S^2)}{(z^2 + \rho_0^2)}$$

$$\times \cos^2\theta \exp[-k^2\sigma_I^2 \sin^2\theta/2]$$

$$\times \exp[ik\cos\theta(z_2 - z_1)]\rho_0 d\rho_0,$$

where

$$\cos\theta = z/(z^2 + \rho_0^2)^{1/2} = s_z,$$

$$\sin\theta = \rho_0/(z^2 + \rho_0^2)^{1/2} = s_\perp,$$

and the azimuthal part has been integrated away. S ilarly, for the on-axis spectral density we obtain f Eqs. (18) and (6) [or directly from Eq. (19) by se
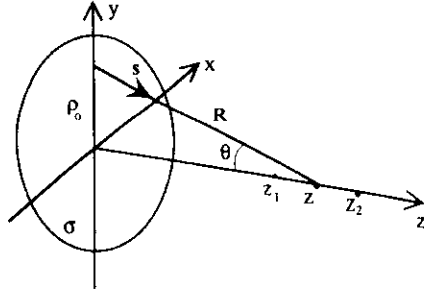
Figure 2. Notation for the calculation of the on-axis spectral density and coherence.

$z_1 = z_2 = z$] the expression

$$S(0;z) = Ak^2\sigma_t^2 \int \frac{\exp(-\rho_0^2/2\sigma_S^2)}{(z^2+\rho_0^2)}$$
$$\times \cos^2\theta\exp[-k^2\sigma_t^2\sin^2\theta/2]\rho_0 d\rho_0. \quad (20)$$

The complex degree of spatial coherence $\mu_l(0;z_1,z_2)$ is then computed on the basis of Eq. (7). The radial integrations in Eqs. (19) and (20) are performed numerically from 0 to some maximum value determined by σ_S.

Some typical results are shown in Figs. 3 and 4. Since the characteristic behavior of GSM and GQH beams is well documented, we focus here on the accuracy of the radiometric method. Thus, the curves in Fig. 3 illustrate the percentage error in the on-axis spectral density, i.e., the quantity

$$d_{lS}(z) = 100 \cdot \left(\frac{S_R - S_W}{S_W}\right), \quad (21)$$

where $S_R(z)$ and $S_W(z)$ are obtained from Eqs. (20) and (8), respectively. The size of the beam at the waist is $\sigma_S = 100\lambda$, and the correlation widths are $\sigma_g = 1.0\sigma_S$, $0.5\sigma_S$, $0.2\sigma_S$, and $0.1\sigma_S$, running from top to bottom in the figure. The maximum propagation distance shown is the Rayleigh range $z_R = 2k\sigma_S^2$ of a corresponding fully coherent beam. Hence with quasihomogeneous beams the axial intensity decays several orders of magnitude, but the radiometric method nonetheless yields the result with a precision better than a tiny fraction of a percent. The accuracy improves with larger source sizes σ_S.

Similarly, the curves in Fig. 4 illustrate the accuracy of the generalized radiometric technique in the calculation of the degree of spatial coherence along the beam

axis. Plotted are the values of the percentage error

$$d_{l\mu}(z_1,z_2) = 100 \cdot \left(\frac{|\mu_R| - |\mu_W|}{|\mu_W|}\right), \quad (22)$$

where $|\mu_R(0;z_1,z_2)|$ and $|\mu_W(0;z_1,z_2)|$ are found numerically on the basis of Eqs. (19) and (8), respectively. The parameters are the same as in Fig. 3 (from top to bottom, as before), except that $z_1 = 2\sigma_S$ and z_2 now varies from $0.5\sigma_S$ to σ_S^2/λ. Again, with quasihomogeneous beams the longitudinal coherence varies considerably over the plotting distance (while increases in σ_g or z_1 naturally reduce the scale of this variation). The accuracy of the radiometric technique is seen to remain excellent.

In Fig. 5 we illustrate the degree of on-axis spatial coherence in a wavefield generated by an effectively incoherent Gaussian source; the bottom curve is $|\mu(0;z_1,z_2)|$ as computed from Eqs. (15) and (7) for $\sigma_S = 100\lambda$, $z_1 = \sigma_S^2/\lambda$, and z_2 ranging from $0.75z_1$ to $1.25z_2$. The generalized radiometric results for $\sigma_g = 0.1\sigma_S$ (top curve) and $\sigma_g = 0.05\sigma_S$ (middle curve) are shown for comparison. It is obvious that the radiometrically obtained results approach the incoherent-source curve as $\sigma_g \to 0$.

4.2. Transverse Profiles of Intensity and Coherence

For the evaluations of the transverse distributions we consider, for simplicity, the geometry illustrated in Fig. 6. One of the observation points is at distance z on the beam axis, while the other is taken (owing to the symmetry) at a separation ρ along the y-axis. Consequently, in this case $R = [z^2 + \rho_{0x}^2 + (\rho/2 - \rho_{0y})^2]^{1/2}$, and we find from
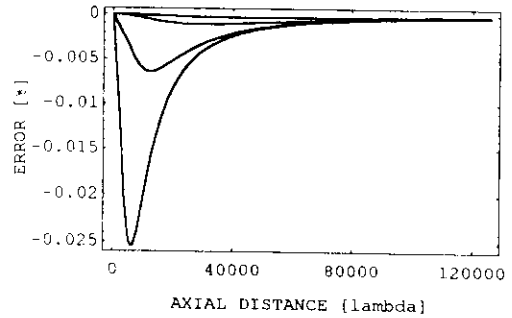

Figure 3. Accuracy of the radiometrically obtained spectral density on the beam axis for a GSM source of waist size $\sigma_S = 100\lambda$ and global degree of coherence $\alpha = \sigma_g/\sigma_S = 1.0, 0.5, 0.2$, and 0.1, from top to bottom, respectively.
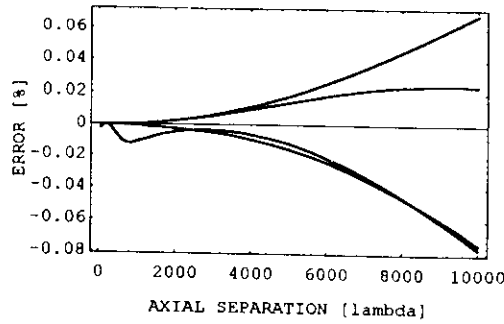
Figure 4. Accuracy of the radiometrically obtained degree of spatial coherence along the beam axis when one point is close to the waist at $z_1 = 2\sigma_S$. The beam parameters corresponding to the curves are, from top to bottom, the same as in Fig. 3.
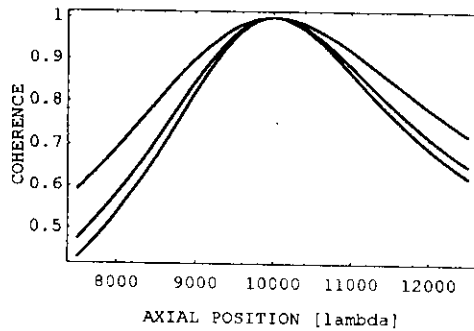

Figure 5. Comparison of the degree of spatial coherence in GQH beams of $\sigma_S = 100\lambda$ and $\alpha = 0.1$ (top curve), $\alpha = 0.05$ (middle curve) with the result in the wavefield produced by a spatially incoherent source (bottom curve, $z_1 = z_R/4\pi$).
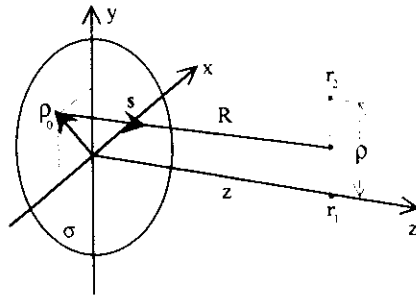

Figure 6. Notation for the calculation of the spectral density and coherence in planes perpendicular to the beam.

Eqs. (5) and (18) that

$$W_t(0,\rho;z) = \frac{A}{2\pi}k^2\sigma_t^2 \iint \frac{\exp(-\rho_0^2/2\sigma_S^2)}{R^2}$$
$$\times \quad \cos^2\theta\exp[-k^2\sigma_t^2\sin^2\theta/2]$$
$$\times \quad \exp[ik\rho(\rho/2 - \rho_{0y})/R]d\rho_{0x}d\rho_{0y}, \quad (23)$$

where $\rho_0 = (\rho_{0x}^2 + \rho_{0y}^2)^{1/2}$ and now

$$\cos\theta = z/R,$$

$$\sin\theta = [\rho_{0x}^2 + (\rho/2 - \rho_{0y})^2]^{1/2}/R.$$

The spectral density is likewise given by

$$S(\rho,z) = \frac{A}{2\pi}k^2\sigma_t^2 \iint \frac{\exp(-\rho_0^2/2\sigma_S^2)}{R^2}$$
$$\times \quad \cos^2\theta\exp[-k^2\sigma_t^2\sin^2\theta/2]d\rho_{0x}d\rho_{0y}, \quad (24)$$

in which R, $\sin\theta$, and $\cos\theta$ are evaluated for point (ρ,z). The complex degree of spatial coherence $\mu_t(0,\rho;z)$ is then again computed in accordance with Eq. (7).

Characteristic results on the transverse distributions are displayed in Figs. 7 and 8. Within the paraxial theory the GSM (and GQH) beam possesses at each plane $z = $ constant a Gaussian intensity variation and the global degree of coherence, $\alpha = \sigma_g/\sigma_S$, remains invariant on propagation. In Fig. 7 we illustrate the percentage error $d_{tS}(\rho)$, defined in complete analogy of Eq. (21) where now $S_R(\rho,z)$ and $S_W(\rho,z)$ are obtained from Eqs. (24) and (8), respectively. The beam parameters σ_S and σ_g (labeling curves from top to bottom) are as in Fig. 3; the propagation distance $z = 2k\sigma_S^2$ is the corresponding fully coherent Rayleigh range. At the maximum transverse distance shown the intensity of the GQH beam with $\alpha = 0.1$ has decreased to 0.61 times of its on-axis value. Since the beams of higher degree of coherence have by that point decayed considerable more, the slight increase in the relative error of the spectral density seen in the graphs is of no practical significance.

In Fig. 8 the analogous percentage error $d_{t\mu}(0,\rho)$ of the transverse distribution of the absolute magnitude of the complex degree of spatial coherence is shown. The quantity $d_{t\mu}(0,\rho)$ is defined as in Eq. (22), but $\mu_R(0,\rho;z)$ and $\mu_W(0,\rho;z)$ are computed on the basis of Eqs. (23) and (8), respectively, using also the definition (7) of the complex degree of coherence. The propagation distance z as well as the beam parameters σ_S and σ_g are the same as in Fig. 7, but this time the curves are labeled from bot-
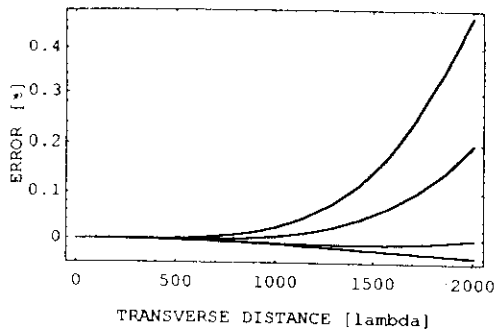
Figure 7. Accuracy of the radiometrically obtained spectral density in a transverse plane, at distance $z = z_R = 2k\sigma_s^2$, of a GSM beam of waist size $\sigma_S = 100\lambda$. For the curves the global degree of coherence, $\alpha = \sigma_g/\sigma_S$, assumes from top to bottom the values $\alpha = 1.0, 0.5, 0.2$, and 0.1, respectively.
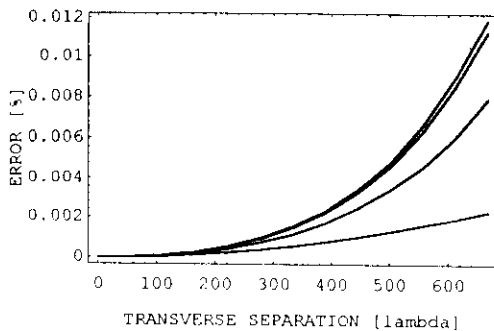

Figure 8. Accuracy of the radiometrically obtained degree of spatial coherence in a transverse plane of a GSM beam when one point is on axis. The geometry and beam parameters are as in Fig. 7, but the global degree of coherence α in curves now decreases from 1.0 to 0.1 going from bottom to top.

tom to top, i.e., the largest error occurs with the smallest degree of global coherence. In each case the degree of spatial coherence at the maximum separation shown in Fig. 8 has fallen to a tiny fraction of its on-axis value (equal to unity). Figures 7 and 8 demonstrate once again that the asymptotic radiometric models are remarkably accurate even in circumstances in which the intensity or coherence attain only very small values.

5. DISCUSSION AND CONCLUSIONS

In this paper we have reviewed a generalized radiometric theory proposed by Foley and Wolf [25,26] for the calculation of the spectral density and the spatial coherence in wavefields generated by quasihomogeneous sources (or, more generally, by sources whose generalized radiance is nonnegative). This radiometric theory, which is not restricted to paraxial waves but holds only in the asymptotic sense as the wavelength $\lambda \to 0$, makes use of simple ray-tracing equations. Hence the calculation of the intensity and coherence distributions in most cases is quick and efficient. The accuracy of these radiometric models has been assessed against earlier analytic results pertaining to paraxial Gaussian Schell-model (GSM) or quasihomogeneous (GQH) beams.

The computations shown in this paper were carried out using a 486 personal computer and Mathematica software with the default precision (16 digits). The results demonstrate that already with relatively small sources (rms beam waist $\sigma_S = 100\lambda$) the asymptotic radiometric theories yield the spectral density and, especially, the spatial coherence with amazing precision for beam fields with varying degrees of global coherence. Furthermore, the calculations indicate that the accuracy generally improves when the source size is increased. The main advantage of these radiometric models, however, is the superior computational speed as compared with the usual diffractive calculations of field intensity and coherence. Similar conclusions were obtained in recent related studies, in which these radiometric theories were applied to the extended line images generated in partially coherent light by generalized holographic axicons [34,35].

ACKNOWLEDGMENTS

REFERENCES

[1] A.T. Friberg, ed., Selected Papers on Coherence and Radiometry, Milestone Series Vol. 69, SPIE Opt. Eng. Press, Bellingham, VA (1993).

[2] E. Collett and E. Wolf, Opt. Commun. 32, 27 (1980).

[3] E. Wolf, J. Opt. Soc. Am. 68, 7 (1978).

[4] H.P. Baltes and B. Steinle, Nuovo Cimento B 41,

428 (1977).

[5] P. De Santis, F. Gori, G. Guattari, and C. Palma, Opt. Commun. 29, 256 (1979).

[6] J.D. Farina, L.M. Narducci, and E. Collett, Opt. Commun. 32, 203 (1980).

[7] J. Deschamps, D. Courjon, and J. Bulabois, J. Opt. Soc. Am. 73, 256 (1983).

[8] A.T. Friberg and R.J. Sudol, Opt. Commun. 41, 383 (1982).

[9] R. Simon, N. Mukunda, and E.C.G. Sudarshan, Opt. Commun. 65, 322 (1988).

[10] A. Gamliel, Opt. Commun. 60, 333 (1986).

[11] T. Shirai and T. Asakura, J. Mod. Opt. 40, 1143 (1993).

[12] H.P. Baltes and B. Steinle, Nuovo Cimento B 44, 423 (1978).

[13] A.T. Friberg and J. Turunen, J. Opt. Soc. Am. A 5, 713 (1988).

[14] Q. He, J. Turunen, and A.T. Friberg, Opt. Commun. 67, 245 (1988).

[15] F. Gori, Opt. Commun. 34, 301 (1980).

[16] A. Starikov and E. Wolf, J. Opt. Soc. Am. 72, 923 (1982).

[17] R. Simon and N. Mukunda, J. Opt. Soc. Am. A 10, 95 (1993).

[18] A.T. Friberg, E. Tervonen, and J. Turunen, J. Opt. Soc. Am. A 11, 1818 (1994).

[19] D. Ambrosini, V. Bagini, F. Gori, and M. Santarsiero, J. Mod. Opt. 41, 1391 (1994).

[20] S. Lavi, R. Prochaska, and E. Keren, Appl. Opt. 27,

3696 (1988).

[21] R. Gase, J. Mod. Opt. 38, 1107 (1991).

[22] M. Zahid and M.S. Zubairy, Opt. Commun. 76, 1 (1990).

[23] C. Palma, P. De Santis, G. Cincotti, and G. Guattari, J. Mod. Opt. 43, 139 (1996).

[24] J. Turunen, E. Tervonen, and A.T. Friberg, J. Appl. Phys. 67, 49 (1990).

[25] J.T. Foley and E. Wolf, J. Mod. Opt. 42, 787 (1995).

[26] E. Wolf, Opt. Lett. 19, 2024 (1994).

[27] A. Walther, J. Opt. Soc. Am. 58, 1256 (1968).

[28] K. Kim and E. Wolf, J. Opt. Soc. Am. A 4, 1233 (1987).

[29] W.H. Carter and E. Wolf, J. Opt. Soc. Am. 67, 785 (1977).

[30] L. Mandel and E. Wolf, J. Opt. Soc. Am. 66, 529 (1976).

[31] L. Mandel and E. Wolf, Optical Coherence and Quantum Optics, Cambridge Univ. Press (1995), Sect. 4.3.2.

[32] A.T. Friberg and R.J. Sudol, Optica Acta 30, 1075 (1983).

[33] J. Rosen and A. Yariv, Opt. Commun. 117, 8 (1995).

[34] S.Yu. Popov and A.T. Friberg, in V.J. Corcovan and T.A. Goldman, eds., Proc. Int. Conf. on Lasers '95, STS, McLean, VA (1996), p. 133.

[35] A.T. Friberg and S.Yu. Popov, Appl. Opt. 35, 3039 (1966).